Antibiofilm activity and mechanisms of Amomum tsao-ko and clove essential oils against *Staphylococcus aureus*

Guoqing Yu[1,2†], Ming Chen[1,2†], Zedong Liao[3†], Yi wu Wen[1,2], Shan Chen[1,2], Yixi Zhou[1,2], Keshan Lin[1,2], Jialin Dai[1,2], Min Dai[1,2*], Fenghui Sun[1,2*]

[1]School of Laboratory Medicine, Chengdu Medical College, Chengdu, China; [2]Sichuan Provincial Engineering Laboratory for Prevention and Control Technology of Veterinary Drug Residue in Animal-Origin Food, Chengdu Medical College, Chengdu, China; [3]Department of Clinical Laboratory, Guangyuan Central Hospital, Guangyuan, Sichuan, China

[†]These authors contributed equally to this work and share first authorship

[*]**Corresponding Authors:** Fenghui Sun and Min Dai, School of Laboratory Medicine, Chengdu Medical College, Chengdu 610500, China. Emails: sunfenghui@cmc.edu.cn; daimin1015@cmc.edu.cn

Academic Editor: Carlos A.F. Oliveira, PhD, Department of Food Engineering, School of Animal Science and Food Engineering, University of São Paulo, Brazil

Received: 3 June 2025; Accepted: 16 December 2025; Published: 20 March 2026

ORIGINAL ARTICLE

Abstract

Staphylococcus aureus biofilms significantly threaten public health by causing persistent infections and foodborne diseases. The rise in antibiotic resistance emphasizes the urgent need for effective non-antibiotic control strategies. This study evaluated the anti-biofilm potential of Amomum tsao-ko (AEO) and clove (CEO) essential oils against *S. aureus* NCTC8325. Gas chromatography–mass spectroscopy analysis revealed distinct chemical profiles, with AEO exhibiting greater diversity. Both essential oils showed potent anti-biofilm activity against *S. aureus* NCTC8325, effectively preventing biofilm establishment, as confirmed by confocal laser scanning microscopy and scanning electron microscopy. The growth curves and crystal violet staining results demonstrated that AEO and CEO effectively inhibit biofilm formation at concentrations of 91.3 μg/mL and 86.3 μg/mL, respectively, without affecting bacterial growth. Transcriptomic profiling revealed that both AEO and CEO exert anti-biofilm effects through significant regulation of multiple molecular pathways. Interestingly, although the specific pathways influenced by AEO and CEO differed, both treatments significantly downregulated the *S. aureus* infection pathway and the expression of key adhesin protein genes within this pathway. Overall, this study provides critical insights into the phenotypic and transcriptional responses of *S. aureus* to AEO and CEO, thereby elucidating the molecular basis of their anti-biofilm activities.

Keywords: *Staphylococcus aureus*; biofilm; Amomum tsao-ko oil; clove oil

Introduction

Staphylococcus aureus is a major pathogen responsible for a wide range of invasive infections in humans, including skin and soft tissue infections, endocarditis, pneumonia, and septicemia as well as severe foodborne illnesses (Chung and Huh, 2015; Hatlen and Miller, 2021; Tong *et al.*, 2015). Moreover, the ability of *S. aureus* to form biofilms markedly enhances its tolerance to antimicrobial agents, facilitating chronic and

recurrent infections that are often difficult to eradicate (Hernández-Cuellar *et al*., 2023; Mahmoudi *et al*., 2019; Piechota *et al*., 2018). In implant-associated infections, *S. aureus* biofilms often colonize medical devices, such as joint replacements, heart valves, and urinary catheters, thus increasing the risk of complications and the likelihood of reoperation (Klinger-Strobel *et al*., 2017; Rahimi *et al*., 2016; Swearingen *et al*., 2016). In chronic wound infections, including diabetic foot ulcers and pressure sores, the presence of *S. aureus* biofilms delays wound healing and predispose patients to recurrent or persistent infections. Moreover, *S. aureus* biofilms that develop on food-processing surfaces contribute to foodborne outbreaks, posing significant challenges to food safety and infection control (Cascioferro *et al*., 2021; Silva *et al*., 2021; Vergara *et al*., 2017).

Biofilms are highly organized microbial consortia composed of extracellular DNA, lipids, proteins, and polysaccharides that adhere to both biotic and abiotic surfaces. They serve as protective barriers that shield bacterial cells from environmental stresses, such as ultraviolet (UV) radiation, extreme temperature or pH, high salinity, nutrient deprivation, and exposure to antibiotics or disinfectants (Yin *et al*., 2019). Compared to their planktonic counterparts, biofilm-embedded bacteria display markedly enhanced resistance to antimicrobial treatments, complicating eradication efforts and contributing to persistent implant-associated infections (Reis *et al*., 2020) and recurrent foodborne diseases (Guo *et al*., 2023). Given the high resistance of biofilms to conventional antibiotics, the development of safe and effective alternative strategies to mitigate biofilm-associated health risks has become an urgent global priority (Rather *et al*., 2021). Current biofilm management strategies encompass diverse approaches, including anti-biofilm peptides (e.g., LL-37) (Ridyard *et al*., 2021), bacteriophage therapy (Pires *et al*., 2022), electromagnetic interventions, antibacterial coatings (Arciola *et al*., 2018; Khatoon *et al*., 2018), and treatments based on natural products.

Among these, plant-derived essential oils have gained considerable attention due to their low toxicity, safety, biodegradability, and environmental compatibility, making them promising candidates for controlling biofilm-associated infections and for using in food preservation (Li *et al*., 2022b; Melander *et al*., 2020). Essential oils extracted from diverse plant sources, such as *Cinnamomum verum* (Yanakiev *et al*., 2020), *Artemisia dracunculus* (Mohammadi Pelarti *et al*., 2021), *Leptospermum scoparium* (Pedonese *et al*., 2022), *Thymbra capitata* (Almeida *et al*., 2022), *Salvia fruticosa*, and *Origanum vulgare* (Ersanli *et al*., 2023), have demonstrated strong anti-biofilm and biofilm-dispersing activity, highlighting their therapeutic potential against *S. aureus* biofilm-associated infections. Among these natural products, Amomum tsao-ko essential oil (AEO) and clove essential oil (CEO) exhibit a wide range of biological activities, including antioxidant (Xie *et al*., 2022), anti-*Trichomonas vaginalis* (Dai *et al*., 2016a), antitumor (Zhang *et al*., 2015), anti-inflammatory (Kim *et al*., 2016), and antiviral effects (Liñán-Atero *et al*., 2024). AEO and CEO have shown significant antibacterial activity against *S. aureus* (Li *et al*., 2022a; Min *et al*., 2016; Yan *et al*., 2025). However, the molecular mechanisms underlying their inhibitory effects on *S. aureus* biofilm formation remain poorly understood, and it is unclear whether these essential oils act through shared or distinct regulatory pathways.

In the present study, we conducted a comprehensive comparative analysis of AEO and CEO to elucidate their anti-biofilm mechanisms against *S. aureus*. The investigation included chemical composition profiling of each essential oil, antimicrobial assays, biofilm formation and disruption assays (crystal violet [CV] staining), ultrastructural characterization by microscopy, and transcriptomic sequencing integrated with molecular validation. Through this multifaceted approach, we systematically examined the inhibitory concentrations, anti-biofilm efficacy, affected molecular pathways, and key regulatory genes involved in the actions of AEO and CEO, providing new insights into their mechanisms of biofilm suppression.

Materials and Methods

Source and preparation of essential oils and *S. aureus* strain

Amomum tsao-ko was purchased from Beijing Tongren Drug Store (China). The dried fruits were crunched, and the essential oil was extracted as per the protocols described by Dai *et al*. (2016b). The extracted oil was stored at 4°C for further use. The CEO was purchased from Shanghai Yuan Ye Biotechnology Co. Ltd. (catalog number: 8000–34–8; China). *S. aureus* NCTC8325 was obtained from the National Collection of Type Cultures and preserved at –80°C in laboratory. Before experimentation, the bacterial strain was first cultured on nutrient agar (Aoboxing, Beijing, China) at 37°C for 24 h, and single colonies were subsequently inoculated into nutrient broth and incubated at 37°C with continuous shaking at 200 rpm for 24 h.

Characterization of AEO and CEO chemical composition using gas chromatography–mass spectrometry (GC-MS)

The chemical compositions of AEO and CEO were analyzed by GC–MS on the Agilent Technologies

7890B GC system coupled with a 5977B inert mass selective detector (MSD) and controlled via the Agilent ChemStation software (Agilent Technologies Co. Ltd., Santa Clara, CA, USA). AEO analysis was performed on an Agilent 19091S-433 column (30 m × 0.25 mm × 0.25 μm). Samples (1 μL) were injected by using an Agilent G4513A autosampler in split mode at a ratio of 20:1, with helium acting as a carrier gas at a flow rate of 1.0 mL/min. The GC oven was programmed as follows: initial temperature 60°C held for 5 min, ramped to 110°C at 1°C/min, and held for 5 min, increased to 180°C at 5°C/min and held for 3 min, and finally heated to 240°C at 3°C/min and held for 5 min. Mass spectrometer operated in electron impact (EI) mode with a scan range of 50–800 amu, an ionization energy of 70 eV, and ion source and quadrupole temperatures set at 240°C and 150°C, respectively. CEO analysis followed a similar protocol, with a modified oven program: initial temperature 40°C held for 30 min, then ramped to 220°C at 5°C/min and held for 30 min. Compound identification was achieved by comparing the obtained mass spectra with reference spectra in the NIST 17.L library (National Institute of Standards and Technology, USA; https://webbook.nist.gov), and the relative component abundances were calculated from peak areas using the Mass Hunter B.07.00 software.

Analysis of bacterial growth in the presence of AEO and CEO

A single colony of *S. aureus* was inoculated into Mueller–Hinton broth (MHB; Solarbio, Beijing, China) and cultured overnight. The resulting bacterial suspension was adjusted to an optical density at 600 nm (OD_{600}) of 0.6 and diluted 1:100 in fresh MHB. The aliquots were then added to MHB containing either AEO (final concentrations: 11.4, 22.8, 45.6, 91.3, 182.5, 365, and 730 μg/mL) or CEO (final concentrations: 10.8, 21.5, 43.1, 86.3, 172.5, 345, and 690 μg/mL). The control did not contain any essential oil. The bacterial growth was monitored by measuring OD_{600} at intervals of over 24 h using a microplate reader (BioTek, Winooski, VT, USA). All experiments were conducted in triplicate.

Assessment of antibacterial activity of AEO and CEO by MIC and MBC assays

The minimum inhibitory concentration (MIC) of AEO and CEO against *S. aureus* NCTC8325 was determined using 96-well microtiter plates in accordance with the guidelines of the Clinical and Laboratory Standards Institute (CLSI). Briefly, 100 μL of bacterial suspension adjusted to 1.5×10^6 CFU/mL in MHB (Solarbio) was added to each well, along with serial dilutions of AEO (0–1,380 μg/mL) or CEO (0–1,460 μg/mL) prepared in MHB. The plates were incubated at 37°C for 18 h, and the lowest concentration of essential oils with no visible growth of microorganisms was defined as MIC. To determine minimum bactericidal concentration (MBC), 10 μL of culture from the wells showing no visible growth was plated onto Mueller–Hinton agar (MHA; Solarbio) and incubated at 37°C for 24 h. The MBC was defined as the lowest concentration at which no bacterial colonies were observed. All experiments were performed in triplicate.

Evaluation of anti-biofilm activity of AEO and CEO via CV assay

The inhibitory effects of AEO and CEO on biofilm formation were assessed by using the CV staining method as described by Ersanli *et al*. (2023). Briefly, exponential-phase *S. aureus* cells (100 μL, 0.5 McFarland) were added to a 96-well microtiter plate containing 100 μL of tryptic soy broth (TSB; Solarbio) supplemented with 1% glucose and sub-inhibitory concentrations of AEO or CEO. After incubation at 37°C for 24 h, the planktonic cells were removed, and the wells were gently rinsed thrice with phosphate-buffered saline (PBS). The biofilms were stained with 1% CV for 20 min at room temperature, followed by three washes with PBS, air drying, and solubilization in 95% ethanol. The absorbance was measured at 570 nm by using a microplate reader. Wells without essential oil treatment served as controls. The minimum biofilm inhibitory concentration (MBIC) was defined as the lowest concentration of AEO or CEO at which OD_{600} displayed no significant difference when compared to the TSB blank control. The biofilm inhibition rate (%) was calculated as follows:

$$\text{Biofilm inhibition rate (\%)} = ([OD_{control} - OD_{inhibition}] \div OD_{control}) \times 100\%.$$

The disruptive effects of AEO and CEO on mature biofilms were evaluated similarly. Exponential-phase *S. aureus* cells (100 μL) were first cultured in a 96-well microtiter plate containing 100 μL of TSB with 1% glucose and incubated at 37°C for 24 h to allow formation of biofilm. The preformed biofilms were then treated with varying concentrations of AEO (91.3–2,920 μg/mL) or CEO (86.3–2760 μg/mL) at 37°C for 24 h. After treatment, the essential oils were removed, and the biofilms were stained and solubilized as described earlier. Absorbance at 570 nm was measured to assess biofilm disruption. Wells treated with sterile TSB served as blank control. The minimum biofilm eradication concentration (MBEC) was defined as the lowest concentration of essential oils that shows no significant difference in

values compared to the TSB blank control. The biofilm elimination rate (%) was calculated as follows:

Biofilm elimination rate (%) = ([$OD_{control}$ - $OD_{disruption}$] ÷ $OD_{control}$) × 100%.

All experiments were performed in triplicate.

Microscopic examination of *S. aureus* biofilms following AEO and CEO treatment

For confocal laser scanning microscopy (CLSM) analysis, *S. aureus* biofilms were treated with AEO (365 μg/mL) or CEO (345 μg/mL) in 8-well chamber slides (Nunc Lab-Tek; Thermo Fisher Scientific, MA, USA) with 400 μL per well. Following incubation at 37°C for 24 h, the biofilms were gently rinsed thrice with sterile PBS, air-dried at room temperature for 20 min, fixed with 5% formaldehyde for 5 min, rehydrated with 95% ethanol for 5 min, and stained with 0.1% (w/v) acridine orange solution for 15 min in the dark. The control samples were processed identically in the absence of essential oils. The biofilm images were acquired at 488 nm using a CLSM (A1R MP+; Nikon Ltd., Japan).

For scanning electron microscopy (SEM) analysis, *S. aureus* biofilms were formed on glass slides in 8-well chamber slides (400 μL/well) in the presence of AEO (365 μg/mL) or CEO (345 μg/mL). After incubation at 37°C for 24 h, the slides were washed with PBS, fixed with 5% formaldehyde for 5 min, and dehydrated through a graded ethanol series (50%, 70%, 90%, and 100%) for 2 min each. The morphological changes in bacterial cells following essential oil treatment were observed by SEM (Helios G4 UC type, Aztec Live ULTIM; Thermo Fisher).

Quantification of extracellular proteins and polysaccharides and viable cell counts in biofilms

The extracellular proteins content was determined by using a previously reported method with minor modifications (Gao *et al*., 2022). Log-phase *S. aureus* cells were diluted as 1:100 in fresh TSB supplemented with 0.5% (w/v) glucose and exposed to varying concentrations of AEO (45.6, 91.3, and 182.5 μg/mL) or CEO (43.1, 86.3, and 172.5 μg/mL) for 24 h to allow the formation of mature biofilms. Untreated *S. aureus* cells served as controls. Following the incubation, the samples were washed and resuspended in PBS. Extracellular proteins were isolated via centrifugation and quantified using a bicinchoninic acid (BCA) protein assay kit (Solarbio) in accordance with the manufacturer's instructions.

The extracellular polysaccharides content was determined by using a previously reported method albeit with minor modifications (Liu *et al*., 2017). Briefly, 2 mL of the sample was mixed with 1 mL of 6% (w/v) phenol solution, followed by the rapid addition of 5 mL of concentrated sulfuric acid. The reaction mixture was incubated in a water bath at 90°C for 15 min and then cooled to room temperature. The absorbance of the mixture was measured at 490 nm using a UV-visible spectrophotometer.

Biofilm viability was assessed by using a method as described previously with minor modifications (Qian *et al*., 2020). Briefly, after 24-h treatment with AEO or CEO in a 6-well plate, the matured biofilms were disrupted in an ultrasonic water bath. The resulting suspensions were washed thrice with 200 μL of 10-mM PBS and serially diluted in 10-fold increments with PBS. Aliquots of 10 μL from each dilution were plated onto tryptic soy agar (TSA) and incubated at 37°C for 24 h. Bacterial viability was determined by enumerating the colony-forming units (CFUs).

RNA extraction, sequencing, and quantitative reverse transcription–polymerase chain reaction (qRT-PCR) validation

A total of nine samples were used for RNA-seq analysis, which comprised three biological replicates per group. *S. aureus* strain NCTC8325 was cultured in TSB medium with or without AEO (91.3 μg/mL) or CEO (86.3 μg/mL) at 37°C for 24 h. Total RNA was extracted following the manufacturer's protocol using the RNAprep Pure Cell/Bacteria kit (TIANGEN Biotech, Beijing, China). The RNA samples were then submitted to Shanghai Meiji Biotechnology Co. Ltd. for sequencing.

The resulting clean reads were aligned to the *S. aureus* subsp. aureus reference genome (GenBank accession GCA_000013425.1) using HISAT2 (v2.1.0) (Kim *et al*., 2019). Differentially expressed genes (DEGs) between the AEO and CEO treatment groups and the control group were identified using the DESeq2 package (v1.38.3) (Quinn *et al*., 2018) in R software with a fold change of ≥1.5 and a significance threshold ($P < 0.05$). To investigate biological functions and pathways associated with DEGs, Gene Ontology (GO) and Kyoto Encyclopedia of Genes and Genomes (KEGG) enrichment analyses were performed using the R package clusterProfiler, with a focusing on terms with $P < 0.05$. The Raw sequence data reported in this paper were deposited in the Genome Sequence Archive in National Genomics Data Center, China National Center for Bioinformation/Beijing Institute of Genomics, Chinese Academy of Sciences (Project Number: PRJCA050085), which are publicly accessible at https://ngdc.cncb.ac.cn/gsa.

To validate RNA-seq results, qRT-PCR was performed. The RNA samples were prepared as described above. Total RNA was reverse-transcribed into complementary DNA (cDNA) by using PrimeScript™ FAST RT Reagent Kit with genomic DNA (gDNA) eraser (Takara, Japan). qRT-PCR reactions were conducted using the TB Green® Premix Ex Taq™ II FAST qPCR kit (Takara) on a CFX Connect real-time PCR system (Bio-Rad Laboratories, Hercules, CA, USA), following the manufacturer's instructions. Primers were designed using the Primer 5.0 software (PREMIER Biosoft, Canada), which are listed in Supplementary Table S1. The gene expressions were normalized to the triosephosphate isomerase (TPI) of *S. aureus*, and the relative expression of target genes was calculated by using the two-delta-delta-C-T ($2^{-\Delta\Delta CT}$) method.

Statistical analysis

Data were presented as mean ± standard deviation (SD). All statistical analyses were conducted utilizing GraphPad Prism 9.0. The data were analyzed using one-way analysis of variance (ANOVA), where $P < 0.05$ was considered to indicate statistical significance. Every experiment was repeated thrice.

Results

Chemical composition and comparison of AEO and CEO

The GC-MS analysis revealed distinct chemical profiles for CEO and AEO (Figure 1), with the principal constituents summarized in Tables 1 and 2. In AEO, 12 major components (relative abundance > 1.0%) were identified, including eucalyptol (30.58%), geraniol (13.10%), citral (7.19%), α-phellandrene (4.22%), 2,6-octadien-1-ol, 3,7-dimethyl-, acetate, (Z)- (2.95%), α-terpinyl formate (2.75%), β-methyl-cinnamaldehyde (2.32%), bicyclo[3.1.1] heptane, 6,6-dimethyl-2-methylene-, (1S)- (1.90%), (E)-2-octenal (1.79%), (1R)-2,6,6-trimethylbicyclo[3.1.1] hept-2-ene (1.61%), 1H-indene-4-carboxaldehyde, 2,3-dihydro (1.53%), and 2-dodecenal (1.18%). In contrast, the CEO was dominated by four major constituents (relative abundance > 1.0%): eugenol (76.35%), caryophyllene (9.69%), humulene (2.39%), and cyclohexane, 1,3,5-triphenyl- (1.24%).

Based on structural classification, these components were grouped into six categories: aromatics, alcohols, aldehydes, alkenes, monoterpenes, and others. Comparative profiling revealed notable compositional differences between two essential oils: AEO exhibited greater chemical diversity, characterized by higher proportions of alcohols, aldehydes, and miscellaneous compounds, whereas aromatics predominated CEO (Figure 2). Given the compositional differences and the observed similar anti-biofilm activity of AEO and CEO against *S. aureus*, we further investigated their potential mechanisms of action.

Antibacterial and anti-biofilm effects of AEO and CEO against *S. aureus*

The antibacterial activities of AEO and CEO were evaluated by determining their MIC, MBC, and growth curves. As shown in Figures 3A and 3B, both essential oils markedly inhibited *S. aureus* growth in a concentration-dependent manner, as reflected by decreasing OD at 600 nm (OD_{600}). Notably, significant reductions in OD at 600 nm were observed at concentrations of 730 μg/mL for AEO and 690 μg/mL for CEO. MIC determination yielded comparable antibacterial potencies, 730 μg/mL for AEO and 690 μg/mL for CEO, consistent with cell density data (Supplementary Figure S1). MBC values were substantially higher than their respective MICs, indicating that bactericidal activity required higher concentrations than those needed for growth inhibition. Specifically, MBC for AEO was 1.45 mg/mL (approximately twice its MIC), while that for CEO was 2.76 mg/mL (approximately four-fold its MIC). Collectively, these results indicate that both AEO and CEO can suppress *S. aureus* proliferation, although their bactericidal thresholds differ.

The anti-biofilm potential of AEO and CEO was subsequently assessed across a concentration gradient (Figures 3C and 3D). AEO and CEO significantly inhibited biofilm formation induced by *S. aureus*. At 91.3 μg/mL, AEO reduced biofilm biomass by 37.693% ± 5.214%, whereas CEO achieved a 39.774% ± 5.404% reduction at 86.3 μg/mL (Figures 3E and 3F). The MICs of biofilm, determined through CV staining, were 730 μg/mL for AEO and 690 μg/mL for CEO, aligning with their MIC values. These results indicated that the sub-MIC values of AEO (11.4, 22.8, 45.6, 91.3, 182.5, and 365 μg/mL) and CEO (10.8, 21.5, 43.1, 86.3, 172.5, and 345 μg/mL) significantly inhibited *S. aureus* NCTC8325 biofilm formation in a dose-dependent manner.

Disruption of *S. aureus* biofilms by AEO and CEO

The ability of AEO and CEO to disrupt pre-established *S. aureus* biofilms was also examined (Figure 4). Biofilm disruption increased progressively with increasing concentrations of both essential oils, with nearly complete biofilm eradication observed at 2,900 μg/mL for AEO and 1,380 μg/mL for CEO. Accordingly, the minimum

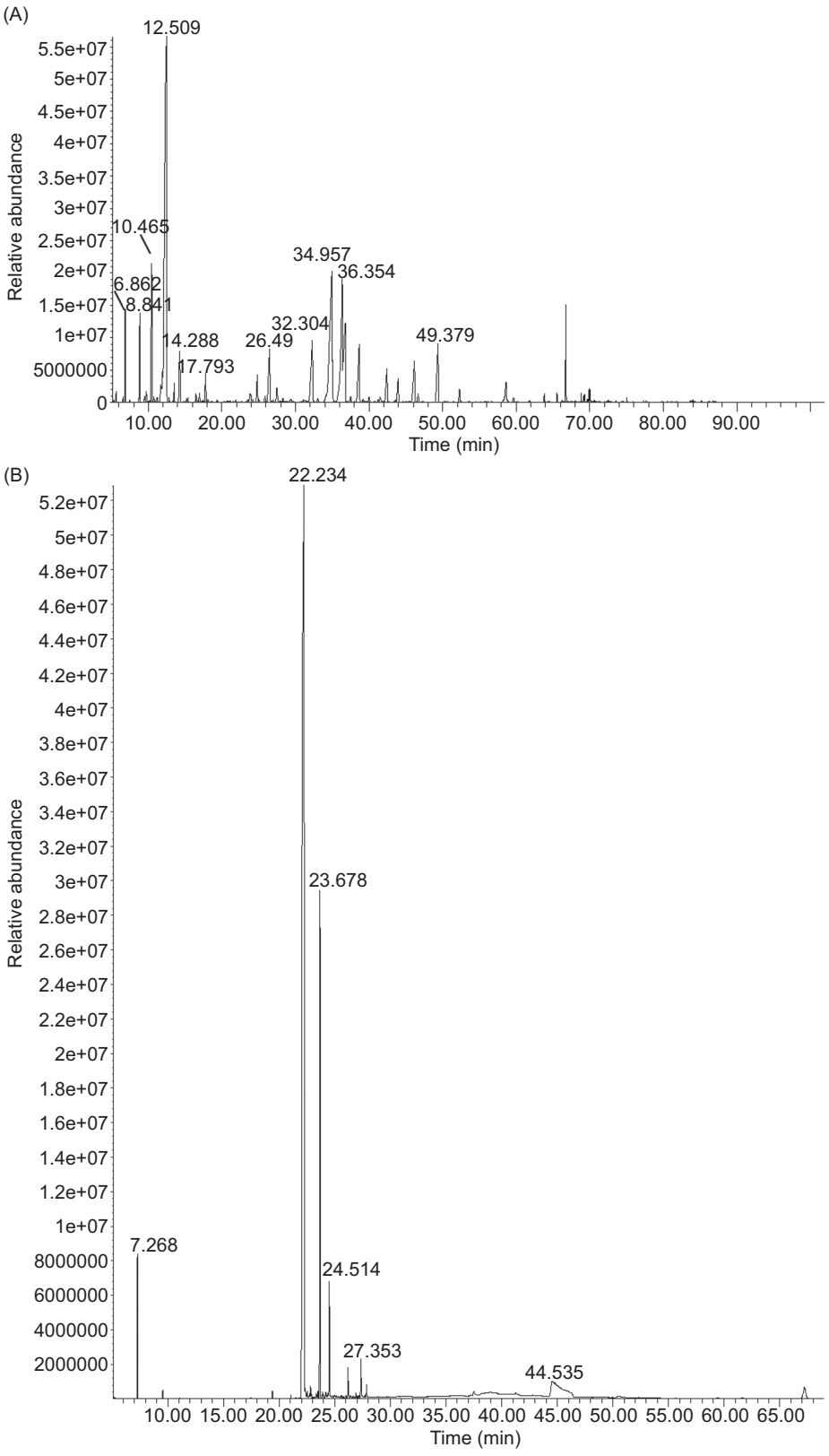

Figure 1. The gas chromatography-mass spectrometer analysis of AEO (A) and CEO (B).

Table 1. The components of AEO identified by GC-MS.

No.	Compound name	Molecular formula	Relative content/%	Retention time (min)
1	2-n-Butyl furan	$C_8H_{12}O$	0.041	5.329
2	Heptanal	$C_7H_{14}O$	0.165	5.637
3	Bicyclo[3.1.0]hex-2-ene, 4-methyl-1-(1-methylethyl)-	$C_{10}H_{16}$	0.1	6.582
4	(1R)-2,6,6-Trimethylbicyclo[3.1.1]hept-2-ene	$C_{10}H_{16}$	1.614	6.862
5	Camphene	$C_{10}H_{16}$	0.05	7.475
6	Bicyclo[3.1.0]hexane, 4-methylene-1-(1-methylethyl)-	$C_{10}H_{16}$	0.067	8.698
7	Bicyclo[3.1.1]heptane, 6,6-dimethyl-2-methylene-, (1S)-	$C_{10}H_{16}$	1.901	8.841
8	6-methyl-5-Hepten-2-one	$C_8H_{14}O$	1.154	9.504
9	β-Myrcene	$C_{10}H_{16}$	0.322	9.71
11	α-Phellandrene	$C_{10}H_{16}$	4.219	10.465
12	3-Carene	$C_{10}H_{16}$	0.138	10.746
13	1-methyl-4-(1-methylethyl)-1,3-Cyclohexadiene	$C_{10}H_{16}$	0.183	11.173
14	p-Cymene	$C_{10}H_{14}$	1.742	11.682
15	1,3,5-Cycloheptatriene, 3,7,7-trimethyl-	$C_{10}H_{14}$	1.035	11.939
16	Eucalyptol	$C_{10}H_{18}O$	30.575	12.509
17	trans-β-Ocimene	$C_{10}H_{16}$	0.082	12.833
18	(Z)-3,7-dimethyl-1,3,6-Octatriene,	$C_{10}H_{16}$	0.361	13.52
19	(E)-2-Octenal	$C_8H_{14}O$	1.791	14.288
20	p-Cresol	C_7H_8O	0.044	14.803
21	Cyclooctyl alcohol	$C_8H_{16}O$	1.088	15.187
22	1-Octanol	$C_8H_{18}O$	0.117	15.393
23	Cyclohexene, 1-methyl-4-(1-methylethylidene)-	$C_{10}H_{16}$	0.212	16.468
24	Phenol, 2-methoxy-	$C_7H_8O_2$	1.066	16.661
25	3-Methyl-2-(2-methyl-2-butenyl)-furan	$C_{10}H_{14}O$	0.082	17.455
26	Linalool	$C_{10}H_{18}O$	0.765	17.793
27	2-Nonanol	$C_9H_{20}O$	1.024	17.941
28	Nonanal	$C_9H_{18}O$	0.075	18.102
29	Fenchol	$C_{10}H_{18}O$	1.031	18.613
30	γ-Terpinene	$C_{10}H_{16}$	0.07	19.354
31	6-Octenal, 3,7-dimethyl-, (R)-	$C_{10}H_{18}O$	1.029	22.711
32	Phenol, 2,5-dimethyl-	$C_8H_{10}O$	0.028	23.32
33	endo-Borneol	$C_{10}H_{18}O$	1.093	23.545
34	Terpinen-4-ol	$C_{10}H_{18}O$	0.907	24.816
35	α-TERPINYL FORMATE	$C_{11}H_{18}O_2$	2.75	26.49
36	Decanal	$C_{10}H_{20}O$	0.147	28.304
37	Neral	$C_{10}H_{16}O$	3.83	32.304
38	2-Cyclohexen-1-one, 2-methyl-5-(1-methylethyl)-, (S)-	$C_{10}H_{16}O$	1.048	32.474
39	Geraniol	$C_{10}H_{18}O$	13.098	34.957
40	Citral	$C_{10}H_{16}O$	7.193	36.354
41	(1S-endo)Bicyclo[2.2.1]heptan-2-ol, 1,7,7-trimethyl-, acetate	$C_{12}H_{20}O_2$	1.042	37.058
42	Phenol, 2-methyl-5-(1-methylethyl)-	$C_{10}H_{14}O$	0.213	40.028
43	1H-Indene-4-carboxaldehyde, 2,3-dihydro	$C_{10}H_{10}O$	1.527	42.44
44	2-Oxabicyclo[2.2.2]octan-6-ol, 1,3,3-trimethyl-, acetate	$C_{12}H_{20}O_3$	1.064	43.609
45	2,6-Octadiene, 2,6-dimethyl-	$C_{10}H_{18}$	0.041	45.594
46	β-methyl-Cinnamaldehyde	$C_{10}H_{10}O$	2.32	46.181
47	2,6-Octadien-1-ol, 3,7-dimethyl-, acetate, (Z)-	$C_{12}H_{20}O_2$	2.95	49.379
48	(E)-2-Decenyl acetate	$C_{12}H_{22}O_2$	0.484	52.299

(continues)

Table 1. Continued.

No.	Compound name	Molecular formula	Relative content/%	Retention time (min)
49	(1R,9R,E)-4,11,11-Trimethyl-8-methylenebicyclo[7.2.0] undec-4-ene	$C_{15}H_{24}$	1.046	56.152
50	2-Dodecenal	$C_{12}H_{22}O$	1.181	58.616
51	Z-2-Dodecenol	$C_{12}H_{24}O$	0.198	59.642
52	[3aS-(3aα,3bβ,4β,7α,7aS*)]-octahydro-7-methyl-3-methylene-4-(1-methylethyl)-1H-Cyclopenta[1,3]cyclopropa[1,2]benzene	$C_{15}H_{24}$	0.033	60.188
53	α-Muurolene	$C_{15}H_{24}$	1.057	61.813
54	Naphthalene, 1,2,3,5,6,8a-hexahydro-4,7-dimethyl-1-(1-methylethyl)-, (1S-cis)	$C_{15}H_{24}$	0.199	63.832
55	Cubenene	$C_{15}H_{24}$	1.023	64.28
56	Cyclohexanemethanol-4-Ethenyl-α,α,4-trimethyl-3-(1-methylethenyl)	$C_{15}H_{26}O$	0.183	65.56
57	Guaiol	$C_{15}H_{26}O$	0.015	67.979
58	1,5-Dodecadiene	$C_{12}H_{22}$	1.138	68.841
59	Naphthalene, 1,2,3,4,4a,7-hexahydro-1,6-dimethyl-4-(1-methylethyl)-	$C_{15}H_{24}$	0.094	69.165
60	2-Naphthalenemethanol, 1,2,3,4,4a,5,6,7-octahydro-α,α, 4a,8-tetramethyl-, (2R-cis)-	$C_{15}H_{26}O$	0.123	69.295
61	Naphthalene, 1,2,3,5,6,7,8,8a-octahydro-1, 8a-dimethyl-7-(1-methylethenyl)-, [1R-(1α,7β,8aα)]-	$C_{15}H_{24}$	1.011	69.56
62	Bicyclo[4.4.0]dec-1-ene, 2-isopropyl-5-methyl-9-methylene-	$C_{15}H_{24}$	0.07	69.703
63	2-Naphthalenemethanol, decahydro-α,α,4a-trimethyl-8-methylene-[2R-(2α,4a.α,8αβ)]	$C_{15}H_{26}O$	0.215	69.926
64	β-Panasinsene	$C_{15}H_{24}$	0.195	70.053
65	tau-Cadinol	$C_{15}H_{26}O$	0.123	70.176
66	Naphthalene, 1,2,3,5,6,7,8,8a-octahydro-1, 8a-dimethyl-7-(1-methylethenyl)-, [1S-(1α,7α,8aα)]-	$C_{15}H_{24}$	0.136	70.62
67	9H-Fluoren-9-one	$C_{13}H_{8}O$	0.014	72.417
68	(E)-β-Famesene	$C_{15}H_{24}$	0.026	72.519
69	(E)-3-Butylidene-4,5-dihydroisobenzofuran-1(3H)-one	$C_{12}H_{14}O_2$	0.111	72.707
70	Phenanthrene	$C_{14}H_{10}$	0.023	73.566

Table 2. The components of CEO identified by GC-MS.

No.	Compound name	Molecular formula	Relative content/%	Retention time (min)
1	Phenol, 4-(2-propenyl)-	$C_9H_{10}O$	0.16	19.392
2	Eugenol	$C_{10}H_{12}O_2$	76.348	22.234
3	Copaene	$C_{15}H_{24}$	0.244	22.523
4	(-)-Tricyclo[6.2.1.0(4,11)]undec-5-ene, 1,5,9,9-tetramethyl- (isocaryophyllene-I1)	$C_{15}H_{24}$	0.225	22.722
5	Naphthalene, 1,2,4a,5,8,8a-hexahydro-4, 7-dimethyl-1-(1-methylethyl)-, (1α,4a.β,8a.α)-(+/-)-	$C_{15}H_{24}$	0.239	22.834
6	1H-Cyclopropa[a]naphthalene, decahydro-1, 1,3a-trimethyl-7-methylene-, [1aS-(1a.α,3a.α,7a.β,7b.α)]	$C_{15}H_{24}$	1.094	22.898
7	Bicyclo[7.2.0]undec-4-ene, 4,11,11-trimethyl-8-methylene-,[1R-(1R*,4Z,9S*)]-	$C_{15}H_{24}$	0.151	23.333
8	2,10,10-Trimethyltricyclo[7.1.1.0(2,7)]undec-6-en-8-one	$C_{14}H_{20}O$	0.169	23.381
9	1S,2S,5R-1,4,4-Trimethyltricyclo[6.3.1.0(2,5)]dodec-8(9)-ene	$C_{15}H_{24}$	1.163	23.489
10	Caryophyllene	$C_{15}H_{24}$	9.692	23.678

(continues)

Table 2. Continued.

No.	Compound name	Molecular formula	Relative content/%	Retention time (min)
11	Tricyclo[4.1.0.0(2,4)]heptane, 3,3,7,7-tetramethyl-5-(2-methyl-1-propenyl)-	$C_{15}H_{24}$	1.055	23.872
12	(2S,4aR,8aR)-4a,8-Dimethyl-2-(prop-1-en-2-yl)-1,2,3,4,4a,5,6,8a-octahydronaphthalene	$C_{15}H_{24}$	0.164	23.931
13	γ-Muurolene	$C_{15}H_{24}$	0.168	24.163
14	(+)-epi-Bicyclosesquiphellandrene	$C_{15}H_{24}$	0.108	24.253
15	4,11,11-trimethyl-8-methylenebicyclo[7.2.0]undec-3-ene	$C_{15}H_{24}$	1.104	24.4
16	Humulene	$C_{15}H_{24}$	2.388	24.514
17	Naphthalene, 1,2,4a,5,8,8a-hexahydro-4,7-dimethyl-1-(1-methylethyl)-, (1α,4a.β,8a.α)-(+/-)-	$C_{15}H_{24}$	1.149	24.929
18	1-Isopropyl-4,7-dimethyl-1,2,3,4,5,6-hexahydronaphthalene	$C_{15}H_{24}$	0.162	24.987
19	α-Muurolene	$C_{15}H_{24}$	0.171	25.631
20	Naphthalene, 1,2,3,4,4a,7-hexahydro-1,6-dimethyl-4-(1-methylethyl)-	$C_{15}H_{24}$	1.043	26.406
21	Caryophyllenyl alcohol	$C_{15}H_{26}O$	0.817	27.353
22	4,4'-(Hexafluoroisopropylidene)diphenol	$C_{15}H_{10}F_6O_2$	0.284	37.505
23	Cyclohexane, 1,3,5-triphenyl-	$C_{24}H_{24}$	1.236	44.535
24	cis-Calamenene	$C_{15}H_{22}$	0.67	26.192

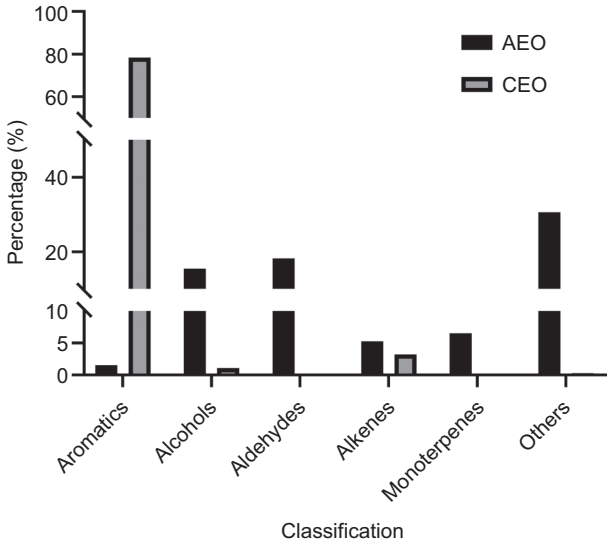

Figure 2. Comparison of components in the AEO and CEO compound categories.

biofilm eradication concentrations were determined to be 2,900 μg/mL for AEO and 1,380 μg/mL for CEO (Table 3).

Confocal laser scanning microscopy revealed that *S. aureus* formed thick, multilayered biofilms with tightly packed, evenly distributed cells in the control group (Figure 5A). Exposure to either AEO (365 μg/mL) or CEO (345 μg/mL) markedly reduced biofilm density, and yielded predominantly monolayered, dispersed bacterial structures (Figures 5B and 5C).

Scanning electron microscopy observations were consistent with the CLSM results. Untreated *S. aureus* cultures formed dense, compact, and well-organized biofilms, with cells forming a continuous, paving-stone-like structure on glass surfaces (Figures 6A and 6B). Treatment with AEO (365 μg/mL) or CEO (345 μg/mL) led to pronounced reductions in cell adhesion and disrupted biofilm integrity, characterized by enlarged intercellular gaps and reticular fractures within the extracellular matrix (Figures 6C–6F).

Effects of AEO and CEO on extracellular matrix components and viable cell counts in *S. aureus* biofilms

Extracellular proteins and polysaccharides are key structural components of *S. aureus* biofilms. In this study, the effects of AEO and CEO on the contents of these extracellular polymers as well as on the viable bacterial counts within the biofilms were assessed. As shown in Figure 7, both extracellular polymer levels and viable bacterial counts in the biofilms decreased in a concentration-dependent manner of either essential oil. Neither statistically significant reduction of extracellular polymer content nor viable cell counts was observed at the lower concentrations of 91.3 μg/mL

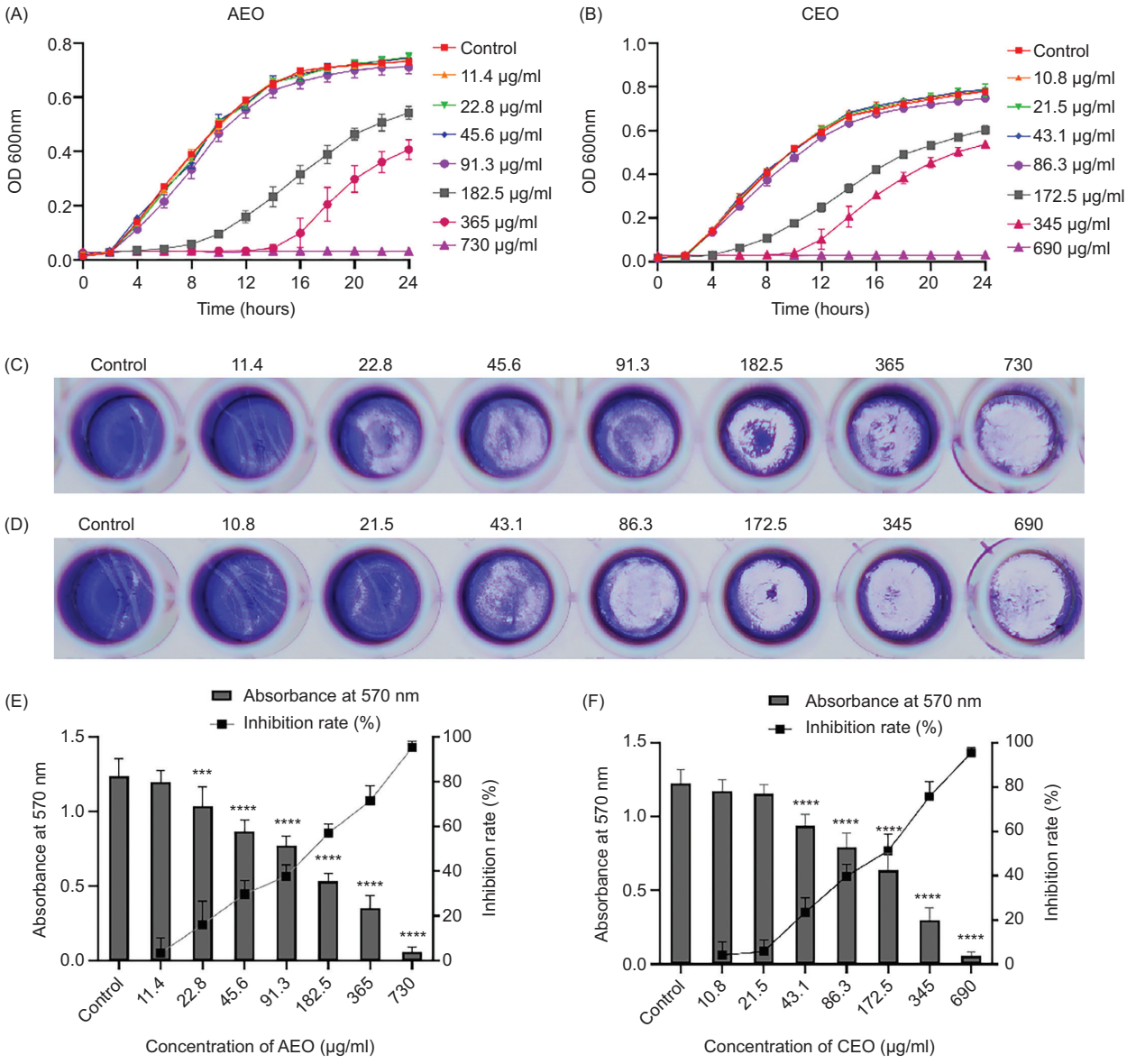

Figure 3. Effects of AEO (A) and CEO (B) at different concentrations on the activity of *S. aureus* NCTC8325 assessed by the growth curve assay. Effect of AEO (C and E) and CEO (D and F) with sub-minimum inhibitory concentrations on the formation of *S. aureus* biofilms assessed by crystal violet staining. ***$P < 0.001$, ****$P < 0.0001$ compared with the control group.

(AEO) and 86.3 μg/mL (CEO). In contrast, at the same concentrations, both essential oils significantly inhibited biofilm formation, as measured by CV assay (Figures 3E and 3F).

Transcriptomic responses of *S. aureus* to AEO and CEO treatment

Correlation heat map analysis revealed tight clustering of biological replicates within the AEO- and CEO-treated and control groups, confirming the stability and reproducibility of the RNA-seq data (Figure 8A).

Comparative transcriptomic profiling identified 835 DEGs (427 upregulated and 408 downregulated) in the AEO-treated group and 593 DEGs (329 upregulated and 264 downregulated) in the CEO-treated group, compared to the control (Figure 8B). All DEGs of biofilms after AEO and CEO treatment are listed in Supplementary Tables S2 and S3. KEGG pathway enrichment analysis showed that downregulated DEGs in both groups were significantly enriched in the *S. aureus* infection pathway, which includes multiple genes associated with adhesion and virulence. This transcriptional pattern provides a molecular correlate to phenotypic findings (Figures 3C and 3D).

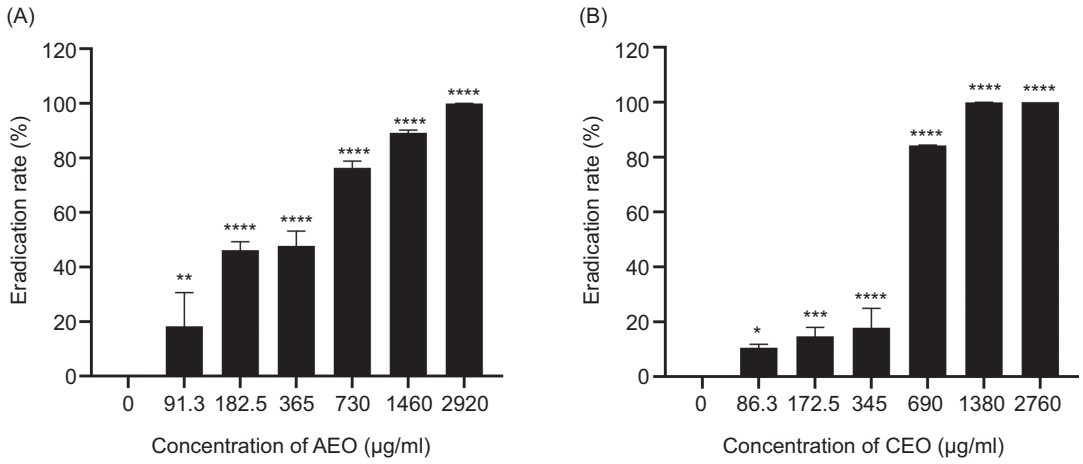

Figure 4. The eradication effect of different concentrations of AEO (A) and CEO (B) on preformed biofilm formation of *S. aureus* NCTC8325, **P* < 0.05, ***P* < 0.01, ****P* < 0.001, *****P* < 0.0001 compared with the 0 μg/ml group.

Table 3. Comparison of the eradication rates of AEO and CEO on preformed biofilms.

Types of essential oils	Concentrations (μg/ml)	Eradication rate (%)
Amomum tsao-ko essential oil	0	0
	91.3	18.27 ± 12.39
	182.5	46.16 ± 3.16
	365	47.76 ± 5.39
	730	76.37 ± 2.53
	1460	89.15 ± 1.08
	2920	99.92 ± 0.08
Clove essential oil	0	0
	86.3	10.54 ± 1.31
	172.5	14.66 ± 3.35
	345	17.81 ± 7.15
	690	84.25 ± 0.16
	1380	99.91 ± 0.03
	2760	99.96 ± 0.02

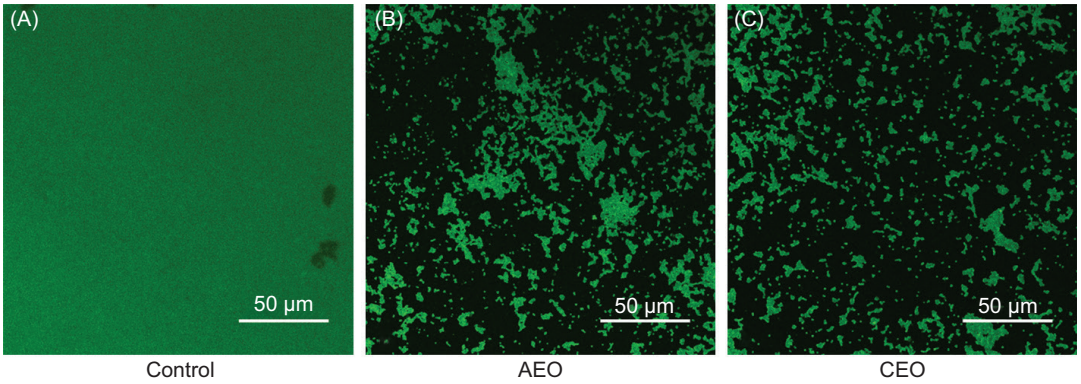

Figure 5. Confocal laser scanning microscopy images of biofilms treated or untreated with AEO and CEO at 400 x magnification. Scale bar: 50 μm. (A) Untreated *S. aureus* biofilm morphology. (B) The morphology of biofilm treated with AEO at 365 μg/ml. Scale bar: 50 μm. (C) The morphology of biofilm treated with CEO at 345 μg/ml. Scale bar: 50 μm.

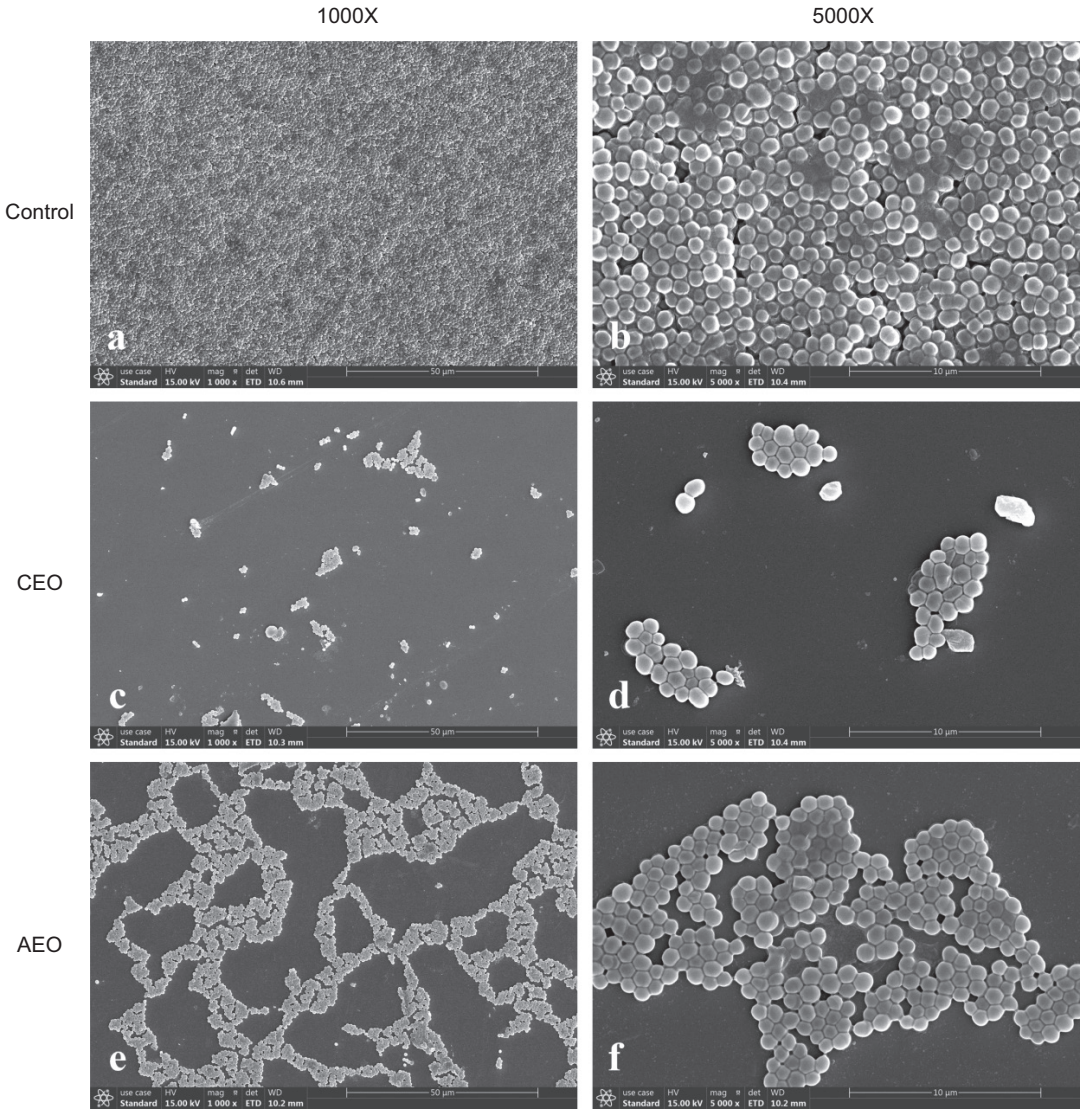

Figure 6. Scanning electron microscope images of biofilms treated or untreated with AEO and CEO at 1000 x or 5000 x magnification. (A, B) Untreated *S. aureus* biofilm morphology. Scale bar: 50 μm, 10 μm. (C, D) The morphology of biofilm treated with CEO at 345 μg/ml. Scale bar: 50 μm, 10 μm. (E, F) The morphology of biofilm treated with AEO at 365 μg/ml. Scale bar: 50 μm, 10 μm.

In contrast, upregulated DEGs were mainly enriched in pathways related to amino acid metabolism and transport, including cysteine and methionine metabolism, monobactam biosynthesis, lysine biosynthesis, valine, leucine and isoleucine biosynthesis, glycine, serine and threonine metabolism, and ABC transporters. Additionally, treatment-specific enrichment patterns were observed: riboflavin metabolism was uniquely upregulated in AEO-treated samples (Figure 8C), whereas atrazine degradation, beta-Lactam resistance, and phenylalanine, tyrosine, and tryptophan biosynthesis and quorum sensing were exclusive to CEO treatment (Figure 8E). Collectively, KEGG analysis revealed that both AEO and CEO downregulate the *S. aureus* infection pathway while differentially modulating specific metabolic pathways.

To validate these findings, the expressions of biofilm-related genes (*icaB*, *icaC*, *agrB*, *fnbB*, and *clfB*) were further examined. The qRT-PCR results showed trends consistent with the transcriptomic data, confirming the stability and reliability of transcriptome analysis (Supplementary Figure S2).

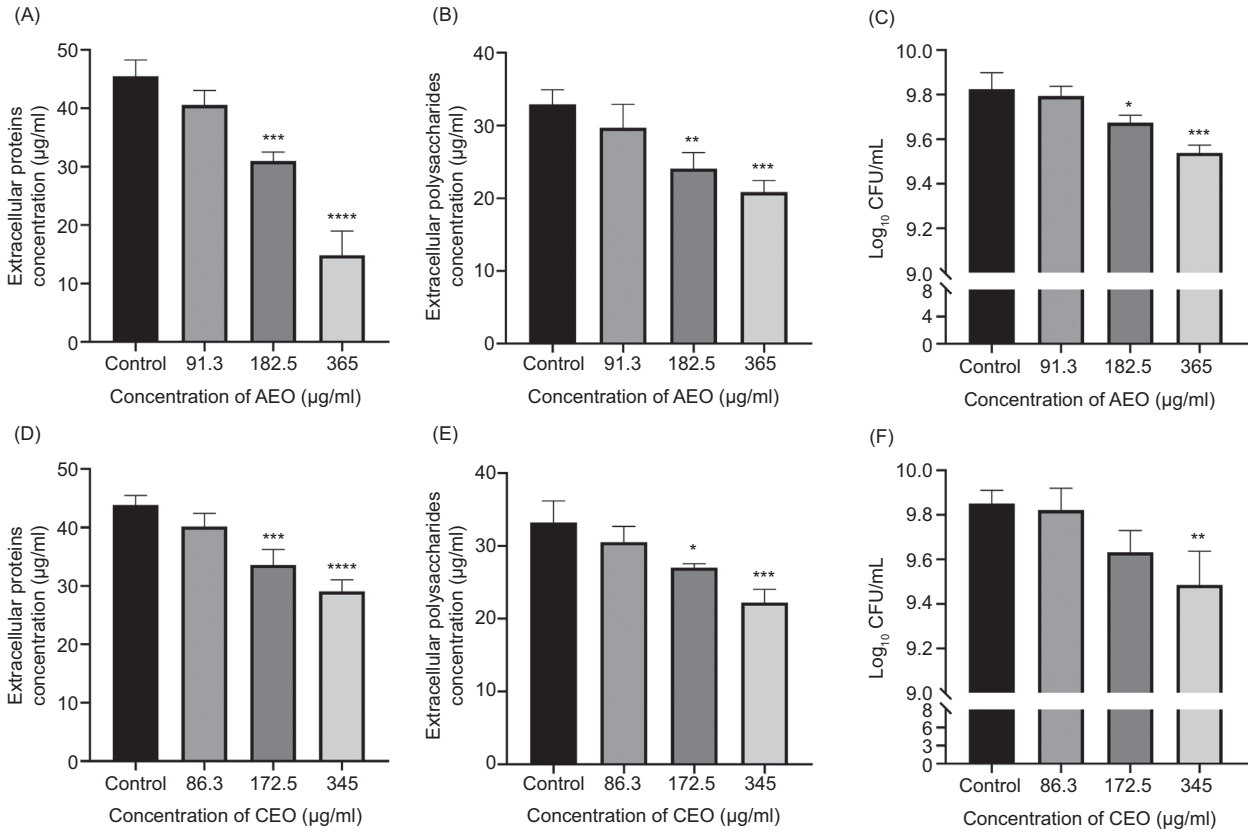

Figure 7. Effects of AEO and CEO on the release of extracellular protein andextracellular polysaccharides of *S. aureus*. (A) Release of extracellular proteins after AEO treatment, (B) Release of extracellular polysaccharide after AEO treatment, (D) Release of extracellular proteins after CEO treatment, (E) Release of extracellular polysaccharide after CEO treatment, and the effects of AEO (C) and CEO (F) on viable bacteria in biofilms. *$P < 0.05$, **$P < 0.01$, ***$P < 0.001$, ****$P < 0.0001$ compared with the control group.

Discussion

Anti-biofilm potential of plant-derived essential oils

Plant-derived natural extracts possess diverse bioactive compounds with significant antimicrobial potential (Aziz *et al*., 2018). Among them, AEO and CEO effectively inhibit the growth and biofilm formation of multiple pathogenic bacteria (Elbestawy *et al*., 2023; Lee *et al*., 2022; Li *et al*., 2022b; Rahman *et al*., 2017; Somrani *et al*., 2022). These properties make them attractive candidates for applications in food packaging (Vasile *et al*., 2017) and preservation (He *et al*., 2024; Valarezo *et al*., 2025).

Consistent with previous findings, our results demonstrated that both AEO and CEO exert substantial anti-biofilm activity at sub-inhibitory concentrations, indicating that their effects extend beyond direct antibacterial action to include modulation of biofilm formation pathways. Notably, the biofilm formed by *S. aureus* ATCC43300 was significantly inhibited and eradicated following the treatment with AEO and CEO (Supplementary Figure S3). These results highlighted the potential of plant-derived essential oils as natural, non-antibiotic agents for preventing and controlling biofilm-associated *S. aureus* contamination in food-related environments.

Biofilm regulatory networks and AEO mechanisms

Transcriptomic analysis revealed significant downregulation of the *S. aureus* infection pathway following AEO treatment, with the serine-aspartate repeat protein *SdrC/D*, fibrinogen-binding protein *fib*, iron-regulated surface determinant protein A of *isdA*, chemotaxis inhibitory protein of staphylococci *chp*, and virulence factor *hlg* genes showing marked downregulation in this pathway. These genes have been demonstrated to be closely associated with biofilm formation (Alabdullatif *et al*., 2022; Chen *et al*., 2020, 2022; Sultan *et al*., 2018). Specifically, *SdrC/D*, *fib*, and *isdA* promote biofilm formation by encoding proteins that facilitate attachment

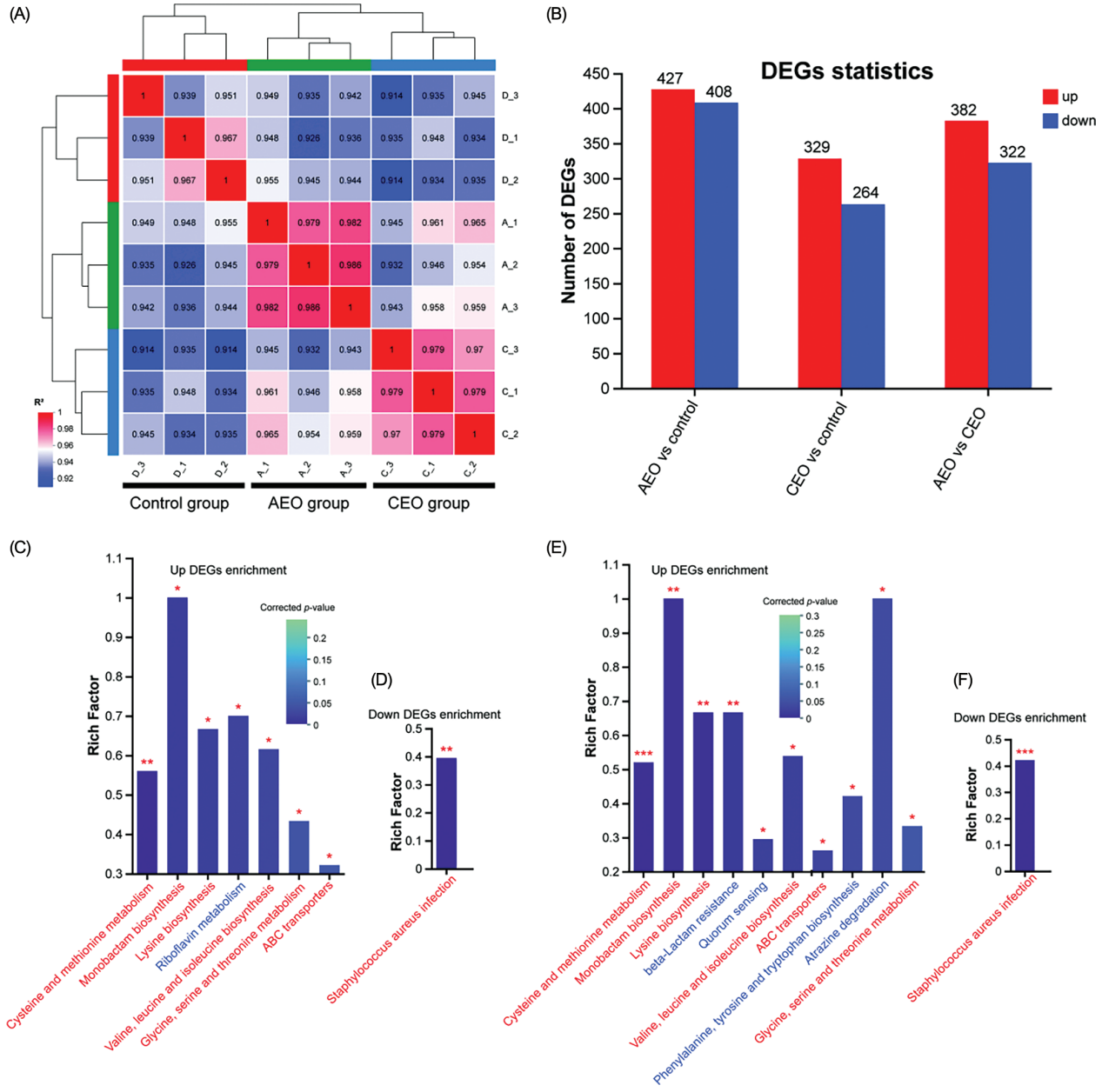

Figure 8: The biofilms of *S. aureus* exposed to AEO and CEO exhibited an altered transcriptomic profile. (A) Hierarchical clustering analysis (heat map) of DEGs in the AEO group, CEO group, and control group. (B) Statistical analysis of up-regulated and down-regulated genes between AEO group and control group, CEO group and control group, and AEO group and control group. (C) KEGG pathways of upregulated DEGs of biofilm in the AEO group. (D) KEGG pathways of downregulated DEGs of biofilm in the AEO group. (E) KEGG pathways of upregulated DEGs of biofilm in the CEO group. (F) KEGG pathways of down-regulated DEGs of biofilm in the CEO group. Pathways highlighted in blue are uniquely enriched in this group, while those in red represent shared enriched pathways between both essential oil treatment groups. *$P < 0.05$, **$P < 0.01$, ***$P < 0.001$.

and colonization of *S. aureus* (Foster *et al.*, 2020; Pant *et al.*, 2022; Roman *et al.*, 2016; Yu *et al.*, 2024a). Hence, the weakened biofilm formation ability following AEO treatment (96.3 μg/mL) could result from the concurrent downregulation of these key adhesion and virulence genes (Figures 3C and 3E).

In addition, AEO treatment significantly upregulated genes involved in amino acid biosynthesis, amino acid metabolism, and riboflavin metabolism. Amino acid and riboflavin homeostasis are known to influence biofilm formation and stability (Böttcher *et al.*, 2022; Mitra *et al.*, 2012). Therefore, these metabolic adjustments may

represent a part of the bacterial response to AEO exposure, although their specific role in the observed biofilm inhibition requires further elucidation.

Notably, a previous study proposed that AEO inhibits biofilm formation by regulating biofilm-associated programmed cell death operons and adhesin genes expression (Yan *et al*., 2025). Discrepancy between our findings and those reports may arise from differences in experimental conditions. In the current study, AEO was applied at a sub-inhibitory concentration (91.3 μg/mL; 1/8 MIC), which does not affect bacterial growth, whereas the previous study employed 0.25 mg/mL, a higher concentration that could trigger distinct stress and regulatory responses.

The CEO interferes with adhesion and quorum-sensing systems

In contrast to AEO, the CEO appears to modulate *S. aureus* biofilm formation through a distinct yet complementary network of regulatory pathways. Consistent with previous reports (Li *et al*., 2025), transcriptomic analysis revealed significant enrichment of quorum-sensing pathways following the CEO treatment, a feature absent in the AEO-treated group. This divergence potentially reflects the compositional heterogeneity of plant-derived essential oils, which influences their molecular interactions and mechanisms of action (Neagu *et al*., 2023). Similar to AEO, exposure to CEO suppressed the *S. aureus* infection pathway with *SdrC/D*, staphylococcal protein *AspA*, *fib*, *chp*, and *hlp* genes showing reduced expression in this pathway. Given the established roles of these factors in adhesion and virulence (Mamdoh *et al*., 2023), their coordinated downregulation offered a transcriptional-level insight that aligns with the observed inhibition of biofilm formation by CEO (Figures 3D and 3F). Additionally, CEO exposure enriched pathways related to amino acid biosynthesis and metabolism. However, the functional role of these metabolic shifts in regulating *S. aureus* biofilm dynamics warrants further investigation.

Comparative mechanisms and implications for food industry applications

Most prior studies have focused on the anti-biofilm effects of single essential oils, without accounting for interspecies variations in chemical composition that may alter their molecular targets and efficacy. For instance, *agrC* was previously identified as a key target gene for CEO (Li *et al*., 2025). In this study, the same *S. aureus* strain was used for both CEO- and AEO-related antimicrobial and anti-biofilm assays, thereby minimizing potential errors arising from strain variability. Through this controlled experimental design, we conducted a systematic and comparative investigation into the mechanisms of CEO and AEO against *S. aureus* biofilms. Microscopic analyses revealed comparable morphological alterations across treatments, consistent with the observed transcriptomic profiles and pathway enrichment patterns. These findings collectively demonstrated that both essential oils exert inhibitory effects on *S. aureus* biofilms, converging on specific molecular pathways, including amino acid metabolism and synthesis pathways, riboflavin metabolism pathways, and *S. aureus* infection pathway.

However, translating these findings into practical applications within the food industry remains challenging. Essential oils are highly sensitive to processing parameters, such as temperature and pH, and their antimicrobial efficacy can be influenced by interactions within complex food matrices. Therefore, developing controlled-release delivery systems, such as nanoemulsions, and assessing their effects on key sensory attributes, including color, flavor, and texture, are essential steps toward practical implementation (Dghais *et al*., 2023; Mahdi *et al*., 2023; Yu *et al*., 2024b). Moreover, conducting *in situ* or pilot-scale studies under realistic processing conditions will be crucial to validate these approaches and support the integration of essential oils into food safety management frameworks.

Conclusion

At sub-inhibitory concentrations, two structurally distinct essential oils, AEO and CEO, exhibited potent inhibitory effects on *S. aureus* biofilm formation and integrity. CLSM and SEM imaging confirmed pronounced disruption of biofilm architecture and cell adhesion. Transcriptomic analyses revealed that AEO primarily modulates amino acid biosynthesis, general metabolism, and riboflavin metabolism pathways, while CEO predominantly targets quorum-sensing system and amino acid metabolic processes. Moreover, both oils converge on a shared mechanism involving downregulation of *SdrC/D*, *isdA*, *spA*, *fib*, *chp*, and *hlp* within the *S. aureus* infection pathway, resulting in impaired bacterial adhesion, virulence, and biofilm establishment. The complementary mechanisms of action not only offer a theoretical foundation for understanding the anti-biofilm efficacy of both essential oils but also provide a scientific basis for developing combined applications or customized strategies for broad-spectrum biofilm control in the food industry.

Mandatory Disclosure on Use of Artificial Intelligence

The authors declare that Al-assisted tools were used as follows: The DeepSeek3.2 had been used to polish the language. All references have been manually verifed for accuracy and relevance.

Data Availability Statement

All data are available in this manuscript.

Author Contributions

Fenghui Sun conceived and designed the project. Guoqing Yu, Ming Chen, and Zedong Liao performed experiment. Shan Chen, Yixi Zhou, Yiwu Wen, and Keshan Lin analyzed the data. Guoqing Yu and Jialin Dai drafted the manuscript. Fenghui Sun and Min Dai modified the manuscript. All authors contributed to the article and approved the submitted version.

Conflict of Interest

The authors declared that the research was conducted in the absence of any commercial or financial relationships that could be construed as a potential conflict of interest.

Funding

This study was supported by the National Natural Science Foundation of China (82102442, 32270449, and 82472328), the Sichuan Science and Technology Program (2025YFHZ0215 and 2024YFFK0090), the CMC Excellent-Talent Program (2024yxGzn06), the Open Fund of Development and Regeneration Key Laboratory of Sichuan Province (24LHFYSZ1-36), the Open Fund of Sichuan Provincial Engineering Laboratory for Prevention and Control Technology of Veterinary Drug Residue in Animal-Origin (23LHNBZZD01), the Health Commission of Sichuan Province Medical Science and Technology Program (24WSXT036), and the Sichuan College Students' Innovation and Entrepreneurship Training Program (S202213705051).

References

Alabdullatif, M. and Alzahrani, A. 2022. Expression of biofilm-associated genes in Staphylococcus aureus during storage of platelet concentrates. Transfusion and Apheresis Science 61(6): 103456. https://doi.org/10.1016/j.transci.2022.103456

Almeida, L., Lopes, N., Gaio, V., Cavaleiro, C., Salgueiro, L., Silva, V., Poeta, P. and Cerca, N. 2022. Thymbra capitata essential oil has a significant antimicrobial activity against methicillin-resistant *Staphylococcus aureus* pre-formed biofilms. Letters in Applied Microbiology 74(5): 787–795. https://doi.org/10.1111/lam.13665

Arciola, C.R., Campoccia, D. and Montanaro, L. 2018. Implant infections: adhesion, biofilm formation and immune evasion. Nature Reviews Microbiology 16(7): 397–409. https://doi.org/10.1038/s41579-018-0019-y

Aziz, Z. A. A., Ahmad, A., Setapar, S.H.M., Karakucuk, A., Azim, M.M., Lokhat, D., Rafatullah, M., Ganash, M., Kamal, M.A. and Ashraf, G.M. 2018. Essential oils: extraction techniques, pharmaceutical and therapeutic potential—a review. Current Drug Metabolism 19(13): 1100–1110. https://doi.org/10.2174/1389200219666180723144850

Böttcher, B., Driesch, D., Krüger, T., Garbe, E., Gerwien, F., Kniemeyer, O., Brakhage, A.A. and Vylkova, S. 2022. Impaired amino acid uptake leads to global metabolic imbalance of *Candida albicans* biofilms. NPJ Biofilms and Microbiomes 8: 78. https://doi.org/10.1038/s41522-022-00341-9

Cascioferro, S., Carbone, D., Parrino, B., Pecoraro, C., Giovannetti, E., Cirrincione, G. and Diana, P. 2021. Therapeutic strategies to counteract antibiotic resistance in MRSA biofilm-associated infections. ChemMedChem 16(1): 65–80. https://doi.org/10.1002/cmdc.202000677

Chen, J.W., Chen, J.L., Wang, Z.W., Chen, C.C., Zheng, J.X., Yu, Z.J., Deng, Q.W., Zhao, Y.X. and Wen, Z.W. 2022. 20S-ginsenoside Rg3 inhibits the biofilm formation and haemolytic activity of *Staphylococcus aureus* by inhibiting the SaeR/SaeS two-component system. Journal of Medical Microbiology 71(10): 001587 https://doi.org/10.1099/jmm.0.001587

Chen, L., Tang, Z.Y., Cui, S.Y., Ma, Z.B., Deng, H., Kong, W.L., Yang, L.W., Lin, C., Xiong, W.G. and Zeng, Z.L. 2020. Biofilm production ability, virulence and antimicrobial resistance genes in *Staphylococcus aureus* from various veterinary hospitals. Pathogens (Basel, Switzerland) 9(4): 264. https://doi.org/10.3390/pathogens9040264

Chung, D.R. and Huh, K. 2015. Novel pandemic influenza A (H1N1) and community-associated methicillin-resistant *Staphylococcus aureus* pneumonia. Expert Review of Anti-Infective Therapy 13(2): 197–207. https://doi.org/10.1586/14787210.2015.999668

Dai, M., Peng, C., Peng, F., Xie, C.B., Wang, P.J. and Sun, F.H. 2016a. Anti-*Trichomonas vaginalis* properties of the oil of Amomum tsao-ko and its major component, geraniol. Pharmaceutical Biology 54(3): 445–450. https://doi.org/10.3109/13880209.2015.1044617

Dai, M., Peng, C. and Sun, F.H. 2016b. Anti-infectious efficacy of essential oil from Caoguo (*Fructus tsaoko*). Journal of Traditional Chinese Medicine (Chung I Tsa Chih Ying Wen Pan) 36(6): 799–804. https://doi.org/10.1016/s0254-6272(17)30018-3

Dghais, S., Ben Jemaa, M., Chouchen, M., Jallouli, S., Ksouri, R. and Falleh, H. 2023. Nano-emulsification of cinnamon and curcuma essential oils for the quality improvement of minced meat beef. Foods (Basel, Switzerland) 12(2): 235. https://doi.org/10.3390/foods12020235

Elbestawy, M.K.M., El-Sherbiny, G.M. and Moghannem, S.A. 2023. Antibacterial, antibiofilm and anti-inflammatory activities of eugenol clove essential oil against resistant *Helicobacter pylori*. Molecules (Basel, Switzerland) 28(6): 2448. https://doi.org/10.3390/molecules28062448

Ersanli, C., Tzora, A., Skoufos, I., Fotou, K., Maloupa, E., Grigoriadou, K., Voidarou, C.C. and Zeugolis, D.I. 2023. The assessment of antimicrobial and anti-biofilm activity of essential oils against *Staphylococcus aureus* strains. Antibiotics (Basel, Switzerland) 12(2): 384. https://doi.org/10.3390/antibiotics12020384

Foster, C.E., Kok, M., Flores, A.R., Minard, C.G., Luna, R.A., Lamberth, L.B., Kaplan, S.L. and Hulten, K.G. 2020. Adhesin genes and biofilm formation among pediatric *Staphylococcus aureus* isolates from implant-associated infections. PloS One 15(6): e0235115. https://doi.org/10.1371/journal.pone.0235115

Gao, K.K., Su, B., Dai, J., Li, P., Wang, R.M. and Yang, X.H. 2022. Anti-biofilm and anti-hemolysis activities of 10-hydroxy-2-decenoic acid against *Staphylococcus aureus*. Molecules 27(5): 1485. https://doi.org/10.3390/molecules27051485

Guo, N., Bai, X., Shen, Y. and Zhang, T.H., 2023. Target-based screening for natural products against *Staphylococcus aureus* biofilms. Critical Reviews in Food Science and Nutrition 63(14): 2216–2230. https://doi.org/10.1080/10408398.2021.1972280

Hatlen, T.J. and Miller, L.G., 2021. Staphylococcal skin and soft tissue infections. Infectious Disease Clinics of North America 35(1): 81–105. https://doi.org/10.1016/j.idc.2020.10.003

He, Y.X., Yuan, Y., Gao, Y.Y., Chen, M.H., Li, Y.Y., Zou, Y., Liao, L.K., Li, X.T., Wang, Z., Li, J.H. and Zhou, W. 2024. Enhancement of colorimetric pH-sensitive film incorporating Amomum tsao-ko essential oil as antibacterial for mantis shrimp spoilage tracking and fresh-keeping. Foods (Basel, Switzerland) 13(11): 1638. https://doi.org/10.3390/foods13111638

Hernández-Cuellar, E., Tsuchiya, K., Valle-Ríos, R. and Medina-Contreras, O. 2023. Differences in biofilm formation by methicillin-resistant and methicillin-susceptible *Staphylococcus aureus* strains. Diseases 11(4): 160. https://doi.org/10.3390/diseases11040160

Khatoon, Z., McTiernan, C.D., Suuronen, E.J., Mah, T.-F. and Alarcon, E.I. 2018. Bacterial biofilm formation on implantable devices and approaches to its treatment and prevention. Heliyon 4(12): e01067. https://doi.org/10.1016/j.heliyon.2018.e01067

Kim, M.-S., Ahn, E.-K., Hong, S.S. and Oh, J.S. 2016. 2,8-Decadiene-1,10-diol inhibits lipopolysaccharide-induced inflammatory responses through inactivation of mitogen-activated protein kinase and nuclear factor-κB signaling pathway. Inflammation 39(2): 583–591. https://doi.org/10.1007/s10753-015-0283-1

Kim, D., Paggi, J.M., Park, C., Bennett, C. and Salzberg, S.L. 2019. Graph-based genome alignment and genotyping with HISAT2 and HISAT genotype. Nature Biotechnology 37(8): 907–915. https://doi.org/10.1038/s41587-019-0201-4

Klinger-Strobel, M., Stein, C., Forstner, C., Makarewicz, O. and Pletz, M.W., 2017. Effects of colistin on biofilm matrices of Escherichia coli and *Staphylococcus aureus*. International Journal of Antimicrobial Agents 49(4): 472–479. https://doi.org/10.1016/j.ijantimicag.2017.01.005

Lee, S.Y., Shetye, G.S., Son, S.-R., Lee, H., Klein, L.L., Yoshihara, J.K., Ma, R., Franzblau, S.G., Cho, S. and Jang, D.S. 2022. Anti-microbial activity of aliphatic alcohols from Chinese black cardamom (Amomum tsao-ko) against Mycobacterium tuberculosis H37Rv. Plants (Basel, Switzerland) 12(1): 34. https://doi.org/10.1016/j.ijantimicag.2017.01.005

Li, H., Li, J., Hua, Z.C., Aziz, T., Khojah, E., Cui, H.Y. and Lin, L. 2025. Transcriptomic combined with molecular dynamics simulation analysis of the inhibitory mechanism of clove essential oil against *Staphylococcus aureus* biofilm and its application on surface of food contact materials. Food and Bioproducts Processing 150: 131–140. https://doi.org/10.1016/j.fbp.2025.01.009

Li, W.D., Li, J.J., Qin, Z., Wang, Y., Zhao, P.Y. and Gao, H.Y. 2022a. Insights into the composition and antibacterial activity of Amomum tsao-ko essential oils from different regions based on GC-MS and GC-IMS. Foods 11(10): 1402. https://doi.org/10.3390/foods11101402

Li, J., Li, C., Shi, C., Aliakbarlu, J., Cui, H. and Lin, L. 2022b. Antibacterial mechanisms of clove essential oil against *Staphylococcus aureus* and its application in pork. International Journal of Food Microbiology 380: 109864. https://doi.org/10.1016/j.ijfoodmicro.2022.109864

Liñán-Atero, R., Aghababaei, F., García, S.R., Hasiri, Z., Ziogkas, D., Moreno, A. and Hadidi, M. 2024. Clove essential oil: chemical profile, biological activities, encapsulation strategies, and food applications. Antioxidants (Basel, Switzerland) 13(4): 488. https://doi.org/10.3390/antiox13040488

Liu, M., Wu, X., Li, J., Liu, L., Zhang, R., Shao, D. and Du, X. 2017. The specific anti-biofilm effect of gallic acid on *Staphylococcus aureus* by regulating the expression of the ica operon. Food Control 73: 613–618. https://doi.org/10.1016/j.foodcont.2016.09.015

Qian, W., Liu, M., Fu, Y., Zhang, J., Liu, W., Li, J., Li, X., Li, Y., and Wang, T. 2020. Antimicrobial mechanism of luteolin against *Staphylococcus aureus* and *Listeria monocytogenes* and its antibiofilm properties. Microbial pathogenesis, 142, 104056. https://doi.org/10.1016/j.micpath.2020.104056

Mahdi, A.A., Al-Maqtari, Q.A., Al-Ansi, W., Hu, W., Hashim, S.B.H., Cui, H.Y. and Lin, L. 2023. Replacement of polyethylene oxide by peach gum to produce an active film using *Litsea cubeba* essential oil and its application in beef. International Journal of Biological Macromolecules 241: 124592. https://doi.org/10.1016/j.ijbiomac.2023.124592

Mahmoudi, H., Pourhajibagher, M., Chiniforush, N., Soltanian, A.R., Alikhani, M.Y. and Bahador, A. 2019. Biofilm formation and antibiotic resistance in meticillin-resistant and meticillin-sensitive *Staphylococcus aureus* isolated from burns. Journal of Wound Care 28(2): 66–73. https://doi.org/10.12968/jowc.2019.28.2.66

Mamdoh, H., Hassanein, K.M., Eltoony, L.F., Khalifa, W.A., Hamed, E., Alshammari, T.O., Abd El-Kareem, D.M. and El-Mokhtar, M.A. 2023. Clinical and bacteriological analyses of biofilm-forming *Staphylococci*-isolated from diabetic foot ulcers. Infection and Drug Resistance 16: 1737–1750. https://doi.org/10.2147/IDR.S393724

Melander, R.J., Basak, A.K. and Melander, C. 2020. Natural products as inspiration for the development of bacterial antibiofilm agents. Natural Product Reports 37(11): 1454–1477. https://doi.org/10.1039/d0np00022a

Mitra, S., Thawrani, D., Banerjee, P., Gachhui, R. and Mukherjee, J. 2012. Induced biofilm cultivation enhances riboflavin production by an intertidally derived *Candida famata*. Applied Biochemistry and Biotechnology 166(8): 1991–2006. https://doi.org/10.1007/s12010-012-9626-7

Mohammadi Pelarti, S., Karimi Zarehshuran, L., Babaeekhou, L. and Ghane, M. 2021. Antibacterial, anti-biofilm and anti-quorum sensing activities of *Artemisia dracunculus* essential oil (EO): a study against *Salmonella enterica* serovar Typhimurium and *Staphylococcus aureus*. Archives of Microbiology 203(4): 1529–1537. https://doi.org/10.1007/s00203-020-02138-w

Neagu, R., Popovici, V., Ionescu, L.E., Ordeanu, V., Popescu, D.M., Ozon, E.A. and Gîrd, C.E. 2023. Antibacterial and antibiofilm effects of different samples of five commercially available essential oils. Antibiotics (Basel, Switzerland) 12(7): 1191. https://doi.org/10.3390/antibiotics12071191

Pant, N., Miranda-Hernandez, S., Rush, C., Warner, J. and Eisen, D.P. 2022. Non-antimicrobial adjuvant therapy using ticagrelor reduced biofilm-related *Staphylococcus aureus* prosthetic joint infection. Frontiers in Pharmacology 13: 927783. https://doi.org/10.3389/fphar.2022.927783

Pedonese, F., Longo, E., Torracca, B., Najar, B., Fratini, F. and Nuvoloni, R. 2022. Antimicrobial and anti-biofilm activity of manuka essential oil against Listeria monocytogenes and *Staphylococcus aureus* of food origin. Italian Journal of Food Safety 11(1): 10039. https://doi.org/10.4081/ijfs.2022.10039

Piechota, M., Kot, B., Frankowska-Maciejewska, A., Grużewska, A. and Woźniak-Kosek, A. 2018. Biofilm formation by methicillin-resistant and methicillin-sensitive *Staphylococcus aureus* strains from hospitalized patients in Poland. BioMed Research International 2018: 4657396. https://doi.org/10.1155/2018/4657396

Pires, D.P., Meneses, L., Brandão, A.C. and Azeredo, J. 2022. An overview of the current state of phage therapy for the treatment of biofilm-related infections. Current Opinion in Virology 53: 101209. https://doi.org/10.1016/j.coviro.2022.101209

Qiu, M., Long, N.N., Gao, M.X., Zhou, Y.Y., Sun, F.H., Lin, L. and Dai, M. 2019. In vitro anti-MRSA effect of clove oil combined with β-lactam antibiotics against methicillin-resistant *Staphylococcus aureus*. Chinese Herbal Medicines 50(7): 1629–1635. https://doi.org/10.7501/j.issn.0253-2670.2019.07.020

Quinn, T.P., Crowley, T.M. and Richardson, M.F. 2018. Benchmarking differential expression analysis tools for RNA-Seq: normalization-based vs. log-ratio transformation-based methods. BMC Bioinformatics 19(1): 274. https://doi.org/10.1186/s12859-018-2261-8

Rahimi, F., Katouli, M. and Karimi, S. 2016. Biofilm production among methicillin resistant *Staphylococcus aureus* strains isolated from catheterized patients with urinary tract infection. Microbial Pathogenesis 98: 69–76. https://doi.org/10.1016/j.micpath.2016.06.031

Rahman, M.R.T., Lou, Z., Yu, F., Wang, P. and Wang, H. 2017. Anti-quorum sensing and anti-biofilm activity of *Amomum tsaoko* (*Amommum tsao-ko* Crevost et Lemarie) on foodborne pathogens. Saudi Journal of Biological Sciences 24(2): 324–330. https://doi.org/10.1016/j.sjbs.2015.09.034

Rather, M.A., Gupta, K. and Mandal, M. 2021. Microbial biofilm: formation, architecture, antibiotic resistance, and control strategies. Brazilian Journal of Microbiology 52(4): 1701–1718. https://doi.org/10.1007/s42770-021-00624-x

Reis, S.V.D., Couto, N.M. G. de, Brust, F.R., Trentin, D.S., Silva, J.K.R. da, Arruda, M.S.P., Gnoatto, S.C.B. and Macedo, A.J. 2020. Remarkable capacity of Brosimine B to disrupt methicillin-resistant *Staphylococcus aureus* (MRSA) preformed biofilms. Microbial Pathogenesis 140: 103967. https://doi.org/10.1016/j.micpath.2020.103967

Ridyard, K.E. and Overhage, J. 2021. The potential of human peptide LL-37 as an antimicrobial and anti-biofilm agent. Antibiotics (Basel, Switzerland) 10(6): 650. https://doi.org/10.3390/antibiotics10060650

Roman, A.Y., Devred, F., Lobatchov, V.M., Makarov, A.A., Peyrot, V., Kubatiev, A.A. and Tsvetkov, P.O. 2016. Sequential binding of calcium ions to the B-repeat domain of SdrD from *Staphylococcus aureus*. Canadian Journal of Microbiology 62(2): 123–129. https://doi.org/10.1139/cjm-2015-0580

Silva, V., Almeida, L., Gaio, V., Cerca, N., Manageiro, V., Caniça, M., Capelo, J.L., Igrejas, G. and Poeta, P. 2021. Biofilm formation of multidrug-resistant MRSA strains isolated from different types of human infections. Pathogens (Basel, Switzerland) 10(8): 970. https://doi.org/10.3390/pathogens10080970

Somrani, M., Debbabi, H. and Palop, A. 2022. Antibacterial and antibiofilm activity of essential oil of clove against Listeria monocytogenes and *Salmonella enteritidis*. Food Science and Technology International (Ciencia Y Tecnologia De Los Alimentos Internacional) 28(4): 331–339. https://doi.org/10.1177/10820132211013273

Sultan, A.R., Swierstra, J.W., Lemmens-den Toom, N.A., Snijders, S.V., Hansenová Maňásková, S., Verbon, A. and van Wamel, W.J.B. 2018. Production of staphylococcal complement inhibitor (SCIN) and other immune modulators during the early stages of *Staphylococcus aureus* biofilm formation in a mammalian cell culture medium. Infection and Immunity 86(8): e00352-18. https://doi.org/10.1128/IAI.00352-18

Swearingen, M.C., Granger, J.F., Sullivan, A. and Stoodley, P. 2016. Elution of antibiotics from poly (methyl methacrylate) bone cement after extended implantation does not necessarily clear the infection despite susceptibility of the clinical isolates. Pathogens and Disease 74(1): ftv103. https://doi.org/10.1093/femspd/ftv103

Tong, S.Y.C., Davis, J.S., Eichenberger, E., Holland, T.L. and Fowler, V.G. 2015. *Staphylococcus aureus* infections: epidemiology, pathophysiology, clinical manifestations, and management. Clinical Microbiology Reviews 28(3): 603–661. https://doi.org/10.1128/CMR.00134-14

Valarezo, E., Ledesma-Monteros, G., Jaramillo-Fierro, X., Radice, M. and Meneses, M.A. 2025. Antioxidant application of clove (*Syzygium aromaticum*) essential oil in meat and meat products: a systematic review. Plants 14(13): 1958. https://doi.org/10.3390/plants14131958

Vasile, C., Sivertsvik, M., Miteluț, A.C., Brebu, M.A., Stoleru, E., Rosnes, J.T., Tănase, E.E., Khan, W., Pamfil, D., Cornea, C.P., Irimia, A. and Popa, M.E. 2017. Comparative analysis of the composition and active property evaluation of certain essential oils to assess their potential applications in active food packaging. Materials 10(1): 45. https://doi.org/10.3390/ma10010045

Vergara, A., Normanno, G., Di Ciccio, P., Pedonese, F., Nuvoloni, R., Parisi, A., Santagada, G., Colagiorgi, A., Zanardi, E., Ghidini, S. and Ianieri, A. 2017. Biofilm formation and its relationship with the molecular characteristics of food-related methicillin-resistant *Staphylococcus aureus* (MRSA). Journal of Food Science 82(10): 2364–2370. https://doi.org/10.1111/1750-3841.13846

Xie, L.B., Yu, D., Li, Y.N., Ju, H.D., Chen, J., Hu, L.X. and Yu, L.Q. 2022. Characterization, hypoglycemic activity, and antioxidant activity of methanol extracts from Amomum tsao-ko: *in vitro* and *in vivo* studies. Frontiers in Nutrition 9: 869749. https://doi.org/10.3389/fnut.2022.869749

Yan, Z.F., Guo, J.R., Chen, Q.M., Wan, S.B., Qin, Z. and Gao, H.Y. 2025. Antibiofilm activity of Amomum tsaoko essential oil on *Staphylococcus aureus* and its application in pork preservation. Foods (Basel, Switzerland) 14(4): 662. https://doi.org/10.3390/foods14040662

Yanakiev, S. 2020. Effects of cinnamon (Cinnamomum spp.) in dentistry: a review. Molecules (Basel, Switzerland) 25(18): 4184. https://doi.org/10.3390/molecules25184184

Yin, W., Wang, Y.T., Liu, L. and He, J. 2019. Biofilms: the microbial "protective clothing" in extreme environments. International Journal of Molecular Sciences 20(14): 3423. https://doi.org/10.3390/ijms20143423

Yu, J.Y., Han, W.H., Xu, Y.L., Shen, L., Zhao, H.L., Zhang, J., Xiao, Y.H., Guo, Y.J. and Yu, F.Y. 2024a. Biofilm-producing ability of methicillin-resistant *Staphylococcus aureus* clinically isolated in China. BMC Microbiology 24: 241. https://doi.org/10.1186/s12866-024-03380-8

Yu, X.H., Hu, E.H., Liu, F.Y., Zhang, Y., Li, W.W., Lyu, Y.M., Li, F.W., Wang, D.J. and Jin, W.B. 2024b. Preparation and characterization of polyphenol-chitosan conjugate-eugenol essential oil microcapsule and its effect on storage behavior of cherry tomato. Journal of Food Science 89(12): 9577–9594. https://doi.org/10.1111/1750-3841.17524

Zhang, T.-T., Lu, C.-L. and Jiang, J.-G. 2015. Antioxidant and anti-tumour evaluation of compounds identified from fruit of *Amomum tsaoko* Crevost et Lemaire. Journal of Functional Foods 18: 423–431. https://doi.org/10.1016/j.jff.2015.08.005

Supplementary Material

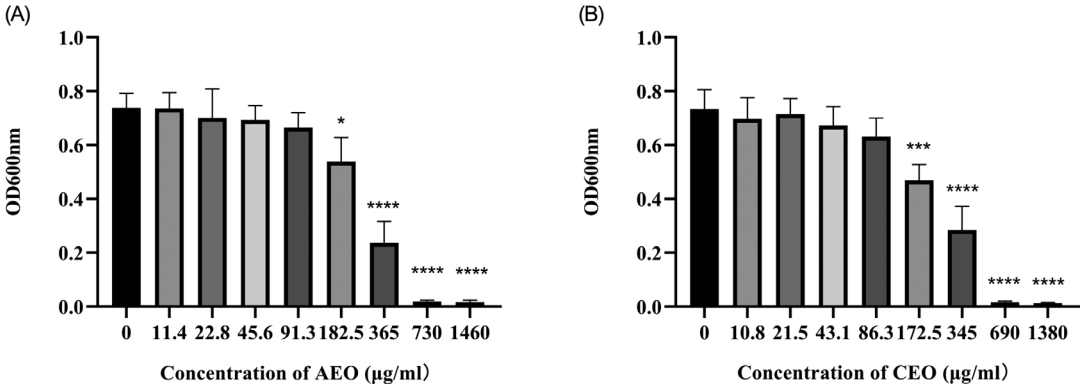

Figure S1. Effect of (A) AEO and (B) CEO on the growth of *S. aureus* NCTC8325; **P* < 0.05, ****P* < 0.001, *****P* < 0.0001.

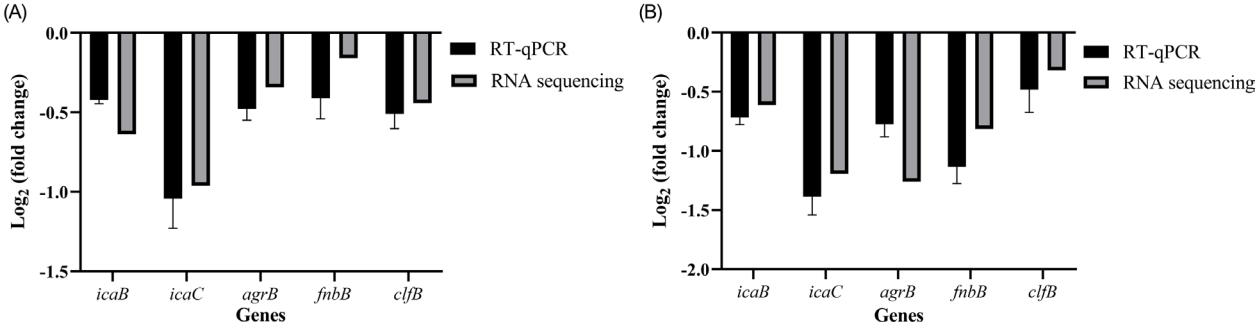

Figure S2. Expression of DEGs with (A) AEO treaded and (B) CEO treaded as verified by qRT-PCR. The resulting data were derived from the average of three independent replicates.

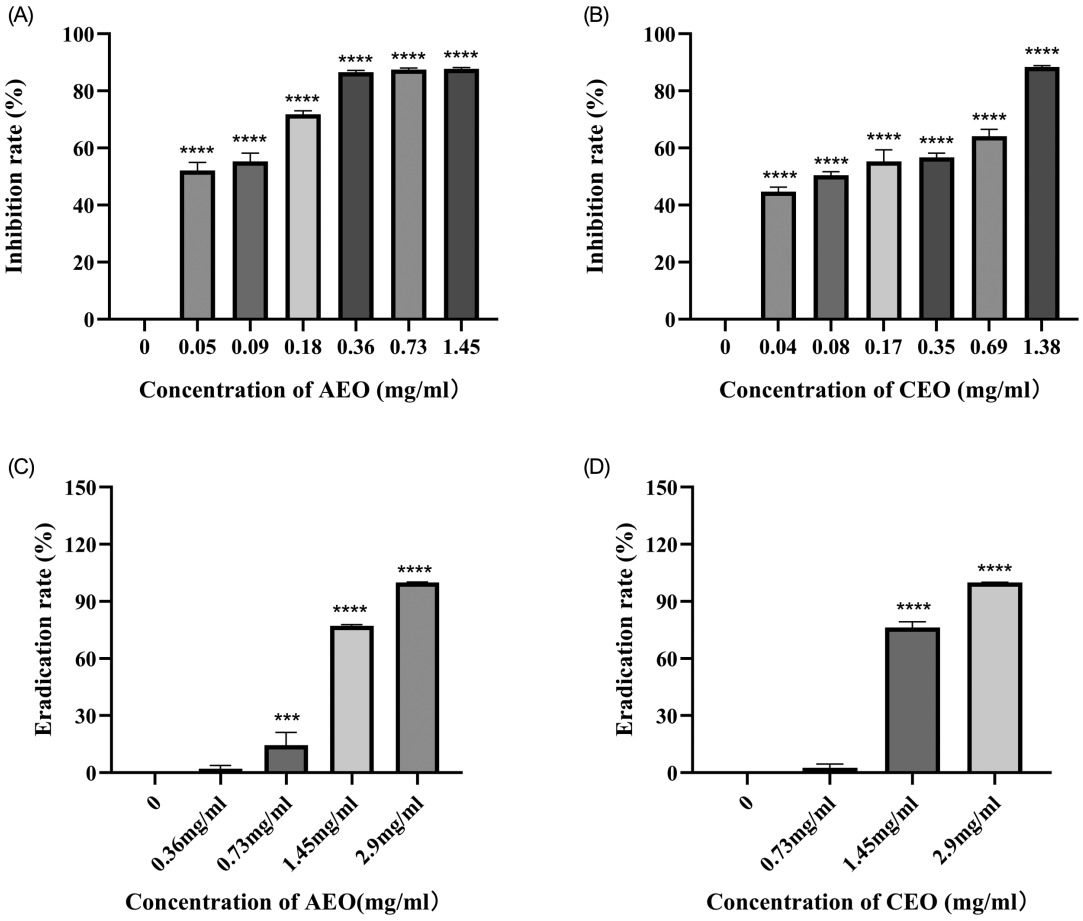

Figure S3. The inhibitory and eradication effect of different concentrations of (A and C) AEO and (B and D) CEO on biofilm formation of *S. aureus* ATCC43300; ***$P < 0.001$, ****$P < 0.0001$.

Table S1. List of primers used for quantitative real-time PCR analysis.

Gene	Forward primer (5'→3')	Reverse primer (5'→3')
Tpi	CGTTGTTATCGGTCATTCT	TTACCACTTTCACGCTCTT
icaC	GAGCAATGTTGTGTATTATCATTA	GTCTAAGATCATCGCCATCAA
icaB	ATGGTCAAGCCCAGACAGAG	AGTATTTTCAATGTTTAAAGCA
agrB	ATTGACCAGTTCGCCACG	AGCTAAGACCTGCATCCC
fnbB	TTCTCCATTGGCGGCTCTG	CTCAGGGCGACGGTAAAGA
clfB	ATTTGGGATAGGCAATCATCA	TTCGGAATCTGCACTTGC

Table S2. The DEGs of biofilm in AEO treatment group and control group of *S. aureus* NCTC8325.

gene_id	gene_name	log_2(FC)	*p*.adjust
SAOUHSC_02892	——	4.9812973627227	1.2616085922635E-155
SAOUHSC_02460	——	4.3088781511459	4.0635963128018E-92
SAOUHSC_02640	hrtA	–3.802970628	4.0640919448465E-59
SAOUHSC_02873	copA	3.7046325222782	8.8688713861986E-56
SAOUHSC_02641	hrtB	–5.343341594	7.5528083913832E-50
SAOUHSC_02893	——	4.5552888598952	1.5652210469833E-34
SAOUHSC_00812	clfA	1.9504973458514	1.5146165396167E-33
SAOUHSC_02848	ptsG	2.0772464277297	1.6801475083043E-33
SAOUHSC_00142	——	–2.776732187	6.0683623075041E-32
SAOUHSC_03033	hoxN	2.2237163741004	4.784610999134E-29
SAOUHSC_00061	ohyA	1.9464333783259	9.0513878172858E-29
SAOUHSC_02814	——	1.7126741408113	5.4075165665171E-28
SAOUHSC_02829	——	1.8343579907581	1.3209478387551E-26
SAOUHSC_02098	vraR	2.1686262969553	6.9602914668914E-26
SAOUHSC_02590	——	1.5997556678808	1.2922178905178E-25
SAOUHSC_02381	dps	–1.765520514	7.1420756252086E-25
SAOUHSC_00181	——	2.6794894898484	9.4426265439069E-25
SAOUHSC_00581	rclA	1.7225969808557	5.8042746405277E-24
SAOUHSC_02813	——	1.6827511424034	2.7368026752143E-23
SAOUHSC_02828	catE	2.1740963078149	6.2923184432628E-23
SAOUHSC_01235	pyrH	–1.765205942	1.6658831257075E-22
SAOUHSC_02597	glvC	1.7242782443076	7.2253258636296E-22
SAOUHSC_00582	——	1.5474379567862	1.0526395335E-21
SAOUHSC_02243	hlg	–1.947125352	3.3099765805128E-21
SAOUHSC_02874	copZ	2.9507060405206	3.8500292210671E-21
SAOUHSC_02812	——	1.5500213138257	4.7703423953641E-21
SAOUHSC_00180	——	3.0520024220722	5.5174893289492E-21
SAOUHSC_00155	ptsG	1.6034774005267	2.9861509000346E-18
SAOUHSC_00160	——	3.1908779837242	1.026674599099E-17
SAOUHSC_00179	——	2.4668264181715	6.2798263854998E-17
SAOUHSC_00320	ssuE	1.9733539708746	8.7066059838313E-17
SAOUHSC_02706	sbi	–2.442659459	8.7066059838313E-17
SAOUHSC_02923	——	2.4712156535685	1.158293276562E-16
SAOUHSC_01945	epiG	1.3234239223971	1.2845502829073E-16
SAOUHSC_01918	——	0.99828261499905	7.2775550161543E-16
SAOUHSC_02108	ftnA	–1.699417059	2.9629155700788E-15
SAOUHSC_02988	asp1	1.3463898104289	3.4353765625306E-15
SAOUHSC_02729	cycA	1.5559741490099	4.9707304251896E-15
SAOUHSC_00319	——	1.874663933	5.496095540563E-15
SAOUHSC_01266	korA	–1.469714042	5.9062918122696E-15
SAOUHSC_00529	fusA	0.98102644445459	9.8277066240848E-15
SAOUHSC_02241	hlg	–1.595043198	9.8958318563622E-15
SAOUHSC_00604	——	1.9512631866334	9.8958318563622E-15
SAOUHSC_01728	——	1.9382876212222	1.2880474785413E-14
SAOUHSC_02708	hlg	–2.399305887	1.2880474785413E-14
SAOUHSC_00382	——	1.2478572104542	1.8657591064733E-14

(continues)

Table S2. Continued.

gene_id	gene_name	log_2(FC)	*p*.adjust
SAOUHSC_01034	trkA	1.420742469	2.2024057841483E-14
SAOUHSC_01702	mtnN	–1.318316913	3.1402195072145E-14
SAOUHSC_02360	tdk	–1.578232195	4.214817143322E-14
SAOUHSC_00158	scrA	2.1032959204232	4.3044357105817E-14
SAOUHSC_01193	fakA	–1.530285043	4.4783265237087E-14
SAOUHSC_00141	——	–1.221573595	8.0510472678167E-14
SAOUHSC_02830	ldhA	1.6720397734479	4.0050713272812E-13
SAOUHSC_00027	rlmH	–1.222058769	8.6264149062115E-13
SAOUHSC_00178	ganQ	1.7916760822216	9.4897681399537E-13
SAOUHSC_00455	——	–1.171123493	9.9980433614548E-13
SAOUHSC_03019	ecfA	2.1454054116014	9.9980433614548E-13
SAOUHSC_02709	hlg	–1.833758745	1.1157515919315E-12
SAOUHSC_00195	fadA	2.5327815633557	4.0870893121845E-12
SAOUHSC_00499	pdxS	–1.259035745	4.1951724798027E-12
SAOUHSC_02912	phnB	1.3366145663388	5.2304711259553E-12
SAOUHSC_02430	fecB	–1.73556977	6.2890726506754E-12
SAOUHSC_02809	gntR	–1.170405289	8.6425682610342E-12
SAOUHSC_00376	——	–1.518739649	9.0181387320184E-12
SAOUHSC_00613	——	–1.254862483	1.7348077595516E-11
SAOUHSC_01124	——	1.4259904693141	1.8894742973471E-11
SAOUHSC_02862	clpL	1.035932333	2.5098246075334E-11
SAOUHSC_02383	——	–0.797197675	2.5098246075334E-11
SAOUHSC_01606	pepT	0.99514006311724	2.6142711138323E-11
SAOUHSC_01232	rpsB	–1.388009815	2.6810271362762E-11
SAOUHSC_00025	——	–1.22589015	3.100909907834E-11
SAOUHSC_00241	rbsU	–1.240644312	4.9906066867976E-11
SAOUHSC_01649	gluP	–1.206044898	5.0079867959024E-11
SAOUHSC_02113	rumA	1.2370441711399	5.265572569033E-11
SAOUHSC_01919	——	1.1247891229871	6.0647277378333E-11
SAOUHSC_03020	mtsT	2.259395698	6.2691437423439E-11
SAOUHSC_02888	——	2.4263129659648	6.474307291851E-11
SAOUHSC_02987	asp2	1.323870398	1.7161204413649E-10
SAOUHSC_00300	lip	–1.292588319	1.7583005839364E-10
SAOUHSC_01858	——	–1.055156142	1.7595153199587E-10
SAOUHSC_01236	frr	–1.182659004	1.9606554694871E-10
SAOUHSC_01254	——	–1.393000099	2.1797132605756E-10
SAOUHSC_01164	pyrR	–1.805457824	2.2062978734976E-10
SAOUHSC_00533	hchA	1.4873791633483	2.2062978734976E-10
SAOUHSC_00663	——	1.1139905366169	2.4610790920879E-10
SAOUHSC_02990	——	1.3362510095864	2.5760445725243E-10
SAOUHSC_01859	——	–1.275889022	2.8354546903252E-10
SAOUHSC_01192	——	–1.274045354	3.8189640612085E-10
SAOUHSC_00132	——	1.4753222348554	3.8657717496224E-10
SAOUHSC_01114	fib	–1.498428693	4.2421785279374E-10
SAOUHSC_00426	metQ	1.5752537889927	4.4565637500655E-10
SAOUHSC_00067	lutP	–1.28887147	4.8942336691147E-10

(continues)

Table S2. Continued.

gene_id	gene_name	log_2(FC)	*p*.adjust
SAOUHSC_02100	——	1.6472645325183	5.1145382363507E-10
SAOUHSC_03021	——	2.3273293795204	6.5724252540792E-10
SAOUHSC_01886	ribH	1.723885463	6.9079718432259E-10
SAOUHSC_01504	fer	–1.299446587	1.1032913893406E-9
SAOUHSC_02768	cntM	–1.940415404	1.4096457981998E-9
SAOUHSC_00192	——	–2.413024215	2.2558610442588E-9
SAOUHSC_01432	msrA	1.2146134167572	2.9147976683669E-9
SAOUHSC_02359	prfA	–0.943236478	3.1272889685367E-9
SAOUHSC_02924	puuE	2.0361999715529	3.694901236947E-9
SAOUHSC_00607	——	1.3498000335602	3.771413652202E-9
SAOUHSC_00632	mnhG	1.1895665442637	3.771413652202E-9
SAOUHSC_00459	rsmI	–1.410040089	3.9536175731927E-9
SAOUHSC_01701	yqeG	–1.051285728	4.9361794638529E-9
SAOUHSC_02820	——	–1.149959723	5.8859743247679E-9
SAOUHSC_02285	leuA	2.1654765817252	7.2285260357645E-9
SAOUHSC_00457	——	–1.30154422	8.206123139465E-9
SAOUHSC_00893	——	1.3005406653973	1.0347826711068E-8
SAOUHSC_00318	——	1.5054162525125	1.0495589131075E-8
SAOUHSC_01949	nisP	1.4829090114814	1.4610343233936E-8
SAOUHSC_02373	ldmS	1.2307060790119	1.5920987724187E-8
SAOUHSC_01395	asd	1.1603445212256	1.6810977264395E-8
SAOUHSC_01018	purD	1.9163346374657	1.9030494576351E-8
SAOUHSC_02860	——	0.73810713423523	1.9075843252861E-8
SAOUHSC_00962	——	2.1389244576378	1.9201157740704E-8
SAOUHSC_02872	——	1.5719624107855	2.072812127203E-8
SAOUHSC_00898	argH	1.7048556847569	2.1823482062348E-8
SAOUHSC_01901	talB	1.2118681053043	2.255409886267E-8
SAOUHSC_02769	cntL	–1.649501546	2.2784901193307E-8
SAOUHSC_01327	katE	1.5196840670131	2.3149946552756E-8
SAOUHSC_00196	fadN	2.6667686786359	2.3868296785886E-8
SAOUHSC_01394	lysC	1.4490292291064	2.4340848426802E-8
SAOUHSC_01267	korB	–1.102606279	2.6636879473733E-8
SAOUHSC_01242	rimP	–1.165504439	2.9040227108662E-8
SAOUHSC_00310	ulaA	2.0372618210809	3.2136711542147E-8
SAOUHSC_00693	cydC	1.0624026473719	3.3507308447202E-8
SAOUHSC_02550	fdhD	1.2458242731354	3.4476937519686E-8
SAOUHSC_02762	——	1.0985457269613	3.5017827159239E-8
SAOUHSC_02864	feoB	1.3210412975431	3.5017827159239E-8
SAOUHSC_01501	——	0.91384852764912	4.5173598531215E-8
SAOUHSC_01744	recJ	–0.833779031	4.6150656536111E-8
SAOUHSC_00191	scn	–1.931656738	4.7201382128235E-8
SAOUHSC_01031	cydA	1.0999936938232	4.7471261830691E-8
SAOUHSC_00369	——	–0.755288521	4.8064417584821E-8
SAOUHSC_00733	hisC	1.5505824027782	4.8215818644781E-8
SAOUHSC_02964	arcR	–1.125819314	4.9202846281603E-8
SAOUHSC_01165	uraA	–1.721357759	5.1056024078757E-8

(continues)

Table S2. Continued.

gene_id	gene_name	log_2(FC)	*p*.adjust
SAOUHSC_00174	lytH	1.9178194620661	5.4775680142448E-8
SAOUHSC_00201	——	1.6205395817783	6.1160969912282E-8
SAOUHSC_00454	holB	–1.472492664	6.6703191363449E-8
SAOUHSC_02099	vraS	1.7887123714184	6.7873529070562E-8
SAOUHSC_02459	——	2.1298276358064	7.1885637959271E-8
SAOUHSC_02646	——	–1.086909873	7.3919239928366E-8
SAOUHSC_00536	ilvE	0.85384214368477	8.3432974665472E-8
SAOUHSC_02698	tcyB	0.96113726501113	9.0454125549615E-8
SAOUHSC_02967	arcD	–1.095501913	9.0525624314575E-8
SAOUHSC_00606	——	1.1133365605302	9.3307233865564E-8
SAOUHSC_00562	pdxK	0.70083697660263	1.1709267565964E-7
SAOUHSC_01431	msrB	0.9736635315573	1.1795329286658E-7
SAOUHSC_01396	dapA	1.4076057152405	1.267018768086E-7
SAOUHSC_00639	——	0.98431731284708	1.308042287639E-7
SAOUHSC_02385	manA	–1.656094794	1.3433436485752E-7
SAOUHSC_02314	kdpD	–1.176000019	1.3441471784766E-7
SAOUHSC_00886	mnhD	1.021794726	1.5549460242702E-7
SAOUHSC_00612	——	–1.475602692	1.7198551635557E-7
SAOUHSC_02659	——	–0.86657217	1.7640076120807E-7
SAOUHSC_02494	rpsE	1.0774829705758	1.9153151873499E-7
SAOUHSC_00531	——	1.0207994865198	1.9483237083018E-7
SAOUHSC_02485	rpoA	0.98664936421144	1.9483237083018E-7
SAOUHSC_01833	serA	1.4030124402198	2.0101788491093E-7
SAOUHSC_01688	lepA	–0.926105825	2.0816969879392E-7
SAOUHSC_00282	——	1.8031855992168	2.1703672993893E-7
SAOUHSC_00036	gloB	1.0489042595484	2.213877428294E-7
SAOUHSC_01324	——	–1.559162063	2.213877428294E-7
SAOUHSC_01234	tsf	–0.833658826	2.2730071874012E-7
SAOUHSC_03027	——	1.5435635171913	2.6206907042282E-7
SAOUHSC_01115	scn	–1.786068561	2.6613816962845E-7
SAOUHSC_01920	——	–1.188349035	2.6920107736567E-7
SAOUHSC_01486	hepT	–0.974020011	2.786512710937E-7
SAOUHSC_01838	degP	0.69578892247868	2.8590885629965E-7
SAOUHSC_01100	trxA	1.2598714653735	3.0243326084651E-7
SAOUHSC_01467	mrcA	0.8489199212754	3.1197694605866E-7
SAOUHSC_02931	——	–1.518982725	3.9892130735909E-7
SAOUHSC_01846	acs	1.1543831492995	4.2982517501031E-7
SAOUHSC_01144	ftsL	–0.921514543	4.7310649800335E-7
SAOUHSC_01601	malZ	0.87970964931241	4.7310649800335E-7
SAOUHSC_02669	ohrR	0.93270869393561	4.9738162412879E-7
SAOUHSC_02117	gatA	–0.681894933	5.1681207361443E-7
SAOUHSC_00788	——	0.95983562438315	5.6024579208098E-7
SAOUHSC_01591	xerD	–0.88950718	6.345770006855E-7
SAOUHSC_02887	——	–2.108541878	6.345770006855E-7
SAOUHSC_00785	trxB	0.88568831767558	6.345770006855E-7
SAOUHSC_01263	rny	0.74312077840188	6.4991559177502E-7

(continues)

Table S2. Continued.

gene_id	gene_name	log_2(FC)	*p*.adjust
SAOUHSC_02276	——	–1.200846005	6.8614955795884E-7
SAOUHSC_01017	purH	1.8239681008547	6.8614955795884E-7
SAOUHSC_02259	yafV	0.76371211104669	7.0484342042583E-7
SAOUHSC_02257	——	–1.318213065	7.3612774155516E-7
SAOUHSC_00530	tuf	0.88010982863816	8.605218241042E-7
SAOUHSC_02161	eap	–1.362122112	8.9442443506994E-7
SAOUHSC_00187	pflD	1.3077396216266	1.022582113361E-6
SAOUHSC_02487	rpsM	1.1376238383284	1.1080367531902E-6
SAOUHSC_01174	——	0.7714391613006	1.1397331615013E-6
SAOUHSC_01813	——	–0.635444279	1.1724134971798E-6
SAOUHSC_01135	psmB	1.3180429461301	1.2067770279042E-6
SAOUHSC_02770	cntK	–1.815728196	1.2929987692554E-6
SAOUHSC_03031	rarD	0.852613455	1.302101213401E-6
SAOUHSC_01243	nusA	–1.104661371	1.3619536745365E-6
SAOUHSC_02495	rplR	1.2105495612959	1.3619536745365E-6
SAOUHSC_00878	ndh	–0.727807139	1.4655955321184E-6
SAOUHSC_00424	metI	1.4916376338483	1.4655955321184E-6
SAOUHSC_02808	gntK	–0.991192077	1.5878748864181E-6
SAOUHSC_01007	folD	0.8012964895053	1.5931258045401E-6
SAOUHSC_01632	gcvPB	1.2804938445621	1.6995405847555E-6
SAOUHSC_00544	sdrC_D_E	–0.881008985	1.7629918905776E-6
SAOUHSC_02638	——	1.1243703510097	1.7769960305983E-6
SAOUHSC_01321	thrC	1.4292484679994	1.8525359216603E-6
SAOUHSC_02142	crtNc	1.2918867202226	1.9939812986937E-6
SAOUHSC_02279	tsaB	–0.956837571	2.0494044760002E-6
SAOUHSC_01050	——	0.86004511570309	2.3980341365731E-6
SAOUHSC_01430	crr	0.81677276743561	2.4037945072122E-6
SAOUHSC_01832	——	1.3434645895408	2.6306541805987E-6
SAOUHSC_02218	——	–2.176422347	2.7269324966812E-6
SAOUHSC_01398	dapH	1.3595060893932	2.9318914524815E-6
SAOUHSC_00366	nfrA1	0.95334369439121	3.0828644417069E-6
SAOUHSC_00398	hsdS	–1.252864968	3.138851619963E-6
SAOUHSC_01203	rnc	–0.889363931	3.2304546821485E-6
SAOUHSC_02286	leuB	2.1674029687986	3.570074303742E-6
SAOUHSC_01397	dapB	1.2457334201434	3.6578898250665E-6
SAOUHSC_00397	hsdM	–1.284892112	3.6578898250665E-6
SAOUHSC_00899	argG	1.595505719	3.6578898250665E-6
SAOUHSC_02284	ilvC	2.1648104934462	3.7283720304394E-6
SAOUHSC_01130	——	1.362858771	3.7283720304394E-6
SAOUHSC_00818	nuc	–2.330755588	3.7283720304394E-6
SAOUHSC_00188	pflA	1.6795915799714	3.9959568830839E-6
SAOUHSC_00013	metX	1.3055306369346	4.0115661551796E-6
SAOUHSC_02337	murA	–0.818231493	4.090585477364E-6
SAOUHSC_01699	aroE	–0.943968868	4.2623747726835E-6
SAOUHSC_00422	mccB	1.693758466	4.3970686599295E-6
SAOUHSC_00638	troR	–0.711222068	4.5582073582414E-6

(continues)

Table S2. Continued.

gene_id	gene_name	log_2(FC)	*p*.adjust
SAOUHSC_01005	——	1.1267472776462	4.5582073582414E-6
SAOUHSC_01663	dnaG	–1.203425839	4.5974884682555E-6
SAOUHSC_00323	——	1.4121618971507	5.1095895039381E-6
SAOUHSC_00217	gutB	1.5444651562851	5.4770152021206E-6
SAOUHSC_02386	——	–1.707961085	6.0531099067213E-6
SAOUHSC_01700	yqeH	–0.903479629	6.0531099067213E-6
SAOUHSC_01224	xerC	0.71095689887434	6.0531099067213E-6
SAOUHSC_02491	secY	0.96882650696268	6.2209841272766E-6
SAOUHSC_00074	sirA	–1.240478978	6.2209841272766E-6
SAOUHSC_01485	ndk	–1.237218696	6.2764333889068E-6
SAOUHSC_01226	hslU	0.79647429284945	6.4955604569037E-6
SAOUHSC_00749	yclQ	1.1581493977705	6.7751496713566E-6
SAOUHSC_00177	ganP	0.95206866305157	7.1728116162158E-6
SAOUHSC_00716	doxD	–1.00005449	7.5134592356348E-6
SAOUHSC_02965	arcC	–1.033022855	8.7968110982036E-6
SAOUHSC_01218	sucD	0.87575604765112	9.4980967689476E-6
SAOUHSC_02169	chp	–1.422733036	9.5400248145019E-6
SAOUHSC_02710	hlg	–1.278970431	9.5762508403461E-6
SAOUHSC_00484	tilS	–0.785413337	9.6184206727799E-6
SAOUHSC_02731	nhaK	0.81282468864351	1.1138008616855E-5
SAOUHSC_00135	——	1.4550401218009	1.1484044529077E-5
SAOUHSC_00939	glbN	0.90753799877592	1.2045373095686E-5
SAOUHSC_00577	mvaK1	–1.059047144	1.2822203190991E-5
SAOUHSC_00170	——	1.5042141195624	1.2843059628798E-5
SAOUHSC_01673	phoH	–0.596982823	1.2990264869554E-5
SAOUHSC_01889	ribD	1.3238483121846	1.3077955753061E-5
SAOUHSC_01460	ypsC	–1.156407427	1.4002408685171E-5
SAOUHSC_00658	dhaM	1.3042013462649	1.4011354658923E-5
SAOUHSC_01981	——	–0.88766314	1.4011354658923E-5
SAOUHSC_01598	rnz	–0.993869863	1.415606339997E-5
SAOUHSC_02611	——	–1.718886651	1.4500345539148E-5
SAOUHSC_00031	——	1.051566049	1.4962059240051E-5
SAOUHSC_02929	acs	0.73781166958883	1.5618338191758E-5
SAOUHSC_02170	——	–0.826092313	1.5618338191758E-5
SAOUHSC_02097	——	–0.699813599	1.5618338191758E-5
SAOUHSC_02282	ilvB	1.7594140165055	1.6598332417975E-5
SAOUHSC_02428	fecC	–1.03530366	1.6598332417975E-5
SAOUHSC_00656	dhaL	1.0617796769587	1.6598332417975E-5
SAOUHSC_00423	metN	1.3500028730269	1.7325848079093E-5
SAOUHSC_02119	putP	0.76849427055951	1.7394839568209E-5
SAOUHSC_02486	rpsK	0.87394654170986	1.7428330354386E-5
SAOUHSC_02287	leuC	1.9739051770443	1.7888890636379E-5
SAOUHSC_02492	rplO	0.97740604786551	1.8019456512616E-5
SAOUHSC_01910	pckA	0.72453129468353	1.8470668925059E-5
SAOUHSC_00024	——	–0.779234508	1.8470668925059E-5
SAOUHSC_02484	rplQ	0.81487881455487	1.8928845931818E-5
SAOUHSC_02972	——	0.93170613373332	1.899164962891E-5

(continues)

Table S2. Continued.

gene_id	gene_name	log_2(FC)	*p*.adjust
SAOUHSC_02899	——	0.8878897176633	1.9516301886993E-5
SAOUHSC_00543	——	–1.237662635	1.9561107224713E-5
SAOUHSC_01944	——	–1.587443683	1.9626636286347E-5
SAOUHSC_00814	——	–2.456916898	2.0333906022291E-5
SAOUHSC_01440	yhhQ	0.74229495009487	2.0420544499808E-5
SAOUHSC_00729	uup	–0.920539002	2.2034260890958E-5
SAOUHSC_02727	——	0.70234483564985	2.2201053132597E-5
SAOUHSC_00199	pct	1.3431376108205	2.4655978213683E-5
SAOUHSC_01887	ribBA	1.3275933933569	2.4712540890603E-5
SAOUHSC_00957	——	0.67961505764179	2.4906311430878E-5
SAOUHSC_02216	dnaC	–3.198478421	2.4906311430878E-5
SAOUHSC_00938	——	0.62050875476907	2.5286078920613E-5
SAOUHSC_02755	——	0.66479416320389	2.9769754510147E-5
SAOUHSC_00259	——	0.91036720908362	3.000648002723E-5
SAOUHSC_02004	ygaC	–0.721072556	3.0893478700069E-5
SAOUHSC_01980	——	–1.108568903	3.358984601784E-5
SAOUHSC_01609	——	0.84878075619446	3.4301163927154E-5
SAOUHSC_01840	sgtA	–0.92456214	3.4803988314131E-5
SAOUHSC_00006	gyrA	–0.59206397	3.5227949000157E-5
SAOUHSC_00520	rplJ	0.81285487137708	3.5688784108203E-5
SAOUHSC_00004	recF	–0.841898608	3.6897732895182E-5
SAOUHSC_01866	——	–0.614907108	4.0336484453081E-5
SAOUHSC_00202	——	2.050742718	4.0354250452079E-5
SAOUHSC_00329	tatA	0.91564114694227	4.0726937123846E-5
SAOUHSC_01416	sucB	0.76806815390388	4.2876020507266E-5
SAOUHSC_00927	oppA	1.4035113740206	4.3019809401867E-5
SAOUHSC_01888	ribE	1.4310408772433	4.4094853999669E-5
SAOUHSC_01588	scpB	–0.63447059	4.4125198176013E-5
SAOUHSC_00912	clpB	–1.367444112	4.4147060485985E-5
SAOUHSC_02299	rsbW	–0.818768336	4.4382706724802E-5
SAOUHSC_01319	lysC	1.5339905768234	4.5592957341217E-5
SAOUHSC_02274	——	–0.740637127	4.6175213073212E-5
SAOUHSC_02782	——	–3.386641207	4.724136698367E-5
SAOUHSC_02790	——	–0.934517826	5.0590345646185E-5
SAOUHSC_01487	ubiE	–0.742706289	5.108089618296E-5
SAOUHSC_02273	rex	0.67220360683395	5.108089618296E-5
SAOUHSC_01391	——	–0.794745852	5.2419707200431E-5
SAOUHSC_01672	ybeY	–0.740916808	5.2419707200431E-5
SAOUHSC_02910	——	0.97430495361603	5.2640225710056E-5
SAOUHSC_00060	yjbB	–1.205301197	5.2666802546175E-5
SAOUHSC_02766	nikB	1.2519725557457	5.4265742373214E-5
SAOUHSC_00427	sle1	–1.696658801	5.4265742373214E-5
SAOUHSC_02496	rplF	1.0370504433076	5.4265742373214E-5
SAOUHSC_02926	——	0.89574701749456	5.9632241526965E-5
SAOUHSC_02302	rsbU_P	–0.636212453	6.0054675876317E-5
SAOUHSC_00441	——	–0.823328991	6.3542705191209E-5
SAOUHSC_01245	——	–0.818268962	6.3741408216915E-5

(continues)

Table S2. Continued.

gene_id	gene_name	log_2(FC)	*p*.adjust
SAOUHSC_02083	——	–2.110135261	6.3928856471631E-5
SAOUHSC_00925	oppD	1.3154230728937	6.5076916859738E-5
SAOUHSC_02697	tcyC	1.0795333631125	6.623373618737E-5
SAOUHSC_00527	rpsL	0.76136310425248	6.6485505776462E-5
SAOUHSC_00542	——	–1.441896551	6.662419092466E-5
SAOUHSC_02557	utp	1.1586475003163	6.8107302538879E-5
SAOUHSC_00742	nrdA	0.84712916280095	7.0974952170256E-5
SAOUHSC_02579	——	–0.873787918	7.1970840877363E-5
SAOUHSC_01183	fmt	–0.873805641	7.1970840877363E-5
SAOUHSC_01914	——	0.75622646536486	7.2743516561471E-5
SAOUHSC_00896	——	0.91272890551378	7.3291327052038E-5
SAOUHSC_01238	cdsA	–0.773868658	7.769383892833E-5
SAOUHSC_00816	——	–1.364933249	7.9835073017244E-5
SAOUHSC_01785	rpmI	–0.974098803	8.3309641127194E-5
SAOUHSC_02909	pyrD	0.99099899617615	8.441461524136E-5
SAOUHSC_00833	——	–0.662933194	8.6008675436198E-5
SAOUHSC_00204	hmp	1.88043129	8.7083209541794E-5
SAOUHSC_02705	——	–1.20184885	8.7157622247231E-5
SAOUHSC_02155	——	0.7246741351582	8.9553383140847E-5
SAOUHSC_02225	——	–2.871615937	9.1090618941427E-5
SAOUHSC_00233	lrgB	1.7438428827185	9.3550104175566E-5
SAOUHSC_00216	gatC	1.6311447369707	9.4224611328021E-5
SAOUHSC_01776	hemA	0.61223292618069	9.8628837161943E-5
SAOUHSC_02012	sgtB	1.13858998	9.8980704336643E-5
SAOUHSC_00039	——	–0.75603706	0.00011254746927737
SAOUHSC_01337	tktA	0.66028110406041	0.00011546611584799
SAOUHSC_02050	xtmA	–2.513805821	0.00011852325728609
SAOUHSC_00232	lrgA	2.0333074572107	0.00011864716120214
SAOUHSC_02663	——	1.1960247762784	0.00011979550583824
SAOUHSC_02752	pbuE	0.85920167301195	0.00012521025674799
SAOUHSC_02986	asp3	1.228018497	0.00012586178769824
SAOUHSC_00949	——	1.3081680800067	0.00012677160404406
SAOUHSC_02740	norB	0.7131648475486	0.00013360855061271
SAOUHSC_02365	murA	0.79094758100558	0.00013826782982012
SAOUHSC_01979	——	–1.313672425	0.0001407966179671
SAOUHSC_01322	thrB	1.3081408568848	0.00014276877254412
SAOUHSC_00907	——	–1.181019406	0.00014389095491554
SAOUHSC_01320	hom	1.0954106268487	0.00014417310988861
SAOUHSC_02233	——	–2.291856564	0.00014999712202225
SAOUHSC_01341	sbcD	–1.057480168	0.00015186113820447
SAOUHSC_00313	——	1.5605581280396	0.00015331534078012
SAOUHSC_01086	htsB	–2.181859866	0.00015541206749219
SAOUHSC_00834	——	0.90782133907405	0.00017105417905049
SAOUHSC_02281	ilvD	1.2616245803529	0.00017737336172205
SAOUHSC_01281	hfq	0.79363357450001	0.00018598632368092

(continues)

Table S2. Continued.

gene_id	gene_name	log_2(FC)	*p*.adjust
SAOUHSC_01684	——	–0.67040399	0.00018598632368092
SAOUHSC_01784	rplT	–1.124134336	0.00019780007236985
SAOUHSC_02357	tsaC	–0.623896866	0.00020645707135993
SAOUHSC_01225	hslV	0.69134399882815	0.00021420721038494
SAOUHSC_00671	——	–1.526200981	0.00021420721038494
SAOUHSC_00603	iolS	0.73799727573021	0.00021420721038494
SAOUHSC_02869	——	0.67337238708461	0.0002159891044956
SAOUHSC_02723	glxK	1.1603438262809	0.00022408666398701
SAOUHSC_00037	sqr	1.0065120221462	0.00022737438134033
SAOUHSC_00803	rnr	0.79274236003244	0.00022742873766978
SAOUHSC_01399	——	1.181944902	0.00023911250369481
SAOUHSC_00139	——	1.1271448045949	0.00024236460801637
SAOUHSC_02048	——	–2.102104406	0.0002453997135816
SAOUHSC_02861	ogt	0.74324364865061	0.00024625293444165
SAOUHSC_03023	drp35	0.80064003366824	0.00024789568525541
SAOUHSC_00005	gyrB	–0.667940907	0.0002534735352978
SAOUHSC_02049	xtmB	–2.377399199	0.00025698954877978
SAOUHSC_02152	——	0.84859471870235	0.0002685692017341
SAOUHSC_01081	isdA	–0.974210796	0.0002685692017341
SAOUHSC_02724	——	1.1890603064121	0.00027090022845609
SAOUHSC_00156	——	0.74585536011486	0.00027298178420151
SAOUHSC_00752	murB	–0.59699814	0.00027298178420151
SAOUHSC_00787	rapZ	0.6978494006767	0.00027985194968928
SAOUHSC_01725	mnmA	0.6723424734556	0.00027985194968928
SAOUHSC_01676	——	0.67435131831284	0.00030008335339525
SAOUHSC_01204	smc	–0.715331471	0.00030575778848748
SAOUHSC_00610	——	–0.934534939	0.00031632536552256
SAOUHSC_01786	infC	–0.915036664	0.00031725438092777
SAOUHSC_00339	yitJ	1.5064247600219	0.00032768891961698
SAOUHSC_01447	——	1.0858936368554	0.000336364019618
SAOUHSC_02841	——	–0.649977794	0.00033709490983796
SAOUHSC_00171	ggt	1.0296488331367	0.00034207952606835
SAOUHSC_02087	——	–1.007252513	0.00034422022430859
SAOUHSC_00528	rpsG	0.7756532030178	0.00035426805412294
SAOUHSC_01792	dnaB	–0.789108572	0.00035436415262318
SAOUHSC_00660	——	0.59436485715263	0.00035808753513769
SAOUHSC_01032	cydB	1.2572440498275	0.00036203221211971
SAOUHSC_02500	rplE	0.86729133830553	0.00036281956632696
SAOUHSC_02221	——	–2.500520833	0.00036384184517165
SAOUHSC_02905	——	1.0827334229132	0.00036989758058432
SAOUHSC_00157	murQ	0.92096607785789	0.00038446180365827
SAOUHSC_01932	hsdS	–0.767907741	0.0003932543181325
SAOUHSC_00748	yclP	1.1712648935539	0.00040246771199353
SAOUHSC_00926	oppF	1.2766816488827	0.00041055052954774
SAOUHSC_01456	——	0.90848903201456	0.00041128645776735
SAOUHSC_02519	——	–0.91637934	0.00041340744921797
SAOUHSC_03022	——	0.99517393617284	0.00041542569467627

(continues)

Table S2. Continued.

gene_id	gene_name	log_2(FC)	*p*.adjust
SAOUHSC_00687	——	–1.501065191	0.00046715949977282
SAOUHSC_00628	mnhD	0.88667180990839	0.0004727336753236
SAOUHSC_00401	——	0.89605549271202	0.00047297405820049
SAOUHSC_01166	pyrB	–1.125685092	0.00048473504404233
SAOUHSC_01992	——	–1.097885023	0.00048855636212426
SAOUHSC_01016	purN	1.4271621219011	0.00049405438706804
SAOUHSC_00711	tlyC	–0.699381895	0.00049491295442334
SAOUHSC_02388	czrA	–0.783768371	0.00050019968397397
SAOUHSC_01249	ribF	0.68614861881995	0.00050613854162159
SAOUHSC_02750	——	1.1093077064074	0.00050976738665013
SAOUHSC_02871	——	1.0242284494396	0.00051818972641696
SAOUHSC_01276	glpK	0.72039854228438	0.00055459349491295
SAOUHSC_01129	arcC	1.4279820008591	0.00055459349491295
SAOUHSC_02501	rplX	0.78987986940924	0.0005817041719656
SAOUHSC_02776	——	–0.923504163	0.00065837543296324
SAOUHSC_01107	rdgB	0.82241655838859	0.00071870442781973
SAOUHSC_00828	lysE	1.3069324858313	0.00071870442781973
SAOUHSC_01400	alr	1.1793230512366	0.00071872151074164
SAOUHSC_01998	——	0.74176418046096	0.00072476518835959
SAOUHSC_02898	——	1.1388051878438	0.00074734069207905
SAOUHSC_00895	gudB	0.61587322092061	0.00075893458616713
SAOUHSC_02490	adk	1.0725001450267	0.00078105816899077
SAOUHSC_01822	tpx	0.60081626600434	0.00078105816899077
SAOUHSC_00279	——	–1.656392723	0.00078105816899077
SAOUHSC_00905	addA	0.60865213060246	0.00079319859537426
SAOUHSC_00987	sspB	–1.059866769	0.00079320009392889
SAOUHSC_00086	butA	0.74485285132525	0.00082406857339829
SAOUHSC_01223	trmFO	0.66775525711813	0.00082406857339829
SAOUHSC_00466	ispE	–0.841845266	0.00083536959824597
SAOUHSC_02880	crtQ	–0.780897883	0.00084966231483705
SAOUHSC_03040	——	0.68371902470449	0.00084986103613254
SAOUHSC_00163	——	–1.384047486	0.00088665732500688
SAOUHSC_01933	hsdM	–1.041419253	0.00089464869992345
SAOUHSC_00198	fadD	1.2470087582431	0.00089644463229002
SAOUHSC_01237	uppS	–0.857724648	0.00090025880069743
SAOUHSC_02163	——	–1.804591427	0.0009054806535344
SAOUHSC_02767	nikA	0.95926529230569	0.001002643951747
SAOUHSC_02822	fbp3	0.89185551202985	0.001030479523687
SAOUHSC_01359	mprF	0.88342320130448	0.0010443969799012
SAOUHSC_02613	——	0.62433319969881	0.0010575294131972
SAOUHSC_01589	scpA	–0.904014237	0.0010659810924538
SAOUHSC_02256	——	–2.698703421	0.0010847568701898
SAOUHSC_02400	mtlA	–0.85791204	0.0010867295460565
SAOUHSC_01051	——	0.83579710329041	0.0010950980272323
SAOUHSC_01364	tyrA2	0.80775648258042	0.0011038017961222
SAOUHSC_01604	——	0.8616477319511	0.001105204924745
SAOUHSC_00869	dltA	0.63561940689759	0.0011471838599693

(continues)

Table S2. Continued.

gene_id	gene_name	log_2(FC)	*p*.adjust
SAOUHSC_02154	——	0.6625571206276	0.0011482540937695
SAOUHSC_01738	hisS	–0.601616701	0.0011899929058341
SAOUHSC_02660	corA	–0.827108121	0.0011948199701533
SAOUHSC_00715	saeR	–0.909591934	0.0012021906769381
SAOUHSC_00312	ulaC	1.7133405322355	0.0012088655069429
SAOUHSC_02502	rplN	0.79692626688573	0.0012130206333667
SAOUHSC_01347	acnA	0.82806691833106	0.0012166420610098
SAOUHSC_00138	——	1.4854856092355	0.0012232709118883
SAOUHSC_02081	——	–2.470078256	0.001245796468778
SAOUHSC_01182	def	–0.935956018	0.0012753699906644
SAOUHSC_02866	——	1.7017219390292	0.0012897423095112
SAOUHSC_02217	——	–2.575811769	0.0013042310663652
SAOUHSC_02855	——	–2.147594831	0.0013042310663652
SAOUHSC_02390	——	–2.439311318	0.0013184453549366
SAOUHSC_00239	rbsK	–0.850842275	0.0013646672990422
SAOUHSC_00169	——	1.643496139	0.001386148908563
SAOUHSC_00421	mccA	1.4691350093593	0.0014458862541992
SAOUHSC_02167	scn	–1.057618738	0.001487001738164
SAOUHSC_00058	norB	0.80149050817919	0.0014940708612686
SAOUHSC_02030	——	–2.224800921	0.001535113619989
SAOUHSC_02907	——	0.95525235433018	0.001535113619989
SAOUHSC_01839	tyrS	–0.802117719	0.0015718942117767
SAOUHSC_01893	arsB	0.75412654873182	0.0015898449482923
SAOUHSC_02842	——	–4.738446419	0.0015954901289791
SAOUHSC_00213	——	1.0788125411575	0.0016024843213554
SAOUHSC_02023	lytD	–2.147454084	0.0016345739409906
SAOUHSC_03012	hisC	1.4857007688068	0.0016369901029372
SAOUHSC_02763	nikE	1.1649001975917	0.0016882612253098
SAOUHSC_02280	tsaE	–1.056593006	0.0017392247638007
SAOUHSC_01146	mraY	–0.659590133	0.0017867040074626
SAOUHSC_02047	——	–1.793019154	0.0018363228344796
SAOUHSC_01685	hrcA	–0.793184439	0.0018567635858638
SAOUHSC_00726	——	–1.974705372	0.0018620798094155
SAOUHSC_01141	bshC	0.79911321863463	0.0018815501070408
SAOUHSC_00182	——	–3.460275865	0.0018815501070408
SAOUHSC_02288	leuD	1.6803318939333	0.0019131146501275
SAOUHSC_02823	——	0.66390952985922	0.0019179791772793
SAOUHSC_01690	holA	–1.26538842	0.0019281974988374
SAOUHSC_02127	sspB2	–1.276159861	0.0019349474228985
SAOUHSC_01764	comC	–1.77942091	0.0019626183627635
SAOUHSC_01718	——	–2.050420515	0.0019978479120243
SAOUHSC_A01455	——	0.80630753756607	0.0019978479120243
SAOUHSC_00667	vraF	0.62902497874303	0.0020094900687048
SAOUHSC_02088	——	–2.253806583	0.0020106434000032
SAOUHSC_01228	codY	0.85678337577574	0.0020224122934266
SAOUHSC_02022	——	–2.149642022	0.002032940629325

(continues)

Table S2. Continued.

gene_id	gene_name	log_2(FC)	*p*.adjust
SAOUHSC_00901	——	0.60963530436617	0.0020379602021924
SAOUHSC_01650	——	–0.967304726	0.002044709435342
SAOUHSC_02498	rpsH	1.0417023907051	0.0020619583209429
SAOUHSC_02033	——	–1.997912806	0.0020619829244471
SAOUHSC_01143	mraW	–0.92140162	0.0020889101792461
SAOUHSC_03013	hisD	1.2223771327029	0.0021092819023411
SAOUHSC_02043	——	–2.047810471	0.0021556373568047
SAOUHSC_01110	——	–1.191676519	0.0021873499377511
SAOUHSC_03049	parB	0.60332391387197	0.0021873499377511
SAOUHSC_01463	——	0.61154665780835	0.0021879549668128
SAOUHSC_02036	——	–1.998777461	0.0022125862846249
SAOUHSC_00808	——	–0.649674714	0.0022373591356237
SAOUHSC_02069	——	–1.765770084	0.0023419259587974
SAOUHSC_02846	ybgC	0.80122999668078	0.0023748537011783
SAOUHSC_01106	murI	0.58523606615258	0.0023748537011783
SAOUHSC_A00992	——	1.2477118063618	0.0023806920233304
SAOUHSC_02020	——	–2.49363233	0.0023874442585099
SAOUHSC_01819	——	–0.982976174	0.0024193528251344
SAOUHSC_01795	coaE	0.6654033924717	0.0024193528251344
SAOUHSC_02025	——	–2.381953952	0.0024232037293029
SAOUHSC_02844	——	0.63390564132853	0.002429287624196
SAOUHSC_02213	——	–4.727397307	0.0024700139519445
SAOUHSC_02220	——	–1.852340329	0.0025216349030413
SAOUHSC_02031	——	–2.171683494	0.0025216349030413
SAOUHSC_01125	——	1.3074574324394	0.0025422585716695
SAOUHSC_01139	——	0.83881892594592	0.0025753326755103
SAOUHSC_00030	——	–1.127832271	0.0025756202948722
SAOUHSC_02041	——	–2.40185731	0.0026147963969672
SAOUHSC_02067	——	–1.645873796	0.0026316646078852
SAOUHSC_00234	yydK	–0.806671548	0.0026750118839433
SAOUHSC_01769	——	0.88482259521018	0.0027038556112162
SAOUHSC_00703	norA	1.0179180721354	0.0027140282284765
SAOUHSC_02336	fabZ	–0.721377964	0.0027359317815305
SAOUHSC_01903	crcB	–1.608530414	0.002752839602963
SAOUHSC_01049	potD	0.61208349081998	0.0028438878149747
SAOUHSC_02118	gatC	–0.69338747	0.0028444418302161
SAOUHSC_00774	——	–1.374190979	0.0028744563553222
SAOUHSC_01331	——	–0.81905892	0.0028744563553222
SAOUHSC_02072	——	–1.738600118	0.0028812751534316
SAOUHSC_00467	purR	–0.855837865	0.0029007674816821
SAOUHSC_00026	——	–2.071564862	0.0029258197560895
SAOUHSC_00304	——	–0.692598095	0.0029289944580668
SAOUHSC_02761	——	–2.0704623	0.0029439927122354
SAOUHSC_00164	——	–0.940306408	0.0030004645194323
SAOUHSC_00888	mnhB	0.66183373995377	0.0030257243474731
SAOUHSC_00998	fmtA	–2.054052774	0.0030257243474731
SAOUHSC_02656	——	0.90923376537765	0.0030548857729542

(continues)

Table S2. Continued.

gene_id	gene_name	log_2(FC)	*p*.adjust
SAOUHSC_00621	——	0.79462830706806	0.0031003211050875
SAOUHSC_00633	nhaK	0.77250369549779	0.0031998410949685
SAOUHSC_00486	ftsH	0.91300031670288	0.0032162139554613
SAOUHSC_02886	——	–3.122234196	0.003257199284888
SAOUHSC_01706	——	–1.073627223	0.0032688625685905
SAOUHSC_00880	yuiF	0.9205825943516	0.0033121606814873
SAOUHSC_00277	——	–1.545681304	0.0033153782403698
SAOUHSC_02078	——	–1.799670057	0.0033252911324729
SAOUHSC_00002	dnaN	–0.6866035	0.0033252911324729
SAOUHSC_01128	argF	1.3135045052554	0.0034129253976715
SAOUHSC_00292	psuG	1.6284944438813	0.0034185524805067
SAOUHSC_01162	lspA	–2.240996055	0.0034273286557622
SAOUHSC_01828	msrC	0.67044009730904	0.0034293469089293
SAOUHSC_00430	——	–0.622882548	0.0034293469089293
SAOUHSC_02219	——	–2.051027502	0.0034315501730998
SAOUHSC_02461	adhR	0.80058212963707	0.0035042290155656
SAOUHSC_01287	glnA	–0.826785183	0.0035830812396922
SAOUHSC_02035	——	–2.046365466	0.0036432534766991
SAOUHSC_02301	rsbU_P	–0.619491533	0.0036555416172794
SAOUHSC_01058	typA	–0.804712608	0.0036555786879194
SAOUHSC_01743	apt	–0.597485456	0.0036641446927368
SAOUHSC_02165	——	–2.767916474	0.0036670270003574
SAOUHSC_02883	——	–1.42940779	0.0036670270003574
SAOUHSC_02070	——	–1.805066927	0.0036670270003574
SAOUHSC_00997	tagT_U_V	0.67167256809137	0.0038350458057047
SAOUHSC_00340	metC	1.3625901997113	0.0039606836641989
SAOUHSC_01275	glpF	0.62846809171942	0.0040012377197584
SAOUHSC_00554	hxlB	0.64587837902261	0.0040744124865834
SAOUHSC_00485	hprT	–1.126374201	0.0040865773138258
SAOUHSC_03015	——	1.4553371245835	0.0041305120147514
SAOUHSC_01328	rpmG	0.9316342743759	0.0041818439957312
SAOUHSC_03017	——	1.4585319479337	0.0041894102334576
SAOUHSC_02576	——	–1.361949498	0.0042513894572127
SAOUHSC_02037	——	–2.398017429	0.0043179433321735
SAOUHSC_02071	——	–1.767268632	0.0043179433321735
SAOUHSC_01894	arsC	0.78331507512243	0.0044068104002757
SAOUHSC_02077	——	–2.063058491	0.0044111220052988
SAOUHSC_02865	feoA	1.6869624154895	0.0044209926226937
SAOUHSC_A02794	——	1.1198890595793	0.00445463866805
SAOUHSC_02901	——	0.78930792692238	0.0045323731294441
SAOUHSC_00961	comK	–0.845698266	0.0045895597652392
SAOUHSC_01285	glnR	–1.04657752	0.0046220726625099
SAOUHSC_02520	glcU	0.97661812316038	0.0047277242828533
SAOUHSC_02266	——	–1.217552675	0.0047471354186771
SAOUHSC_02811	——	0.58995412037613	0.0047585688143394
SAOUHSC_02607	hutU	–1.017558718	0.0048747346485221
SAOUHSC_01583	——	–0.746871354	0.0049332249390055

(continues)

Table S2. Continued.

gene_id	gene_name	log_2(FC)	*p*.adjust
SAOUHSC_02915	——	0.65078906186602	0.0049332249390055
SAOUHSC_01653	——	0.63824116707594	0.0049584930272531
SAOUHSC_00985	menB	0.62367304208472	0.0049866370100624
SAOUHSC_02382	——	0.85470184357212	0.0051020566099379
SAOUHSC_02021	——	–2.117925341	0.0051427334325558
SAOUHSC_01401	lysA	0.74211151448686	0.0051720009329375
SAOUHSC_00721	queC	–0.646058681	0.0052245609904001
SAOUHSC_00521	rplL	0.63534358800663	0.0052671496592183
SAOUHSC_00020	vicR	–0.602611873	0.0052791642631403
SAOUHSC_02584	suhB	–0.807555256	0.0053451550150805
SAOUHSC_01942	sspA	–1.718401812	0.0054795660500871
SAOUHSC_01209	rimM	–0.662104365	0.0058356456478586
SAOUHSC_02840	sdaA	–0.759364687	0.0058541622760534
SAOUHSC_01621	nusB	–1.184244123	0.005977032082323
SAOUHSC_03025	pcp	–0.815875676	0.005977032082323
SAOUHSC_02374	——	0.66777887389162	0.0060789798313242
SAOUHSC_01782	——	–0.878481431	0.0063862432003403
SAOUHSC_02571	——	–1.308199862	0.0064144877886339
SAOUHSC_02064	——	–1.987468103	0.0065921624828931
SAOUHSC_00922	——	–4.479563832	0.0066299711999501
SAOUHSC_00702	——	0.80601792445282	0.0066678216255009
SAOUHSC_01171	pyrF	1.3445535459886	0.006678555882225
SAOUHSC_02160	——	–1.158218526	0.006748464690346
SAOUHSC_00341	metB	1.389863503	0.006748464690346
SAOUHSC_02447	qorA	0.64354020296423	0.0067592054236916
SAOUHSC_02062	——	–1.912510713	0.0067592054236916
SAOUHSC_02764	nikD	0.83669903786048	0.0069761463078693
SAOUHSC_02876	——	0.70936811682049	0.0069887472897586
SAOUHSC_02900	——	0.60388828316752	0.0070635368946344
SAOUHSC_01610	brxA_B	0.64386264288618	0.0071157674034216
SAOUHSC_02110	dnaQ	–0.934038331	0.0071622576754662
SAOUHSC_00293	——	1.2966437543388	0.0072781686272241
SAOUHSC_00278	——	–1.045640003	0.0073046602293607
SAOUHSC_00497	——	–1.342302913	0.0073480264030009
SAOUHSC_01240	proS	0.6338658931313	0.0074425607405437
SAOUHSC_00033	——	1.1582774193079	0.0075178883434295
SAOUHSC_02875	ldhA	0.83166819624266	0.0076705578289656
SAOUHSC_02034	——	–2.221466947	0.007697048339239
SAOUHSC_00276	——	–1.13763954	0.0079589409661745
SAOUHSC_01763	radC	–1.20759201	0.0079589409661745
SAOUHSC_01244	ylxR	–1.129970199	0.0080659189271986
SAOUHSC_00328	tatC	1.0496802049216	0.0087124776104806
SAOUHSC_00500	pdxT	–0.589171955	0.0088755166528908
SAOUHSC_02949	gpx	0.99073525800369	0.0090405784479339
SAOUHSC_02073	——	–1.638965196	0.0092411823302322
SAOUHSC_02897	——	1.1397598129142	0.00931164592645

(continues)

Table S2. Continued.

gene_id	gene_name	log_2(FC)	*p*.adjust
SAOUHSC_03018	ecfT	1.0922757016477	0.0095995843691039
SAOUHSC_02027	——	–2.353189502	0.0096563965404817
SAOUHSC_01030	——	–3.73314688	0.0096695104186138
SAOUHSC_01781	——	–1.047071461	0.0097607751692821
SAOUHSC_00456	——	–0.989794737	0.0097607751692821
SAOUHSC_00257	——	0.78856843255081	0.0098363964043739
SAOUHSC_00759	——	–0.780757398	0.0098707589123868
SAOUHSC_02057	dut	–1.6666671	0.010160846107577
SAOUHSC_02040	——	–2.338255248	0.010195687273837
SAOUHSC_00685	——	–0.92079888	0.010195687273837
SAOUHSC_03036	bceA	1.2897255620959	0.010306566031115
SAOUHSC_01477	——	0.71568498720982	0.010592304436582
SAOUHSC_01957	——	–1.018068389	0.010722614562693
SAOUHSC_02038	——	–2.241425924	0.010802601740402
SAOUHSC_02668	——	–1.927765699	0.010876338829062
SAOUHSC_01503	——	–1.358891696	0.011037836690343
SAOUHSC_00240	rbsD	–1.220502194	0.011080796268671
SAOUHSC_01831	——	0.84395182797049	0.011111467113258
SAOUHSC_03014	hisG	1.9069301181117	0.011160036255582
SAOUHSC_00982	menF	–0.712925358	0.011195551606572
SAOUHSC_01993	——	–0.70254634	0.011822583869766
SAOUHSC_00133	czcD	0.76824217142944	0.012126326245485
SAOUHSC_02231	antB	–2.546762756	0.012649778843239
SAOUHSC_02331	tenA	–1.035350883	0.012702593246921
SAOUHSC_00314	mepR	–0.808216141	0.01311543692801
SAOUHSC_00773	——	0.71046901333826	0.013185667059945
SAOUHSC_00437	treB	–0.60051953	0.013239098115493
SAOUHSC_03037	bceB	0.94331998875374	0.013521640778145
SAOUHSC_01817	——	–0.67490636	0.013948221209387
SAOUHSC_02678	narI	–0.934165271	0.014137526451544
SAOUHSC_01917	——	–1.289428329	0.014280909384703
SAOUHSC_02552	bioY	–0.821563635	0.014280909384703
SAOUHSC_02619	——	–0.598791679	0.014280909384703
SAOUHSC_03051	gidB	0.82616980364886	0.014594621917999
SAOUHSC_02499	rpsN	0.93480935080282	0.014824171705504
SAOUHSC_01514	——	–0.768358006	0.014824171705504
SAOUHSC_01133	eta	0.62254877895523	0.014884925782494
SAOUHSC_03006	lip	0.59862781209824	0.015153483468352
SAOUHSC_02726	——	–1.414877827	0.015400230501069
SAOUHSC_01172	pyrE	1.4485552514404	0.015439887227896
SAOUHSC_01288	——	–3.811558843	0.016115454855777
SAOUHSC_01576	——	–0.681273254	0.016115454855777
SAOUHSC_02019	xlyAB	–2.428175486	0.01612238531556
SAOUHSC_00802	yvaK	0.63689807800653	0.01612238531556
SAOUHSC_01488	hepS	–0.783797744	0.016412859263351
SAOUHSC_00458	——	–1.707699522	0.016461056548549
SAOUHSC_00618	——	–1.791238215	0.016553453142204

(continues)

Table S2. Continued.

gene_id	gene_name	log_2(FC)	*p*.adjust
SAOUHSC_02234	——	–2.294171268	0.016553453142204
SAOUHSC_00637	mntA	–1.096694179	0.016554150402918
SAOUHSC_03028	——	–0.764135035	0.016565364123822
SAOUHSC_00057	——	0.88368145929234	0.01677086480271
SAOUHSC_00189	——	1.6421901651112	0.016787223992936
SAOUHSC_03035	——	–0.792229734	0.016915236705438
SAOUHSC_00988	sspA	–1.113842934	0.01693711641294
SAOUHSC_01655	zurR	–2.142322434	0.017281391479078
SAOUHSC_02904	——	0.81941440036121	0.017305710995056
SAOUHSC_01675	——	0.62274591374192	0.017525413278337
SAOUHSC_00219	gutB	0.81685336238164	0.017558072319894
SAOUHSC_00991	——	1.5492755731708	0.017756254040996
SAOUHSC_00885	mnhE	0.77106731700468	0.017799281818091
SAOUHSC_00714	saeS	–0.802403662	0.017799281818091
SAOUHSC_01941	——	–1.108121536	0.017917177484678
SAOUHSC_01371	trpB	1.0463813044694	0.018046854668778
SAOUHSC_02059	——	–1.919774394	0.01833530407392
SAOUHSC_00864	——	–0.590829132	0.018700527162911
SAOUHSC_01921	——	–0.933011111	0.018780566077746
SAOUHSC_01898	——	–2.886413754	0.018909843138357
SAOUHSC_02810	——	0.69556715264434	0.019339543322982
SAOUHSC_02719	irtA	–0.843680739	0.019664570813431
SAOUHSC_02330	thiD	–0.6352309	0.019760391586309
SAOUHSC_00817	——	–1.019178659	0.019782519389654
SAOUHSC_00910	——	0.72096540452579	0.019788954124306
SAOUHSC_02089	——	–0.60519946	0.019944072934845
SAOUHSC_01947	nisE	0.7920470992125	0.01995894406506
SAOUHSC_01121	hlyII	–0.817904037	0.01995894406506
SAOUHSC_00754	——	–0.650081172	0.01995894406506
SAOUHSC_02992	——	–2.164039064	0.020319566104393
SAOUHSC_01369	trpC	1.4035152860616	0.020351943118331
SAOUHSC_00235	bglFa	–1.369292544	0.020396018194299
SAOUHSC_00420	——	–1.122740258	0.020552393241354
SAOUHSC_02690	znuA	–0.61035693	0.020708243788875
SAOUHSC_01015	purM	1.1636930933983	0.020731331400775
SAOUHSC_02419	——	0.58909533867652	0.021636529245219
SAOUHSC_01794	gap2	0.68396952449671	0.02172620353758
SAOUHSC_01103	sdhC	–0.727491925	0.021756547247796
SAOUHSC_00290	——	0.8219523271376	0.021796927685927
SAOUHSC_00835	——	–1.113660632	0.022193041294005
SAOUHSC_02570	——	–1.299696787	0.022314436575171
SAOUHSC_01801	icd	0.67962843226194	0.022646109278031
SAOUHSC_00200	prsW	–0.782594547	0.022712450520361
SAOUHSC_00968	——	1.4505852401509	0.022717473647869
SAOUHSC_00917	——	–1.022112177	0.022728414685576
SAOUHSC_02214	——	–2.051067494	0.022728414685576

(continues)

Table S2. Continued.

gene_id	gene_name	log_2(FC)	*p*.adjust
SAOUHSC_00236	bglA	–1.094736877	0.023018990592238
SAOUHSC_00381	——	0.80817478299318	0.023083676952628
SAOUHSC_02226	——	–0.648660799	0.023231021880529
SAOUHSC_02321	——	–0.787418672	0.023389922685032
SAOUHSC_00330	——	0.87540008434038	0.023470849623577
SAOUHSC_02200	——	–1.498617675	0.023937644875101
SAOUHSC_00400	——	–0.733413822	0.02464927384671
SAOUHSC_01142	mraZ	–0.591609247	0.024976672266058
SAOUHSC_02356	ywlE	–0.687664984	0.025108804486314
SAOUHSC_02208	——	–3.432304387	0.025506058170281
SAOUHSC_01084	isdD	–1.521630927	0.02559822346451
SAOUHSC_02968	argF	–0.594132946	0.02559822346451
SAOUHSC_02845	——	0.58760898598977	0.02559822346451
SAOUHSC_01073	——	–2.658102428	0.025738732937882
SAOUHSC_01922	——	–0.585532734	0.026223190510839
SAOUHSC_00556	proP	0.66582800506652	0.026228682551156
SAOUHSC_02075	——	–1.831556007	0.026228682551156
SAOUHSC_01978	——	–0.672911165	0.026228682551156
SAOUHSC_00172	——	–0.895757576	0.026343047648901
SAOUHSC_01990	artR	0.77571150290138	0.026580049292468
SAOUHSC_01788	thrS	1.2084533711837	0.026580049292468
SAOUHSC_01156	——	–1.094586239	0.026703816528002
SAOUHSC_01908	——	–0.887743226	0.027235671721787
SAOUHSC_00924	oppC	0.71416719290612	0.027362594148431
SAOUHSC_01951	lanC	0.73303673235637	0.02744948624009
SAOUHSC_00722	pabA	–0.749109024	0.027707183082912
SAOUHSC_02505	rplP	0.61027690113075	0.027778476636522
SAOUHSC_01075	coaD	–1.21604125	0.027778476636522
SAOUHSC_00197	gcdH	1.3511315123024	0.027910205167571
SAOUHSC_02051	——	–1.394658778	0.027947341540468
SAOUHSC_00914	leuA	–1.580240171	0.028080401010494
SAOUHSC_00844	metQ	0.64713778171343	0.028125838898049
SAOUHSC_02074	——	–1.636387491	0.028727128522949
SAOUHSC_01082	isdC	–0.98204651	0.029317929795204
SAOUHSC_02435	sfaA	–0.71122261	0.029342268920983
SAOUHSC_01088	srtB	–5.316863077	0.029501775321837
SAOUHSC_02516	pbuG	0.71269108372256	0.030592856350289
SAOUHSC_00800	——	–2.001992937	0.030725480875481
SAOUHSC_01850	galR	0.66555935381399	0.030817339103509
SAOUHSC_02112	——	0.77381824861303	0.030836171666649
SAOUHSC_01219	——	0.92522580762865	0.031148481668371
SAOUHSC_00399	ssl5_11	–2.410327088	0.031422708759731
SAOUHSC_02065	——	–2.380595453	0.032498925792418
SAOUHSC_00317	glpT	0.62569165242052	0.032941768953837
SAOUHSC_02068	——	–2.15852698	0.033051950980293
SAOUHSC_00274	——	–0.845877289	0.033302246976629
SAOUHSC_00324	rimL	0.6134723542689	0.033364274193339

(continues)

Table S2. Continued.

gene_id	gene_name	log_2(FC)	*p*.adjust
SAOUHSC_01648	gluP	–0.613245004	0.033397443271174
SAOUHSC_02028	——	–2.334725371	0.03340289794433
SAOUHSC_02928	——	–1.500885309	0.033595581090793
SAOUHSC_00413	——	0.83148543937748	0.03366637493725
SAOUHSC_00291	——	1.2267083146962	0.034792509597878
SAOUHSC_00231	lytT	–1.102540385	0.035049535719849
SAOUHSC_00046	——	–1.344194364	0.035688333783466
SAOUHSC_01127	——	0.95576199180297	0.035781257672372
SAOUHSC_02624	corA	–0.890165069	0.036900148741509
SAOUHSC_01865	trmB	–1.080483324	0.037001971094812
SAOUHSC_00767	hpf	0.73421655831958	0.037038824211683
SAOUHSC_01372	trpA	0.58741718354951	0.037133815178602
SAOUHSC_02515	——	0.81440129475115	0.037743187025494
SAOUHSC_02797	——	0.71691343217282	0.037743187025494
SAOUHSC_00874	——	–0.626876421	0.038113902175906
SAOUHSC_02587	——	–1.224423251	0.038507486793224
SAOUHSC_02765	nikC	0.86440182121816	0.038507486793224
SAOUHSC_00275	——	–0.738345374	0.038637163371045
SAOUHSC_01633	gcvPA	0.62302864618816	0.038765456188092
SAOUHSC_00372	xpt	–0.713148211	0.03903068189068
SAOUHSC_01370	trpF	1.4592492213281	0.039306378844032
SAOUHSC_01937	——	–0.915509379	0.03944426085136
SAOUHSC_02029	——	–2.092439802	0.040850624414348
SAOUHSC_00105	phnD	0.89801583083249	0.041383792003912
SAOUHSC_01366	trpE	0.80855226762425	0.041762390259527
SAOUHSC_01835	——	0.61356041531184	0.041777560547371
SAOUHSC_02458	——	2.6135966103724	0.042021968658579
SAOUHSC_02252	——	–1.638597981	0.042183875407435
SAOUHSC_02044	——	–2.181670095	0.043006709194574
SAOUHSC_01356	glcT	–1.774651755	0.043006709194574
SAOUHSC_01897	——	–3.307109832	0.043020861470809
SAOUHSC_01459	——	–0.926396263	0.043410349846806
SAOUHSC_02322	csoR	–0.858567723	0.043511969837176
SAOUHSC_01378	ddpD	0.63725425377979	0.043824588674862
SAOUHSC_01099	mutS2	0.69245974688545	0.044421941619702
SAOUHSC_02247	trkH	0.70303376648886	0.044947637541578
SAOUHSC_00434	——	–0.819805953	0.045006276167895
SAOUHSC_00683	——	–0.825906728	0.045129921203236
SAOUHSC_01913	mutT	–0.777321485	0.046386603751358
SAOUHSC_01793	nrdR	–0.612008268	0.046426970666057
SAOUHSC_02691	yoeB	–0.594867707	0.046498333465394
SAOUHSC_02042	——	–2.454906082	0.047088456586072
SAOUHSC_02757	yefM	–0.839603444	0.047088456586072
SAOUHSC_02605	——	0.5906714171664	0.047412460696636
SAOUHSC_00883	mnhG	0.87879839887552	0.047434326625915
SAOUHSC_02595	——	0.71073654951822	0.048492120110149
SAOUHSC_03001	icaR	0.58794364632224	0.38304719349524

Table S3. The DEGs of biofilm in CEO treatment group and control group of *S. aureus* NCTC8325.

gene_id	gene_name	log_2(FC)	*p*.adjust
SAOUHSC_02098	vraR	3.9374037182547	4.4053908843041E-75
SAOUHSC_02706	sbi	–5.213040911	8.5347228015132E-67
SAOUHSC_02709	hlg	–4.536629128	1.1001718397565E-57
SAOUHSC_01945	epiG	2.3856611773368	9.3865964000736E-48
SAOUHSC_02708	hlg	–5.417785399	2.9177305992439E-47
SAOUHSC_00315	mepA	3.2726302471581	7.287557965092E-41
SAOUHSC_02100	——	3.2345833271841	4.1131874036001E-40
SAOUHSC_02710	hlg	–3.591125574	1.156056265482E-39
SAOUHSC_01114	fib	–3.992813112	2.3896505423458E-37
SAOUHSC_00061	ohyA	2.2800503031939	4.0588100300953E-35
SAOUHSC_01115	scn	–4.348960126	1.3660693556107E-31
SAOUHSC_02099	vraS	3.4856761228027	6.0504217810581E-30
SAOUHSC_02113	rumA	2.1659249503749	1.392742775099E-29
SAOUHSC_01005	——	2.7164693954846	7.031376011763E-29
SAOUHSC_00316	——	2.8992925351583	7.6654497381478E-29
SAOUHSC_02243	hlg	–3.078258946	1.6638422814717E-28
SAOUHSC_00069	spa	–5.106197015	2.689345432167E-28
SAOUHSC_01949	nisP	2.510151239	6.1839651746842E-28
SAOUHSC_02923	——	2.4999299325916	3.22437925072E-26
SAOUHSC_03027	——	3.1296218016411	4.0360601394081E-26
SAOUHSC_02820	——	–2.883015132	7.2722327627275E-26
SAOUHSC_02873	copA	1.8152345124073	2.0593086180334E-25
SAOUHSC_02590	——	1.8012505270384	1.0756753445208E-24
SAOUHSC_00192	——	–4.095993548	1.2775501030963E-24
SAOUHSC_00582	——	2.1547205404715	6.8000628002177E-23
SAOUHSC_02723	glxK	2.9933574843418	1.5846775952864E-22
SAOUHSC_01110	——	–3.994650645	1.7654230990679E-22
SAOUHSC_02724	——	3.2143627345239	1.7932116835135E-22
SAOUHSC_01951	lanC	2.4827983540666	2.1118603700622E-22
SAOUHSC_02241	hlg	–2.567499508	3.3998710389763E-22
SAOUHSC_02012	sgtB	2.6495588281258	5.504400310581E-22
SAOUHSC_00812	clfA	1.945657518	9.2996394670839E-22
SAOUHSC_00898	argH	2.6531564473172	1.0865265180626E-21
SAOUHSC_02814	——	1.5614820429818	1.5847544497922E-21
SAOUHSC_00427	sle1	–3.706132685	4.4737090333122E-21
SAOUHSC_00581	rclA	1.8330014067219	8.7450956409074E-21
SAOUHSC_02813	——	1.5694862604008	1.0844011136282E-20
SAOUHSC_00639	——	2.7083360949173	1.3796355896666E-20
SAOUHSC_01121	hlyII	–3.163262093	4.1278559272817E-20
SAOUHSC_02583	tagT_U_V	1.989213243	6.5756273076215E-20
SAOUHSC_00181	——	2.0549602192638	2.6237063266222E-18
SAOUHSC_02646	——	2.6886622489321	2.732842479236E-17
SAOUHSC_00717	——	–3.133467416	4.2211351770758E-17
SAOUHSC_01394	lysC	1.8606568122063	9.6050141941305E-17
SAOUHSC_00180	——	2.476707528	3.6401345919423E-16
SAOUHSC_01467	mrcA	1.5334735732349	4.0499896226988E-16
SAOUHSC_02365	murA	1.772700211	4.6790009774352E-16

(continues)

Table S3. Continued.

gene_id	gene_name	log_2(FC)	*p*.adjust
SAOUHSC_02769	cntL	–2.922006235	4.9648240231929E-16
SAOUHSC_00300	lip	–1.835900189	6.3832759781087E-16
SAOUHSC_00191	scn	–3.228831152	1.0545783290599E-15
SAOUHSC_00632	mnhG	1.6279943702565	1.4172602129146E-15
SAOUHSC_02830	ldhA	2.078671669	1.8086687441056E-15
SAOUHSC_02872	——	3.0171972170139	1.9053040007786E-15
SAOUHSC_01952	lanB	2.3696686262793	1.0801977881831E-14
SAOUHSC_00899	argG	2.2531079957046	1.3814085992537E-14
SAOUHSC_03021	——	2.4990157181246	5.6645863747289E-14
SAOUHSC_01287	glnA	–1.973007957	6.8262702824545E-14
SAOUHSC_01235	pyrH	–1.622427785	7.5330589536703E-14
SAOUHSC_00262	ftsK	1.4680535193866	1.1169830218236E-13
SAOUHSC_01947	nisE	1.9850771999154	1.9941053624116E-13
SAOUHSC_01159	ileS	–1.336976782	2.4016347824858E-13
SAOUHSC_00060	yjbB	–2.122947995	3.2932235863704E-13
SAOUHSC_00179	——	1.915303136	8.8271522289805E-13
SAOUHSC_02155	——	1.4049943682858	9.9010597924038E-13
SAOUHSC_00901	——	1.7141883255032	1.0376131388839E-12
SAOUHSC_00671	——	–2.654939004	1.0726104945641E-12
SAOUHSC_01395	asd	1.3634700199542	1.2611885080021E-12
SAOUHSC_00992	——	1.4884990656545	1.2628301379701E-12
SAOUHSC_02112	——	2.2348462421978	2.3391290175654E-12
SAOUHSC_00715	saeR	–2.056845531	2.5415552438217E-12
SAOUHSC_01361	tagT_U_V	1.9941883418198	4.3773843746001E-12
SAOUHSC_01236	frr	–1.156739601	6.6521674015585E-12
SAOUHSC_02983	——	1.1737309199208	7.6685307782022E-12
SAOUHSC_03019	ecfA	1.8196733869538	8.2805192936608E-12
SAOUHSC_03023	drp35	1.5547162353652	1.5202075104145E-11
SAOUHSC_02154	——	1.4546261528879	2.0935769076279E-11
SAOUHSC_02888	——	1.7197381487406	2.0935769076279E-11
SAOUHSC_01285	glnR	–2.458041012	6.5130804581423E-11
SAOUHSC_02770	cntK	–2.913194292	6.9268784682736E-11
SAOUHSC_02093	——	2.3418829752262	8.7465718286272E-11
SAOUHSC_01234	tsf	–1.052984368	9.2048704792231E-11
SAOUHSC_02690	znuA	–1.708566962	9.4765606236707E-11
SAOUHSC_00716	doxD	–2.378330956	1.054707727294E-10
SAOUHSC_00994	atl	–2.176446311	1.2698108474831E-10
SAOUHSC_00902	lepB	1.4805414008578	1.5122822504468E-10
SAOUHSC_02984	——	1.1790533570618	1.9556516592895E-10
SAOUHSC_01910	pckA	1.1108510168201	2.3869825982385E-10
SAOUHSC_03020	mtsT	2.0863890974275	2.7108997577069E-10
SAOUHSC_02768	cntM	–2.375880345	4.4547010223403E-10
SAOUHSC_02562	ureE	1.7796438611182	5.4706037141027E-10
SAOUHSC_02565	ureD	1.5924025851041	7.3904900823087E-10
SAOUHSC_00233	lrgB	–2.938257402	7.8381032144616E-10
SAOUHSC_01735	tcdA	–1.058446079	1.1658320821148E-9

(continues)

Table S3. Continued.

gene_id	gene_name	log_2(FC)	*p*.adjust
SAOUHSC_02576	——	–2.73094894	1.2671757067547E-9
SAOUHSC_00691	bacA	1.2989085194526	1.7789582408379E-9
SAOUHSC_00178	ganQ	1.565821082	2.1478812978615E-9
SAOUHSC_01017	purH	1.6751372057562	2.4496270255871E-9
SAOUHSC_01447	——	0.90238270930059	2.759812200409E-9
SAOUHSC_02988	asp1	1.3673320972872	3.1237861379128E-9
SAOUHSC_00818	nuc	–2.43223269	3.4053300384607E-9
SAOUHSC_02828	catE	1.5537485683586	4.5027935533041E-9
SAOUHSC_00259	——	1.3565317150133	5.9897677389357E-9
SAOUHSC_01396	dapA	1.6205298180776	6.3292547333028E-9
SAOUHSC_02705	——	–1.548767516	6.8790692235266E-9
SAOUHSC_02829	——	1.220804377	7.2868121690923E-9
SAOUHSC_01018	purD	1.3797188923761	7.7188886765434E-9
SAOUHSC_02563	ureF	1.7415866051874	7.7188886765434E-9
SAOUHSC_00714	saeS	–1.923105192	8.4264071067202E-9
SAOUHSC_02811	——	1.2105771596579	8.4264071067202E-9
SAOUHSC_02561	ureC	1.8747925344713	9.1264154867342E-9
SAOUHSC_01920	——	–1.738876773	1.3174196548863E-8
SAOUHSC_02924	puuE	1.8543230957225	1.3446246677737E-8
SAOUHSC_01760	——	3.6786328453216	1.7288749734182E-8
SAOUHSC_02990	——	1.1269796619213	2.5472391072666E-8
SAOUHSC_01681	prmA	1.1588141209763	4.4354468958026E-8
SAOUHSC_01320	hom	1.333950489	6.6014037050403E-8
SAOUHSC_01397	dapB	1.4562425854909	1.1221123400686E-7
SAOUHSC_01794	gap2	1.7730395868373	1.1221123400686E-7
SAOUHSC_02564	ureG	1.606132928	1.1986464722427E-7
SAOUHSC_02862	clpL	0.83899273670073	1.2471065140381E-7
SAOUHSC_01275	glpF	1.2611439331926	1.290485890511E-7
SAOUHSC_00939	glbN	1.3882997445526	1.608083257144E-7
SAOUHSC_02163	——	–3.094146165	1.8621227302597E-7
SAOUHSC_02152	——	1.1640113842931	1.8621227302597E-7
SAOUHSC_00167	ddpD	1.5316006204867	2.1764261729609E-7
SAOUHSC_00025	——	–1.021173794	2.2926323843939E-7
SAOUHSC_02864	feoB	1.319494744	2.4603667260399E-7
SAOUHSC_00119	wbjC	1.1399860730821	2.8960430176039E-7
SAOUHSC_02259	yafV	0.83951248445074	3.0681771264401E-7
SAOUHSC_02161	eap	–1.48463818	3.4177909030525E-7
SAOUHSC_02269	scrR	–0.9677133	4.4870474575281E-7
SAOUHSC_01953	nisA	2.5868205680326	5.5167342737171E-7
SAOUHSC_01321	thrC	1.2976715029471	6.5319918705695E-7
SAOUHSC_02558	ureA	2.4208523850594	6.5319918705695E-7
SAOUHSC_02874	copZ	1.8969565179767	6.616205561335E-7
SAOUHSC_01016	purN	1.582302909	8.2805830401518E-7
SAOUHSC_01432	msrA	0.89919939901938	8.9136814348057E-7
SAOUHSC_02855	——	–3.222439096	9.0524333439163E-7
SAOUHSC_00120	wbjD	1.1668900909837	1.0095021626419E-6
SAOUHSC_01165	K02824	uraA	1.1094989681431E-6

(continues)

Table S3. Continued.

gene_id	gene_name	log_2(FC)	*p*.adjust
SAOUHSC_02887	——	——	1.4263718080019E-6
SAOUHSC_02907	——	——	1.535352389973E-6
SAOUHSC_00882	——	——	1.5991575146485E-6
SAOUHSC_02611	——	——	1.8951500583217E-6
SAOUHSC_01431	K07305	msrB	1.8997811415801E-6
SAOUHSC_02987	K12269	asp2	1.9372599051107E-6
SAOUHSC_00422	K17217	mccB	2.0358246199614E-6
SAOUHSC_02669	K23775	ohrR	2.5950561521113E-6
SAOUHSC_01266	K00174	korA	2.8803535251384E-6
SAOUHSC_02731	K24163	nhaK	2.9557676889613E-6
SAOUHSC_01135	K20337	psmB	2.9748543683139E-6
SAOUHSC_02985	K03070	secA	3.2701230585736E-6
SAOUHSC_01918	——	——	3.4574266882087E-6
SAOUHSC_02557	K08717	utp	3.4741444109468E-6
SAOUHSC_01993	K07485	——	3.6066359654912E-6
SAOUHSC_01319	K00928	lysC	4.201752644502E-6
SAOUHSC_02729	K11737	cycA	4.3825779687227E-6
SAOUHSC_02101	——	——	4.4827164034641E-6
SAOUHSC_02244	K01439	dapE	4.555264248543E-6
SAOUHSC_01164	K02825	pyrR	4.6563620701036E-6
SAOUHSC_01584	——	——	5.026178917118E-6
SAOUHSC_02986	K12270	asp3	5.2736658509925E-6
SAOUHSC_02867	——	——	5.3642208970152E-6
SAOUHSC_01430	K02777	crr	5.4913672855992E-6
SAOUHSC_00579	K00938	mvaK2	5.586856752162E-6
SAOUHSC_02906	——	——	6.1730466845622E-6
SAOUHSC_00177	K15771	ganP	6.4662018078283E-6
SAOUHSC_02750	——	——	7.6816542045826E-6
SAOUHSC_02696	——	——	8.0852555345627E-6
SAOUHSC_00056	——	——	8.9587273059529E-6
SAOUHSC_02559	K01429	ureB	9.4575866534518E-6
SAOUHSC_00118	K15894	pseB	1.0193478134913E-5
SAOUHSC_00246	——	——	1.0786181100961E-5
SAOUHSC_00544	K14194	sdrC_D_E	1.1027342428395E-5
SAOUHSC_00323	——	——	1.1749978434396E-5
SAOUHSC_00421	K17216	mccA	1.2244833442702E-5
SAOUHSC_02967	K03758	arcD	1.3703320503854E-5
SAOUHSC_00319	——	——	1.3763313368142E-5
SAOUHSC_00174	lytH	1.6244597407889	1.5541085090437E-5
SAOUHSC_00700	——	1.4520911961235	1.7081973530286E-5
SAOUHSC_02883	——	–2.075625345	1.8361585491648E-5
SAOUHSC_00117	wbpM	0.85915221669567	1.9836568383933E-5
SAOUHSC_02658	——	1.3295834619503	2.2078803336665E-5
SAOUHSC_00217	gutB	1.4332681430091	2.4122518903769E-5
SAOUHSC_00938	——	1.0049661449637	2.413963914016E-5
SAOUHSC_02083	——	–2.073990281	2.5090783946886E-5
SAOUHSC_00572	——	0.88396202972366	2.6427628731007E-5

(continues)

Table S3. Continued.

gene_id	gene_name	log_2(FC)	*p*.adjust
SAOUHSC_01759	mreC	0.81859620567743	2.6740703182172E-5
SAOUHSC_00241	rbsU	–1.006635487	2.7336692610496E-5
SAOUHSC_02402	cmtB	1.419015253	2.9245875990099E-5
SAOUHSC_01416	sucB	0.80424567542452	3.0581874091126E-5
SAOUHSC_02265	agrA	–1.02839374	3.441021787863E-5
SAOUHSC_00341	metB	2.0423969647293	3.4704104042037E-5
SAOUHSC_01469	nth	–0.755667634	3.4704104042037E-5
SAOUHSC_02635	tcaA	1.5867096869989	3.6312009342976E-5
SAOUHSC_02403	mtlD	1.2694521421659	3.6899726221779E-5
SAOUHSC_00584	——	0.72501360103379	3.7068481138674E-5
SAOUHSC_01113	——	–2.744538658	3.7331645928566E-5
SAOUHSC_01813	——	–0.676938301	3.743865763479E-5
SAOUHSC_02812	——	1.0092091660551	3.8837291032656E-5
SAOUHSC_02772	——	0.93308190539749	4.2343532699327E-5
SAOUHSC_01276	glpK	0.97606784371589	4.3745586837103E-5
SAOUHSC_02911	queH	–1.006968396	4.5200700686123E-5
SAOUHSC_02810	——	1.2702352183159	5.2073482601813E-5
SAOUHSC_02571	——	–1.945540744	5.756673238807E-5
SAOUHSC_01456	——	1.2265713029633	5.7646377688721E-5
SAOUHSC_03026	——	1.6192805724273	5.95938920345E-5
SAOUHSC_01972	prsA	1.8721264854143	5.9624573462445E-5
SAOUHSC_02127	sspB2	–1.73558745	5.9910427405557E-5
SAOUHSC_00261	——	1.1087301981543	6.1610113595667E-5
SAOUHSC_01105	sdhB	0.63499034756244	6.9311659309666E-5
SAOUHSC_00232	lrgA	–2.614325891	7.0278278972688E-5
SAOUHSC_01866	——	–0.877617073	7.2158130724295E-5
SAOUHSC_03033	hoxN	1.0308757391713	7.9343990195151E-5
SAOUHSC_01130	——	0.88385699375815	8.5898121573326E-5
SAOUHSC_00320	ssuE	0.99120089272464	8.9618503904541E-5
SAOUHSC_02097	——	–0.812361393	9.3779876664796E-5
SAOUHSC_00142	——	–1.03234865	0.00011129743304742
SAOUHSC_02620	——	0.98361044823215	0.00011129743304742
SAOUHSC_02336	fabZ	–0.951944525	0.00011129743304742
SAOUHSC_02073	——	–2.291074176	0.00011603334285742
SAOUHSC_01819	——	–1.333671402	0.00012209325987465
SAOUHSC_00216	gatC	1.5902994474867	0.00013677090314052
SAOUHSC_00314	mepR	1.1901833678051	0.00014176143915513
SAOUHSC_00949	——	1.1449240937574	0.00014176143915513
SAOUHSC_00199	pct	1.4967533394794	0.00014330465959289
SAOUHSC_01025	——	1.0186228185275	0.00014776274054322
SAOUHSC_01846	acs	0.88174122670418	0.00018712731236004
SAOUHSC_01485	ndk	–1.160150773	0.00018927929387696
SAOUHSC_02833	yydJ	1.4980987051812	0.00019146639240666
SAOUHSC_00074	sirA	–1.230141768	0.00020070718467973
SAOUHSC_02759	——	–1.394458265	0.00020878824435503
SAOUHSC_00424	metI	1.5270173935088	0.00022008171721972
SAOUHSC_00031	——	1.183440709	0.0002235168702752

(continues)

Table S3. Continued.

gene_id	gene_name	log_2(FC)	*p*.adjust
SAOUHSC_01398	dapH	1.1604878163368	0.0002251365830159
SAOUHSC_02023	lytD	–2.562547517	0.00024851220349803
SAOUHSC_02025	——	–2.663283598	0.00026749496898789
SAOUHSC_02915	——	0.83278046772812	0.00027106211749688
SAOUHSC_01893	arsB	1.1291279713158	0.00027106211749688
SAOUHSC_01992	——	–1.183044699	0.00027495532537467
SAOUHSC_00729	uup	–0.819946196	0.00027747941247022
SAOUHSC_01267	korB	–0.886010277	0.00029345376724633
SAOUHSC_02019	xlyAB	–2.61948585	0.00030865133330252
SAOUHSC_02286	leuB	1.513311336	0.00030865133330252
SAOUHSC_00628	mnhD	0.95461240954379	0.00031281649096394
SAOUHSC_02089	——	–0.937315036	0.00032682378537446
SAOUHSC_02285	leuA	1.501022375	0.00034432165764077
SAOUHSC_01838	degP	0.64469166856785	0.00036280601043386
SAOUHSC_00318	——	0.9934244339362	0.00036751627576983
SAOUHSC_02254	groEL	0.95037100081251	0.00037244232291093
SAOUHSC_00828	lysE	1.1254889025656	0.00037978090514859
SAOUHSC_01232	rpsB	–0.959729428	0.00038224508429394
SAOUHSC_01440	yhhQ	0.82802838635069	0.00039302042350687
SAOUHSC_00297	——	0.78820504576823	0.00040661903501959
SAOUHSC_02886	——	–3.854964131	0.00040888044575072
SAOUHSC_00125	——	0.80519530464656	0.0004361102651382
SAOUHSC_01429	——	2.3834611637476	0.00045321715021124
SAOUHSC_02257	——	–1.076058704	0.00045321715021124
SAOUHSC_02905	——	0.96036437075294	0.00045321715021124
SAOUHSC_00195	fadA	1.2111347001879	0.00049500568389971
SAOUHSC_02261	agrB	–1.258926529	0.00049500568389971
SAOUHSC_00974	tarM	–1.390951414	0.00051173113645252
SAOUHSC_02516	pbuG	1.0597660016949	0.00053609813097673
SAOUHSC_00814	——	–1.981207707	0.00055338676970251
SAOUHSC_02022	——	–2.484926009	0.00055338676970251
SAOUHSC_00730	recQ	–0.798135	0.00055343449483335
SAOUHSC_00702	——	1.0364191168842	0.00055714299746504
SAOUHSC_01505	fmnP	–0.935541971	0.00059845072375803
SAOUHSC_00785	trxB	–0.706118164	0.0006026046685049
SAOUHSC_01990	artR	0.82560704108829	0.00061409787446094
SAOUHSC_00455	——	–0.794616589	0.00061774284715685
SAOUHSC_00844	metQ	0.89249767457257	0.00062195511429855
SAOUHSC_02078	——	–2.146322363	0.00064836444148981
SAOUHSC_02049	xtmB	–2.162397551	0.00065157488808932
SAOUHSC_00067	lutP	–0.791856518	0.00065642735919181
SAOUHSC_02251	——	1.3678068058076	0.00067698149717765
SAOUHSC_02644	——	0.82823341915488	0.00070638458751913
SAOUHSC_00423	metN	1.3310082174506	0.00070839469368278
SAOUHSC_01855	——	–0.885968198	0.00071063650518399
SAOUHSC_00160	——	1.3336340684407	0.00072391483770622

(continues)

Table S3. Continued.

gene_id	gene_name	log_2(FC)	*p*.adjust
SAOUHSC_02035	——	–2.490579797	0.00072391483770622
SAOUHSC_00400	——	–1.210874262	0.00074030300702683
SAOUHSC_02255	groES	1.2684526792489	0.00075293836866132
SAOUHSC_02337	murA	–0.783002502	0.0008276923244114
SAOUHSC_03022	——	0.99472614304331	0.00088927058717457
SAOUHSC_00578	mvaD	0.90880306548921	0.00092303675734698
SAOUHSC_00624	——	1.1508236314742	0.00093241120072328
SAOUHSC_00213	——	1.0352366523742	0.00094571822843106
SAOUHSC_01728	——	1.0259056697285	0.00099011049300636
SAOUHSC_00151	——	–0.947777317	0.0010183885603033
SAOUHSC_02030	——	–2.356931423	0.0010363105247461
SAOUHSC_00027	rlmH	–0.7605509	0.0010363105247461
SAOUHSC_00339	yitJ	1.4838457489473	0.0011216534115456
SAOUHSC_00223	tarF	–0.705193603	0.0011775687918753
SAOUHSC_00408	——	1.1124192449307	0.0011989751782817
SAOUHSC_02036	——	–2.227302561	0.0011989751782817
SAOUHSC_00369	——	–0.728111197	0.0012263237539811
SAOUHSC_00886	mnhD	0.79083619092566	0.0012728269294615
SAOUHSC_01399	——	1.0296799605983	0.0012728612877591
SAOUHSC_02043	——	–2.182326835	0.0013005270616331
SAOUHSC_02020	——	–2.769710667	0.0013310431407999
SAOUHSC_02071	——	–1.940700652	0.0013310431407999
SAOUHSC_02048	——	–1.92678267	0.0013310431407999
SAOUHSC_02047	——	–1.983902064	0.0013310431407999
SAOUHSC_00733	hisC	0.89350843037718	0.0013714081971918
SAOUHSC_00196	fadN	1.5964215649375	0.0013789715771421
SAOUHSC_00580	——	0.81341854479336	0.0014182347774305
SAOUHSC_01001	qoxB	0.89124974347561	0.0014394652368104
SAOUHSC_00499	pdxS	–0.717680471	0.0014657235668132
SAOUHSC_00182	——	–3.756629236	0.0015240693061657
SAOUHSC_02081	——	–2.207731237	0.0015393310917238
SAOUHSC_01598	rnz	–0.649636744	0.0015497974677063
SAOUHSC_01000	qoxC	1.1658000991257	0.001559667304985
SAOUHSC_01657	znuC	–1.328491974	0.0015784031631236
SAOUHSC_00571	——	0.9814282242087	0.0015822696419789
SAOUHSC_00500	pdxT	–0.707242277	0.0015881801498488
SAOUHSC_02028	——	–2.435360545	0.0016060287357648
SAOUHSC_01922	——	–0.868440006	0.0016080947631079
SAOUHSC_01832	——	0.99419765018561	0.0016129162977293
SAOUHSC_02080	——	–2.219959573	0.0016129162977293
SAOUHSC_00613	——	–0.693905719	0.0016176827995275
SAOUHSC_01719	——	–0.846987304	0.0017056282022413
SAOUHSC_00004	recF	–0.682200598	0.001724461171991
SAOUHSC_02070	——	–1.997130998	0.0017318432918364
SAOUHSC_02555	——	1.4527880881133	0.0017474662617661
SAOUHSC_02964	arcR	–0.701552575	0.0017521358412912
SAOUHSC_02282	ilvB	1.4457241015634	0.0017568579152808

(continues)

Table S3. Continued.

gene_id	gene_name	log_2(FC)	*p*.adjust
SAOUHSC_02029	——	–2.294862881	0.0018055887254533
SAOUHSC_02031	——	–2.292814776	0.0018113933129247
SAOUHSC_00859	——	–0.846107041	0.0018403794525794
SAOUHSC_02284	ilvC	1.6351097908128	0.0018403794525794
SAOUHSC_02268	sacA	–0.598153213	0.0018598509241493
SAOUHSC_00843	metI	1.3197095229335	0.0018617483779132
SAOUHSC_02430	fecB	–0.929366334	0.0018634712438434
SAOUHSC_00663	——	0.85410431693891	0.0018774604415532
SAOUHSC_01322	thrB	1.0576579275055	0.0018900565454761
SAOUHSC_02119	putP	0.67644246227809	0.0019631198368133
SAOUHSC_00265	——	1.3838332054721	0.0020381321861999
SAOUHSC_01663	dnaG	–0.946536206	0.0020381321861999
SAOUHSC_01400	alr	0.98721079304237	0.002044126558964
SAOUHSC_02264	agrC	–1.355161692	0.002044126558964
SAOUHSC_02260	hld	–3.335088598	0.0021252711300557
SAOUHSC_01046	potA	0.81193395369185	0.0021525144797494
SAOUHSC_02463	hysA	–0.841416154	0.0021543071323346
SAOUHSC_01682	dnaJ	0.92568483618151	0.0021615477638417
SAOUHSC_01035	rnj	–0.773108421	0.0021615477638417
SAOUHSC_00138	——	1.5231160595332	0.0022252539905852
SAOUHSC_00039	——	–0.630639631	0.0022252539905852
SAOUHSC_01917	——	–1.500491516	0.0024515058977306
SAOUHSC_01859	——	–1.149453262	0.0025456565838506
SAOUHSC_01499	bdr	–0.960643249	0.002550162775355
SAOUHSC_02922	ldh	–1.665222381	0.002562934395143
SAOUHSC_00294	——	0.76942425254004	0.002562934395143
SAOUHSC_00024	——	–0.745554645	0.0026833528999581
SAOUHSC_02033	——	–2.046530765	0.0027001599585945
SAOUHSC_02072	——	–1.849055659	0.0027396550045291
SAOUHSC_02062	——	–2.210724858	0.0027715466615032
SAOUHSC_00200	prsW	–1.011365624	0.0028766403979828
SAOUHSC_02782	——	–2.557589442	0.0028766403979828
SAOUHSC_01774	hemC	0.83210745073414	0.0028766403979828
SAOUHSC_02050	xtmA	–1.923274211	0.0029142096165542
SAOUHSC_01941	——	–1.481904321	0.0030366568080707
SAOUHSC_00845	——	–1.254532414	0.0030366568080707
SAOUHSC_00457	——	–0.727909902	0.0030749539120972
SAOUHSC_02767	nikA	–1.014583643	0.0031673454336325
SAOUHSC_00925	oppD	0.9754212470208	0.0031673454336325
SAOUHSC_01746	secDF	–0.87302987	0.0031673454336325
SAOUHSC_00553	hxlA	–0.735437989	0.0031845124834859
SAOUHSC_02426	——	0.96479798418984	0.0031845124834859
SAOUHSC_00484	tilS	–0.693818514	0.0031845124834859
SAOUHSC_01798	——	–1.097538183	0.0032465465112944
SAOUHSC_00407	——	1.5471372735767	0.0033337379050762
SAOUHSC_02931	——	–1.096339665	0.0033803719505524
SAOUHSC_01652	pbp3	–0.62449115	0.0034284033585014

(continues)

Table S3. Continued.

gene_id	gene_name	log_2(FC)	*p*.adjust
SAOUHSC_01895	——	–1.138044456	0.003629313699181
SAOUHSC_00861	lipA	–0.62499942	0.0037173798580694
SAOUHSC_01656	znuB	–0.727718452	0.0037366932486455
SAOUHSC_A02794	——	0.96368518053425	0.0037584047329679
SAOUHSC_00410	——	–1.037952945	0.0038141861824839
SAOUHSC_00987	sspB	–0.863531735	0.0038380367890474
SAOUHSC_02167	scn	–1.055042585	0.0038684082937561
SAOUHSC_00340	metC	1.6677678857224	0.0039774542636294
SAOUHSC_00257	——	0.8838596507653	0.0040196332315527
SAOUHSC_01981	——	–0.749060449	0.0040311741923895
SAOUHSC_00501	nupC	–0.620026298	0.0040311741923895
SAOUHSC_01680	rsmE	0.81953719738372	0.004069564111471
SAOUHSC_02881	crtP	–0.877734969	0.0041261638966891
SAOUHSC_01894	arsC	0.85126094605531	0.0041261638966891
SAOUHSC_02965	arcC	–0.764711577	0.004189512897955
SAOUHSC_02075	——	–2.283653054	0.0041998958674183
SAOUHSC_02389	czcD	–0.588514332	0.0042853960630795
SAOUHSC_02401	mtlR	1.0762846883759	0.0043427930864661
SAOUHSC_00304	——	–0.79929326	0.0045056126596796
SAOUHSC_02041	——	–2.326943219	0.0045722931019095
SAOUHSC_02682	cobA	1.1327999382323	0.0045890347259935
SAOUHSC_02802	fnbB	–0.813815116	0.0046346356571564
SAOUHSC_02287	leuC	1.1805275833712	0.0047602409621069
SAOUHSC_02069	——	–1.701743904	0.004827043420717
SAOUHSC_00248	lytM	–1.470348239	0.0048326479806063
SAOUHSC_00718	——	–1.412442899	0.0048594462562751
SAOUHSC_01921	——	–1.215843637	0.0048594462562751
SAOUHSC_01865	trmB	–1.630592925	0.0049902566700849
SAOUHSC_01470	dnaD	–1.567635041	0.0052454180809356
SAOUHSC_01084	isdD	–1.966545485	0.0053350532686048
SAOUHSC_01369	trpC	1.6928905908343	0.0053630464442212
SAOUHSC_00420	——	–1.415693089	0.0053630464442212
SAOUHSC_02865	feoA	1.7559958594368	0.0054469683750732
SAOUHSC_00459	rsmI	–0.794590674	0.0055866152653913
SAOUHSC_00376	——	–0.924995073	0.0056737921119313
SAOUHSC_00569	——	0.69437231519019	0.006083262961265
SAOUHSC_02034	——	–2.324700661	0.0063367340686587
SAOUHSC_00533	hchA	0.70503375109834	0.0064077380393837
SAOUHSC_00198	fadD	1.1803825886605	0.0064077380393837
SAOUHSC_01984	——	–1.982913102	0.0065046441664453
SAOUHSC_02912	phnB	0.68164726429913	0.0066011039307938
SAOUHSC_00485	hprT	–1.150838863	0.0068837621535287
SAOUHSC_00070	——	–1.607069379	0.0071055466989311
SAOUHSC_02554	fhuD	–0.736641367	0.0071973221617744
SAOUHSC_02038	——	–2.349106362	0.0073061287363225
SAOUHSC_00398	hsdS	–0.696762675	0.007323999690742

(continues)

Table S3. Continued.

gene_id	gene_name	log_2(FC)	*p*.adjust
SAOUHSC_02698	tcyB	0.65214706899893	0.007346472438893
SAOUHSC_03014	hisG	1.9561081601111	0.0074676373742953
SAOUHSC_00926	oppF	0.68348582008041	0.0075254879945249
SAOUHSC_01366	trpE	1.2214541237489	0.0076638388672674
SAOUHSC_01175	——	–0.697406285	0.0076919872988882
SAOUHSC_01283	hflX	–0.738717799	0.0078071523761841
SAOUHSC_00135	——	1.1205897705145	0.0078823483432322
SAOUHSC_00146	yagU	1.1533711067711	0.0079027308860409
SAOUHSC_00732	opuC	–0.973904126	0.0080063639001598
SAOUHSC_02821	——	–2.828766572	0.0080986291482735
SAOUHSC_01367	trpG	1.5354408521836	0.008117058634152
SAOUHSC_01845	fhs	–0.772489049	0.0082631114308812
SAOUHSC_00955	——	1.4763563077387	0.0082728303808098
SAOUHSC_01932	hsdS	–0.697050329	0.0084541206854359
SAOUHSC_00126	wbqP	0.89114922274564	0.0086385737562355
SAOUHSC_00264	——	1.424808308	0.0088853875171341
SAOUHSC_01224	xerC	0.59970467223051	0.0090025383243678
SAOUHSC_02628	——	0.64676182628661	0.0090248145149327
SAOUHSC_02252	——	1.3356005947543	0.0092842399575819
SAOUHSC_01050	——	0.62603057169822	0.0093099456940017
SAOUHSC_01371	trpB	1.1339514851537	0.0093685466680958
SAOUHSC_02722	——	1.265829721	0.0095152780461692
SAOUHSC_01919	——	0.61070577489993	0.0098845449764311
SAOUHSC_00426	metQ	0.8558507016274	0.010254345434558
SAOUHSC_01378	ddpD	0.78149670235145	0.010409358824149
SAOUHSC_01310	clsA_B	–0.623310589	0.01048920636864
SAOUHSC_02737	——	–1.13184977	0.010539784921183
SAOUHSC_00123	——	0.77501562540692	0.010803160178168
SAOUHSC_01053	mntH	–0.887165069	0.010889907675584
SAOUHSC_02150	——	0.99918684271384	0.01101101896572
SAOUHSC_00556	proP	0.84117395986832	0.011092657693992
SAOUHSC_02504	rpmC	0.94708993883567	0.011187758468841
SAOUHSC_02040	——	–2.321366434	0.011288668581717
SAOUHSC_01732	cymR	1.2533941006336	0.011519449852535
SAOUHSC_00127	——	0.68375810802788	0.012327475090331
SAOUHSC_02794	——	0.75190662116386	0.012341931223729
SAOUHSC_00999	qoxD	1.1930475306718	0.012359786531489
SAOUHSC_02936	——	1.0475020572553	0.012433092480013
SAOUHSC_00483	——	–0.772856565	0.01266315317218
SAOUHSC_00982	menF	–0.799557985	0.012675224239772
SAOUHSC_01858	——	–0.716376348	0.012735487710396
SAOUHSC_00997	tagT_U_V	0.68040835548184	0.012735487710396
SAOUHSC_02074	——	–1.891819522	0.012780146088771
SAOUHSC_02643	——	0.84524214995516	0.012963791573159
SAOUHSC_01761	——	1.4964487780231	0.013286910452217
SAOUHSC_02641	hrtB	–1.130792022	0.013475013885289

(continues)

Table S3. Continued.

gene_id	gene_name	log_2(FC)	*p*.adjust
SAOUHSC_02314	kdpD	–0.594283985	0.013739135932453
SAOUHSC_00164	——	–0.890156944	0.013788567117111
SAOUHSC_01015	purM	1.0815961773857	0.013788567117111
SAOUHSC_02256	——	–2.151048217	0.013821414494208
SAOUHSC_02296	sprL	0.71377266195296	0.014038242335137
SAOUHSC_00842	metN	0.92683686075629	0.014460625269325
SAOUHSC_02021	——	–1.904773969	0.014549261665069
SAOUHSC_02281	ilvD	1.0055275009112	0.014549261665069
SAOUHSC_01278	glpA	0.98839899356746	0.014549261665069
SAOUHSC_02003	——	–0.740692206	0.014606782052667
SAOUHSC_02989	secY	1.1019515149419	0.015002300471635
SAOUHSC_02037	——	–2.121411367	0.015057438140545
SAOUHSC_00051	plc	–1.484159155	0.015117706397277
SAOUHSC_02250	xtmA	1.0549842676443	0.015117706397277
SAOUHSC_01827	ezrA	–0.792305537	0.015273721628814
SAOUHSC_02067	——	–1.466351222	0.015273721628814
SAOUHSC_03012	hisC	1.2634632350601	0.015332995542907
SAOUHSC_00903	lepB	0.9085317826467	0.015576064851856
SAOUHSC_01835	——	0.71274962729167	0.015635846608348
SAOUHSC_02160	——	–1.011817438	0.015840551620092
SAOUHSC_00367	——	0.63697018634498	0.016264326636488
SAOUHSC_00927	oppA	0.61716862515199	0.016301546314128
SAOUHSC_02374	——	0.65140153445938	0.016498147277992
SAOUHSC_00397	hsdM	–0.79702771	0.016987855676016
SAOUHSC_02216	dnaC	–1.726556635	0.017395169967262
SAOUHSC_00153	kdcA	–1.157685425	0.017395169967262
SAOUHSC_01014	purF	0.97463902594955	0.017409635013242
SAOUHSC_00687	——	–0.823880584	0.017651902805897
SAOUHSC_00513	rlmB	–0.615721981	0.017891366253773
SAOUHSC_01957	——	–1.556731757	0.01902924322533
SAOUHSC_03015	——	1.3060472051336	0.019161155465064
SAOUHSC_02077	——	–1.884389844	0.019326026892599
SAOUHSC_00755	brxC	0.8801040197605	0.019326026892599
SAOUHSC_02648	lutP	0.76254027567171	0.019674973505926
SAOUHSC_00206	ldh	1.1975153267858	0.01991387184268
SAOUHSC_00627	mnhC	1.5576152766463	0.020325803408133
SAOUHSC_02656	——	0.70680789873821	0.02046863452966
SAOUHSC_01912	——	–0.618565035	0.020845223359725
SAOUHSC_00973	tarM	–1.590034613	0.02087454656448
SAOUHSC_02044	——	–1.808871444	0.021124015792806
SAOUHSC_00983	menD	–0.592091051	0.021624064223988
SAOUHSC_02489	infA	1.9217058568979	0.021738210119006
SAOUHSC_02499	rpsN	0.99698041857665	0.022331103243729
SAOUHSC_01980	——	–0.881628291	0.022604035630873
SAOUHSC_00907	——	–0.792386068	0.022604035630873
SAOUHSC_00924	oppC	0.67039310721848	0.022677695863217
SAOUHSC_00139	——	0.789152165	0.022976941182604

(continues)

Table S3. Continued.

gene_id	gene_name	log_2(FC)	*p*.adjust
SAOUHSC_00306	——	–0.758852116	0.023101924935431
SAOUHSC_00281	——	0.72836030017228	0.023201857398939
SAOUHSC_00230	lytS	–0.741426501	0.023309334594991
SAOUHSC_00543	——	–0.794437393	0.024012485713891
SAOUHSC_00430	——	–0.590903598	0.024029065465179
SAOUHSC_02935	gbsR	0.59242691239871	0.024055687406333
SAOUHSC_00189	——	1.9486005743027	0.025009191984528
SAOUHSC_02556	——	0.97092453348568	0.025109334074636
SAOUHSC_00002	dnaN	–0.706122393	0.025581360055176
SAOUHSC_01833	serA	0.64560442399349	0.02592724734116
SAOUHSC_00795	gapA	–0.860763869	0.026913773607212
SAOUHSC_02930	——	–0.728785976	0.026931312769316
SAOUHSC_00158	scrA	0.7374016350904	0.026931312769316
SAOUHSC_00115	epsB	0.72909256651998	0.027912832989699
SAOUHSC_03017	——	1.2217915847835	0.027915035396921
SAOUHSC_00055	——	0.72773078066525	0.02826304212412
SAOUHSC_00952	——	0.71283337431475	0.028712449099309
SAOUHSC_02288	leuD	1.2731404263906	0.028777724463393
SAOUHSC_03006	lip	–0.615814407	0.02925237542845
SAOUHSC_02425	——	0.60172615227374	0.02925237542845
SAOUHSC_01839	tyrS	–0.596161345	0.029415271688784
SAOUHSC_01814	——	–0.984055167	0.029614605992862
SAOUHSC_02949	gpx	0.73178886028305	0.029614605992862
SAOUHSC_02761	——	–1.746345784	0.029702948062902
SAOUHSC_02169	chp	–0.905097223	0.02981912268268
SAOUHSC_01327	katE	0.70134744937135	0.029923714909207
SAOUHSC_02027	——	–2.072481539	0.029923714909207
SAOUHSC_00487	hslO	–0.81672176	0.030896756398121
SAOUHSC_00245	——	0.73658650340847	0.030896756398121
SAOUHSC_00504	mcsB	0.6751025630853	0.030896756398121
SAOUHSC_01368	trpD	1.0338372042269	0.031573521532115
SAOUHSC_00953	ugtP	0.71385871496396	0.031845479771168
SAOUHSC_02225	——	–1.50044378	0.032390188542466
SAOUHSC_02171	sak	–0.967395266	0.032767791734373
SAOUHSC_01049	potD	0.62999276461192	0.032812214338401
SAOUHSC_00013	metX	0.76822053993132	0.033585449334365
SAOUHSC_01655	zurR	–2.121269244	0.034366458989059
SAOUHSC_00962	——	1.1788745705911	0.034486406603441
SAOUHSC_01112	flr	–1.128399296	0.034753022391816
SAOUHSC_01030	——	–3.315677473	0.03530375301796
SAOUHSC_03018	ecfT	1.2301526827511	0.035309868251534
SAOUHSC_00565	——	0.79570315401162	0.036119645577722
SAOUHSC_02597	glvC	0.60439264048226	0.036119645577722
SAOUHSC_00317	glpT	0.62705245136464	0.036123920498249
SAOUHSC_00007	nnrD	–0.620154003	0.036123920498249
SAOUHSC_01689	rpsT	–0.596296243	0.036267171055774
SAOUHSC_01370	trpF	1.4328471159455	0.036599122535287

(continues)

Table S3. Continued.

gene_id	gene_name	log_2(FC)	*p*.adjust
SAOUHSC_03008	hisF	0.90915417541718	0.037030167846077
SAOUHSC_00121	catB	0.95558860403907	0.037066859416276
SAOUHSC_01991	artQ	0.77995239682822	0.037375544138949
SAOUHSC_02880	crtQ	–0.62193226	0.037422657824837
SAOUHSC_01316	nuc	–0.622076177	0.0374778259104
SAOUHSC_01326	——	0.61158440319035	0.03761562572263
SAOUHSC_02280	tsaE	–0.993900481	0.03761562572263
SAOUHSC_01944	——	–0.824111209	0.038274569951526
SAOUHSC_02233	——	–1.342269012	0.038305833198003
SAOUHSC_03013	hisD	1.05471473	0.039068880547926
SAOUHSC_00258	——	0.59213349092584	0.040505359422045
SAOUHSC_00335	——	0.88371466333511	0.040587226037438
SAOUHSC_02057	dut	–1.397278465	0.041087980967276
SAOUHSC_02064	——	–1.648190976	0.041443935436531
SAOUHSC_00188	pflA	1.0346411558535	0.041443935436531
SAOUHSC_00344	ybiO	0.622289308	0.041576445439207
SAOUHSC_00429	——	–0.670332087	0.042152511866308
SAOUHSC_02766	nikB	–0.766028991	0.042331534923952
SAOUHSC_01717	prtC	–0.731843791	0.042331534923952
SAOUHSC_02087	——	–0.793254499	0.042740960187708
SAOUHSC_01162	lspA	–1.721825481	0.042758572993453
SAOUHSC_01082	isdC	–0.886822112	0.043260661780056
SAOUHSC_00163	——	–1.215351425	0.044251351000612
SAOUHSC_00708	fruA	0.81818010955068	0.044382425323806
SAOUHSC_01466	recU	0.76893983205376	0.044605113483786
SAOUHSC_02670	——	0.72924224432836	0.044605113483786
SAOUHSC_01756	ysxB	1.3453351983125	0.044605113483786
SAOUHSC_01125	——	–0.959254275	0.04706066569654
SAOUHSC_02051	——	–1.360318048	0.047100266010791
SAOUHSC_00299	——	1.3552536186881	0.04734831813698
SAOUHSC_00219	gutB	0.72316706270734	0.047423957542919
SAOUHSC_02016	——	0.65780685310957	0.048108954512002
SAOUHSC_00923	oppB	0.59064755906276	0.048897915770427